

**SKB**

---

**TECHNICAL**  
**REPORT**

---

**93-13**

**A review of the seismotectonics  
of Sweden**

Robert Muir Wood

EQE International Ltd, Warrington, Cheshire, England

April 1993

---

**SVENSK KÄRNBRÄNSLEHANTERING AB**

*SWEDISH NUCLEAR FUEL AND WASTE MANAGEMENT CO*

BOX 5864 S-102 48 STOCKHOLM

TEL 08-665 28 00 TELEX 13108 SKB S

TELEFAX 08-661 57 19

A REVIEW OF THE SEISMOTECTONICS OF SWEDEN

Robert Muir Wood

EQE International Ltd, Warrington, Cheshire, England

April 1993

This report concerns a study which was conducted for SKB. The conclusions and viewpoints presented in the report are those of the author(s) and do not necessarily coincide with those of the client.

Information on SKB technical reports from 1977-1978 (TR 121), 1979 (TR 79-28), 1980 (TR 80-26), 1981 (TR 81-17), 1982 (TR 82-28), 1983 (TR 83-77), 1984 (TR 85-01), 1985 (TR 85-20), 1986 (TR 86-31), 1987 (TR 87-33), 1988 (TR 88-32), 1989 (TR 89-40), 1990 (TR 90-46) and 1991 (TR 91-64) is available through SKB.

A REVIEW OF THE SEISMOTECTONICS OF SWEDEN

Robert Muir Wood

EQE International Ltd  
500 Longbarn Boulevard  
Birchwood  
Warrington  
WA2 OXF  
Cheshire  
England

April 1993

(With contributions from Ove Stephansson, Rutger Wahlström and  
Ronald Arvidsson)

Keywords: Sweden, seismotectonics, seismicity, deglaciation,  
postglacial rebound, neotectonics, stress-field,  
strain-field.

## ABSTRACT

A study has been undertaken of data relating to the seismotectonic state of Sweden, both under current conditions and also through the glaciation/deglaciation cycle. The focus of the study has been to explore primary data on all the separate sources of information bearing on seismotectonics including: a) regional tectonics; b) neotectonic surface faulting; c) geodetic and tide-gauge observations of land-level changes; d) the horizontal strain field; e) Holocene land-level changes; f) historical and instrumental seismicity; g) palaeoseismicity; h) stress determinations, and i) geothermal observations. These data have then been combined into a regional seismotectonic model, relating the distribution, style and rates of seismicity to the seismogenic properties of the crust and the continuing crustal deformation.

From the evidence of the modelled and observed horizontal strainfield and the diversity of focal mechanisms, all the current seismicity of the region appears to be a response to postglacial rebound. Through an understanding of the interaction between the pre-existing tectonic strainfield, and the strainfield resulting from glacial loading and unloading it is possible to make testable predictions about the localisation of deformation and seismicity in Fennoscandia at different stages of the glacial cycle. Immediately following glacial unloading intense deformation was concentrated on the northwestern flank of the downwarped crustal bowl. Currently low-level deformation and associated seismicity is most pronounced around the western margins of the dome of postglacial rebound. While the rebound dome is primarily extensional relieving the high levels of compression that accompanied crustal downwarping, there are also areas of compression and extension associated with flexures in the rebound surface that appear to affect the distribution and style of seismicity. The study shows how the significance and localisation of deformation and seismicity may be predicted both under present conditions and at other stages of the glacial cycle. Strain changes that accompany glacial loading and unloading are likely to have had a pronounced impact on hydrogeology.



## ABSTRACT (SWEDISH)

Denna studie utvärderar seismotektoniska förhållanden i Sverige, både under nuvarande förhållanden och under den senaste glaciation/ deglaciationscykeln. Studien har huvudsakligen gjorts på de ursprungsdata som har funnits tillgängliga inom ämnesområdena; a) regional tektonik, b) neotektoniska förskjutningar av markytan, c) geodetiska observationer, inklusive vattenståndsobservationer, av landhöjning, d) horisontellt deformationsfält (strain), e) Holocen landhöjning, f) jordskalv, både historiska och instrumentella data, g) paleoseismicitet, h) bergspänningsmätningar, och i) geotermala observationer. Dessa data har samlats till en landsomfattande seismotektonisk modell som relaterar jordskalvens fördelning, typ och omfattning till jordskorpan seismogena förhållanden och till dess nuvarande deformation.

Det modellerade och observerade horisontella deformationsfältet tyder på att den nuvarande seismiciteten i Sverige är en effekt av den postglaciala landhöjningen. Denna slutsats stöds även från analyser av jordskalvens fokalmekanismer. Genom att förstå växelverkan mellan det tektoniska deformationsfältet som fanns innan den senaste glaciationen och det deformationsfält som är ett resultat av på- och avlastningen av inlandsisen, är det möjligt att göra testbara förutsägelser av var den huvudsakliga deformationen och seismiciteten i Fennoscandia har skett under olika stadier i den glaciala cykeln.

Omedelbart efter inlandsisens avsmältning förekom en intensiv deformation av berggrunden i den nordvästra delen av den nedtryckta jordskorpan. Idag finns en liten pågående deformation, med tillhörande seismicitet, främst i den västligaste delen. Landhöjning innebär i huvudsak en utvidgning av berggrunden med avlastning av jordskorpan som följd. Det verkar emellertid även finnas områden i Sverige med omväxlande kompression och extension som är associerade med krökningar i landhöjningen, som i sin tur verkar påverka jordskalvens fördelning och typ.

Denna studie visar hur omfattning och fördelning av deformation och seismicitet kan förutsägas under såväl dagens förhållanden som under en glaciationscykel. Den deformation av berggrunden som uppkommer genom på- och avlastning av en inlandsis har troligen även en väsentlig inverkan på berggrundens hydrogeologiska förhållanden.

## ACKNOWLEDGEMENTS

This study was initiated in March 1991, following discussions with Kaj Ahlbom, Ove Stephansson and Chris Talbot in Uppsala in May 1990, and in London with Lars Ericsson and Roy Stanfors in November of the same year. Special thanks are due to Lars Ericsson for promoting the project, and offering considerable assistance with a number of discussions in the course of the research.

Two sections of the work were the responsibility of researchers in Sweden. All the work on instrumental seismicity, including magnitude determinations, establishing regional thresholds and focal mechanism studies (Sections 5.2.6 and 5.3) was undertaken by Ronald Arvidsson and Rutger Wahlström at the Seismological Observatory at Uppsala. The section on Stress (the whole of Section 6) was produced under the direction of Professor Ove Stephansson at the Department of Engineering Geology, at the Royal Institute of Technology in Stockholm. Their assistance, not only with their own sections, but with the wider scope of the report is gratefully acknowledged. Special thanks are also due to Kaj Ahlbom of Conterra AB who provided detailed logs for a number of Swedish boreholes and to Gordon Woo of BEQE who also provided much help with evaluating the limits of statistical analysis for geodetic data, and with compiling seismicity statistics according to a coherent set of magnitudes.

Many other individuals have provided extremely helpful assistance and information in the course of the project, sometimes sharing unpublished manuscripts and data, in particular in the fields of geodetics and geothermics. In particular I would like to thank: Karl Anundsen, University of Bergen; Kakkuri, Finnish Geodetic Institute, Helsinki; Aarne Verio, National Board of Survey, Helsinki; Lars Sjöberg, Department of Geodesy, Royal Institute of Technology, Stockholm; Niels-Axis Mörner, Department of Geology, University of Stockholm; Martin Ekman, National Land Survey, Gavle; Massimo Verdoya, University of Genova; D.S. Parasnis, Lulea University; Ilmo Kukkonen, Geological Survey of Finland, Helsinki; Robert Lagerbäck, Swedish Geological Survey, Uppsala; Christopher Talbot, University of Uppsala; John Adams, Geological Survey of Canada, Ottawa. I would also like to thank Niels-Axel Mörner for taking me to visit some interesting localities in the vicinity of Stockholm, and to Robert Lagerbäck for his extraordinarily resourceful assistance and kindness on two visits to the Lapland late-glacial faults, as well as engaging in many hours of discussion on the significance and origins of these structures.

However with the exception of Sections 5.2.6, 5.3 and all of Section 6, responsibility for the opinions and analysis throughout the remainder of the report remains with the principal author.

## TABLE OF CONTENTS

		Page
	Abstract	
	Acknowledgements	
	Table of Contents	i
	Summary	v
<b>1</b>	<b>INTRODUCTION</b>	<b>1</b>
1.1	QUALITY CONTROL CRITERIA	1
1.2	DATA BASES	2
<b>2.0</b>	<b>TECTONIC BACKGROUND</b>	<b>4</b>
2.1	THE FORMATION OF THE BALTIC SHIELD	4
2.2	CRUSTAL AND LITHOSPHERIC THICKNESS	6
2.3	MAJOR TECTONIC ZONES IN SWEDEN	8
2.4	POST-OROGENIC RIFTING	9
2.4.1	Late Pre-Cambrian rifting	9
2.4.2	Palaeozoic basins	10
2.4.3	Mesozoic and Tertiary tectonics	11
2.4.4	Neogene tectonics	13
2.5	SUMMARY OF PLIO-QUATERNARY TECTONICS	13
<b>3</b>	<b>NEOTECTONICS</b>	<b>17</b>
3.1	MAKING A SCIENCE OF NEOTECTONICS	17
3.1.1	Earthquake geology	18
3.1.2	Demonstrating offset	18
3.1.3	Superficial faulting	19
3.1.4	Neotectonic diagnostics	19
3.1.5	Grading neotectonic claims	20
3.2	SCANDINAVIAN NEOTECTONICS	21
3.3	THE LAPLAND POST-GLACIAL FAULT PROVINCE	21
3.3.1	Orientation	21
3.3.2	Fault groups	23
3.3.3	Age	23
3.3.4	Fault reactivation	28
3.3.5	Fault families	28
3.3.6	Frontal thrusts	30
3.3.7	Analogies to other reverse fault scarps	31
3.3.8	Fault spacing	34
3.3.9	Accompanying earthquakes	34
<b>4</b>	<b>LAND MOVEMENTS</b>	<b>36</b>
4.1	Geodetics	36
4.1.1	Relevelling	37
4.1.2	Tide gauge observations	39
4.1.3	Calibrated geodetic observations	41
4.1.4	Third relevelling surveys	45
4.1.5	Reducing the spatio-temporal scale of observation	45
4.1.6	Horizontal component of deformation	51
4.2	Historic observations of uplift	53
4.3	Holocene uplift	54

5	<b>SEISMICITY</b>	58
5.1	QUALITY CONTROL	58
5.2	HISTORICAL SEISMICITY	58
5.2.1	Historiography	59
5.2.2	Macroseismic monitoring	62
5.2.3	Macroseismic interpretation	63
5.2.4	Locational accuracy	64
5.2.5	Depth estimates	65
5.2.6	Regional magnitude scales	65
5.2.7	Calibrating macroseismic information for magnitude	68
5.2.8	Seismicity statistics	70
5.3	INSTRUMENTAL SEISMOLOGICAL DATA	73
5.3.1	Introduction	73
5.3.2	Seismic instrumentation and threshold magnitudes	73
5.3.3	Epicentre location	83
5.3.4	Focal depth	85
5.3.5	Crustal stresses and earthquake focal mechanisms	88
5.4	PALAEOSEISMICITY	90
5.4.1	Palaeoseismic observations	90
5.4.2	Fennoscandian palaeoseismicity	93
5.4.3	Swedish 'palaeoseismic indicators'	95
5.4.4	Shallow stress-release phenomena?	96
6.	<b>STRESS OBSERVATIONS</b>	98
6.1	INTRODUCTION	98
6.2	SHORT HISTORY OF ROCK STRESS MEASUREMENT	99
6.2.1	Sweden	99
6.2.2	Norway	101
6.2.3	Finland	101
6.3	FENNOSCANDIAN ROCK STRESS DATA BASE (FRSDB)	102
6.3.1	Current state of the FRSDB	102
6.3.2	Stress versus depth	104
6.3.3	Stress magnitude discontinuities	109
6.3.4	Orientation of stresses from FRSDB	110
6.3.5	Scatter in stress magnitudes and orientations	112
6.3.6	Stress state from breakouts and other tests at great depth in the Siljan district	118
6.4	FENNOSCANDIA IN THE CONTEXT OF THE WORLD AND THE EUROPEAN STRESS MAP	121
6.4.1	World Stress Map (WSM)	121
6.4.2	The European Stress Data Base (ESDB)	123
6.4.3	The European Stress Map (ESM)	124
6.4.4	Relationship of the Fenoscandian stress province to Central Europe	126
6.4.5	In-situ stress measurements around the centre of the rebound dome	132

7	<b>GEOHERMAL OBSERVATIONS</b>	134
7.1	BACKGROUND	134
7.2	OBSERVATIONS	135
7.3	PERTURBATIONS TO THE GEOTHERM	135
7.3.1	The record of the vertical component of fluid flow	137
7.4	EXTRAPOLATING THE GEOTHERM TO DEPTH	138
7.4.1	Deep boreholes	139
7.4.2	Radiogenic heat production	141
7.4.3	The Swedish geotherm	141
8	<b>CURRENT SEISMOTECTONICS</b>	142
8.1	TECTONICS OR REBOUND?	142
8.1.1	The tectonic strainfield	143
8.1.2	The rebound strainfield	145
8.1.3	The competing strainfields of rebound and tectonics	147
8.1.4	A tectonic component in addition to rebound?	147
8.1.5	Reconciling stress with strain	148
8.1.6	Modifications of the stress state from strain release	149
8.1.7	Where is permanent strain most likely to occur?	150
8.1.8	Tectonic strain during glacial loading	152
8.2	REBOUND SEISMOTECTONICS: THE REAL WORLD	154
8.2.1	Rebound deformation	154
8.2.2	Rheology and rebound	156
8.3	REBOUND DEFORMATION AND SEISMICITY	157
8.3.1	Depth dependent stress release	158
8.3.2	Deformation around the Baltic shield	158
8.4	SPATIAL AND TEMPORAL VARIATIONS IN SEISMICITY	164
8.4.1	Temporal variations in seismicity	164
8.4.2	Spatio-temporal clustering	166
8.4.3	Seismic swarms	168
8.5	CRUSTAL STRAIN AND GROUNDWATER	169
8.5.1	Hydrogeological consequences of coseismic strain	169
8.5.2	Hydrogeological consequences of rebound strain	169
8.5.3	Horizontal strain and pockmarks	172
8.5.4	Compressional strainfields within the rebound dome	173
9	<b>SEISMOTECTONICS OF THE GLACIATION/ DEGLACIATION CYCLE</b>	176
9.1	ICE LOADING	176
9.1.1	Stress-state during ice loading	177
9.2	DEGLACIATION REBOUND	177
9.2.1	Deglaciation rebound in southern Fennoscandia	179
9.2.2	Deglaciation seismicity in southern Fennoscandia	181

9.2.3	Deglaciation rebound in northern Fennoscandia	183
9.2.4	Deglaciation tectonics in northern Fennoscandia	185
9.2.5	Deglaciation seismicity in northern Fennoscandia	187
9.2.6	Differential vertical uplift	189
9.2.7	The horizontal component of deformation	189
9.3	POST-DEGLACIATION SEISMOTECTONICS	192
9.4	PREVIOUS GLACIATIONS	193
10	<b>CONCLUSIONS</b>	195
10.1	CURRENT SEISMOTECTONICS	195
10.2	DEGLACIATION SEISMOTECTONICS	197
10.3	HYDROGEOLOGICAL IMPACT	198
11	<b>REFERENCES</b>	200

## SUMMARY

This project, entitled "*A review of the seismotectonics of Sweden*", was carried out by EQE International Ltd, England, for Svensk Karnbranslehantering AB (SKB), the Swedish Nuclear Fuel and Waste Management Co. The scientist in charge of the project for EQE and principal author of this report was Dr Robert Muir Wood. Considerable support was provided by Swedish scientists and others, and this is detailed in the acknowledgements.

This project has set out to review all the various forms of data relating to the structure (tectonics), and properties (stress and temperature) of the crust that constrain the distribution and style of deformation (strain and seismicity), both under present day conditions and those prevailing through the glaciation / deglaciation cycle. These data have then been combined in a seismotectonic synthesis in an attempt to understand the causes, styles, sizes and locations of earthquakes in particular through the past 13,000 years since the ice-sheet began to retreat from southern Sweden. The various data-sets are in different stages of integration and in all cases an attempt has been made to apply some kind of quality criteria for revealing the nature of the inherent errors and uncertainties.

Fennoscandia is a cratonic region, stabilised more than 1000 million years ago, and subsequently subject to only modest and declining deformation. The chief phase of post-cratonic tectonics across the shield was an episode of minor late-Precambrian rifting. The last episode of significant tectonic activity within the Baltic Basin involved strike-slip and reverse faulting at the time of the final (ca. 400Ma) Caledonian collision. A localised phase of rifting and volcanism in the Oslo Graben dates from the Permian (ca. 290Ma). Significant subsequent Mesozoic rifting and faulting is concentrated along the Fennoscandian Border Zone and the west Norwegian coast and continental margin. No evidence has been found for any Tertiary faulting within the shield, and any movements through this period are likely to have been minor.

In a review of evidence for neotectonic faulting in Fennoscandia a proposal is made to establish criteria by which neotectonic claims can be graded for their credibility. Many of the localities claimed as neotectonic have not been properly investigated or documented and some probably have a non-neotectonic explanation. However evidence suggestive of neotectonics is known from the Fennoscandian Border Zone in the Kattegat, and in certain localities along the coast of western and northern Norway and Russian Kola. However the most spectacular neotectonic examples are clustered in the Lapland late-glacial fault province that lies in northern Sweden, Finland and Finnmark, Norway.

Almost all the information on continuing deformation in Fennoscandia reflects vertical level changes relative to a sea-level datum. Geodetic releveling data is of different qualities and adjusted to different datums in the various countries of Fennoscandia and it is as yet impossible to obtain a unified geodetic picture of uplift. Published maps of rebound have tended to smooth the data ignoring genuine flexures within the rebound surface, that can be seen when the land-level changes are followed along geodetic survey lines radiating out from the centre of the rebound dome. The dome is almost everywhere convex, in particular in passing towards the Norwegian coast. However some concave 'saddles' also appear to exist within the rebound surface for Sweden. Such flexures may be important for suggesting crustal deformation within the uplift surface.

Repeated short-range levelling studies across prominent structures at a number of localities in Fennoscandia have revealed concentrated (but intermittent and sometimes reversing) zones of deformation with velocities up to 1mm/yr. An attempt to explore the horizontal strain field from triangulation and trilateration data from Finland has revealed that extensional strain dominates although parts of the south-west of the country are in compression. Strain-levels in excess of  $10^{-7}$  were found in this survey although in many cases the inherent errors are as large as the apparent signals. The past pattern of land-level changes is best revealed from studies of the relative elevation of a unique water-level marker in particular the Baltic Ice Lake shoreline, as well as from detailed lake isolation studies.

Throughout much of the historical record there has been a bias whereby the seismicity of Sweden has appeared more pronounced than that of western Norway. This bias has been explored by analysing how information has been recorded at different periods of history. Although there are numerous earthquakes known in Sweden from the late 17th Century right up to the late 19th Century when the regular collection of macroseismic reports was initiated, there is a seismological deficit, both because moderate sized events were unreported, but also because incomplete information has survived of those that are known. Hence it is almost impossible to develop seismicity statistics from the pre-1880 record, except for the largest magnitude events.

Through examining thresholds for detection it has also been possible to establish uniform data-sets for the instrumental period covering the whole of Fennoscandia. The seismicity of Sweden has been consistently low throughout history; more than an order of magnitude lower than for an equivalent area of western and northern Norway and the adjacent continental shelf. The zone of activity in Sweden has been very consistent from the historical through to the instrumental period. By



establishing quality criteria it has been possible to create a list of reliable focal mechanisms for Sweden that reveal a surprising amount of diversity in stress-release processes, and show evidence of extension within the rebound dome. Unambiguous palaeoseismic evidence has been found only to be of significance in the region of the Lapland faults, revealing the strength and duration of the accompanying ground motion.

In-situ stress observations have been collected and compiled from throughout Fennoscandia. These observations reveal that in southern Sweden there is a regionally consistent NW-SE direction of the principal horizontal stress, although there is far more variation in northern Sweden and northern Norway. A number of depth dependent stress discontinuities have been established and a range of stress-states identified from strike-slip to compressional. In the vicinity of the Lansjarv Fault in Swedish Lapland the stress-state was found to be highly anomalous with horizontal stresses significantly less than vertical stresses, revealing the existence of an extensional stress regime.

Geothermal observations have been compiled as part of the European Geotraverse Project and reveal a significant decrease in heatflow into the centre of the Baltic shield from the relatively high values along the Fennoscandian Border Zone. Projecting the surface derived heatflows to depth shows that there are marked differences in the temperature of the lower crust and upper mantle along a north south profile passing through Sweden.

The modelled and observed horizontal strain in the Fennoscandia Shield reveals that current crustal dynamics is all the result of post-glacial rebound. The horizontal lithospheric strainfield associated with the inward motion of mantle material to infill the former downwarped crustal bowl is probably in excess of  $10^{-9}$  per year, two to three orders of magnitude higher than any plausible tectonic strain within the shield. Differences in rheology and topographically controlled variations in the original ice-load, appear to show some control on flexures in the rebound surface, and these in turn appear to give rise to zones of crustal deformation that generate seismicity. In Sweden, earthquake generation may primarily be controlled by a zone of flexure associated with a ridge in the rebound dome, passing along the Gulf of Bothnia, that interconnects with a region of higher heatflow in south-west Sweden and the Kattegat. Inbetween these areas around the central east coast, there is evidence for a saddle in the rebound surface associated with shallow compression. All the larger (M5-6) earthquakes within the 100-300 year historical record have been located within the thinner crust around the western margins of the Fennoscandian rebound dome.

The expansion of the crust during rebound has probably increased crustal porosity, drawing surface water into the

crust to a depth that may be typically of several hundred metres. The region of the central east coast of Sweden subject to shallow reverse fault earthquakes is also one in which there are indications of compressional strain including: saline water close to the surface, low-angle dilated fractures controlling fluid flow, and pockmarks (revealing gas and water release) in the adjacent seafloor.

Over much of the crust of Fennoscandia stresses are returning to the state that prevailed prior to glacial loading, as the subsidence bowl continues to shallow. During the course of glacial loading the downwarped crust beneath the ice-load suffered radial compression as the underlying mantle streamed towards the surrounding forebulge. Subsequent to the removal of the ice-load the vertical stress returned to its pre-glacial state, but horizontal stresses took far longer to respond to the inward flow of mantle material back beneath the region. The impact of this radial flow on the crustal stress-state is very dependent on the disposition of a region of crust relative to the orientation of the underlying tectonically controlled NW-SE principal horizontal stress direction. On the north-west flank of the subsidence bowl in northern Sweden radial increases in stress served to raise the deviatoric stress, tending to take the crust into conditions of failure in the immediate aftermath of unloading. However on the southwestern flank in southern Sweden the radial increase in stress affected the minimum compressive stress state, reducing or leaving unaffected the deviatoric stress and hence giving no cause for major earthquakes during deglaciation.

In a fully elastic medium once rebound is complete stress would return to the tectonic state that prevailed prior to glacial loading. However where there has been non-elastic behaviour involving permanent strain during the glaciation/deglaciation cycle the stress state is unable to recover its preglacial value. Hence significant rotations in stress orientation and stress magnitudes are likely to be a diagnostic of some local permanent strain during the course of the rebound cycle.

The Lapland post-glacial reverse faults moved in conjunction with the deglaciation of the region and all involved the uplift of the eastern block relative to the west, indicating that prior to fault rupture the area to the east was rising far faster than to the west. These faults owe their existence to the very rapid deglaciation of Finland and the Gulf of Bothnia around 9,000BP. The most easterly faults are all located close to the marine limit: the elevation of the contemporary sea-level appears to have determined the limit of the most rapid deglaciation. These faults probably ruptured very deep, possibly passing right through the 40km thick crust. The largest accompanying earthquake had a magnitude estimated as 8.2. The horizontal component of deformation

associated with these fault movements almost entirely reflects compressional strain within the downwarped crustal bowl rather than tectonic strain stored during the existence of the ice-sheet. The current strain regime surrounding these faults is extensional and hence they have no possibility of near-future reverse reactivation. Earlier Quaternary glaciations may have involved centres of load at different distances from the initiation of the ice sheet in the North Swedish mountains, as well as different styles and rates of deglaciation, producing faulting (if at all) in other neighbouring regions.

1

## INTRODUCTION

Sweden lies at the centre of a remarkable tectonic province in which the rates of vertical crustal movement are some of the highest known on Earth and yet the current seismicity is low. Evidence of surface faulting in northern Sweden dating from the end of the last Ice Age reveals that at least part of this same region has had a very high rate of earthquake activity only a few thousand years ago. Such a switch in the level of seismic activity from that more typical of a continental plate boundary to that of a stable continental interior is completely at odds with a conventional tectonic setting. This report concerns regional seismotectonics: the exploration of the causes and geological controls of seismicity.

1.1

### QUALITY CONTROL CRITERIA

Establishing the seismotectonics of an intraplate low seismicity region is always difficult as a result of a shortage of suitable reliable data. When data is scarce there is always a tendency to ignore its inherent uncertainties. For example, seismotectonics would be greatly assisted if it was possible to identify the geological fault that was the origin of every earthquake, but most earthquakes in Sweden involve fault ruptures significantly smaller than  $1 \text{ km}^2$ , and could occur on one of many hundreds of unknown faults within the typically  $>10,000 \text{ km}^3$  volume of locational uncertainty. Even in well studied plate boundary regions almost all small and moderate sized earthquakes do not lie on known surface-mapped faults.

Most examples of over interpretation arise because those building a model are insufficiently familiar with the way in which the original data has been collected and processed. Hence the chief purpose of this project has been to explore all the individual data sources on crustal properties, deformation and seismicity and apply some quality criteria, so that information of dubious quality does not become the focus of analysis, and that correlations are only attempted between data-sets of comparable accuracy. Whatever disputes may

eventually exist as to the integration of different types of data into a seismotectonic understanding it is first necessary to share a common and reliable foundation of knowledge.

The application of quality criteria is relatively complex and has to be developed to complement the particular data-type under scrutiny. For individual parameters one needs to know the reliability of measurement, the consistency of measurement, and the uncertainty (or errors in numerical data sources). For groups of observations one needs to know the degree to which they represent a complete data-set; which observations reveal the general field, and which are local anomalies.

In each of the separate sections that discuss individual sources of data (Sections 2 to 7) an attempt is made to explore how quality criteria can be developed and employed. The application of quality criteria provides a sieve through which high quality data pass. Inevitably at all stages the poorest quality data, or data that do not form part of a complete data-set may have to be discarded.

## 1.2

### **DATA BASES**

In earlier publications on the seismicity and seismotectonics of Sweden, Swedish seismicity has often been considered independent of the rest of Fennoscandia, obscuring regional seismotectonic comparisons. Also no attempt has previously been made to evaluate the degree to which the Swedish earthquake catalogue represents a complete record of all those events that have occurred. In common with other intraplate regions, the hunger for obtaining focal mechanisms has meant that initial publications on the subject contain solutions of relatively poor quality.

Within all seismotectonic studies it is important to obtain a context within which anomalous results can be understood. For example, if it is discovered that movement (larger than the likely observational error) appears to be localised across a narrow zone intersected by a geodetic survey, one could all too

easily extrapolate to believe that such movements are ubiquitous throughout Fennoscandia or alternatively dismiss the observation as a freak. It is only when a survey is undertaken to discover how many prominent structural features appear to show evidence for movement (as has now been undertaken in Finland: Verio, 1990) is it possible to put this single observation in its appropriate context. This context can be difficult to achieve: there is a fundamental bias of reporting whereby it is all too easy to obtain publication of some poorly substantiated claim of neotectonic fault movement, but far less common to find papers reporting that the earlier claims have not been validated.

It is also important in seismotectonic investigation to differentiate between observations that record processes taking place today (most obviously earthquakes), from those that record events in the past (such as faults). Some observations may reflect both present-day and past processes. The stress field and the temperature gradient take time to re-equilibrate once perturbed. Hence both stress and temperature have a memory that could potentially record past events.

## TECTONIC BACKGROUND

Sweden is part of the Baltic Shield, a section of ancient continental crust formed in episodes of continental collision between 3000 and 1500 Ma. Subsequently these orogenic zones became deeply eroded to expose high grade metamorphic and plutonic rocks over much of the present day rock surface. The relatively dense Swedish crust is thicker and colder than average continental crust, although typical of other ancient continental shields. Since the final consolidation of the shield there has only been relatively modest deformation across the region.

### 2.1 THE FORMATION OF THE BALTIC SHIELD

The Baltic Shield grew like a snowball (see Figure 2-1) accreting new sections of continental crust, that may formerly have been island arcs, or parts of other continents. The main phase of shield formation occurred between 3.1 - 1.5 Ga. The latest phase of orogenesis in the Caledonian period reworked the whole western margin of the Shield.

The primary Archaean nucleus that runs from northern Finland across northern Sweden probably dates from 2.9-2.6 Ga, formed in the Lopian orogeny. Other sections of Archaean crust became welded to the original nucleus across the (2.0-1.95 Ga) Kola suture zone to the north. In a series of subsequent episodes, the Baltic Shield continued to expand chiefly towards the south and southwest. Each episode involved continental accretion as well as reworking (through rifting, and collision tectonics) the adjacent edge of the growing Baltic continent.

To the south of the Archaean nucleus, following a phase of rifting prior to 2.0 Ga, there was a major episode of Sveco-Karelian orogenesis, involving a northeastward dipping subduction zone, which helped create or accrete the Svecofennian crust of much of central Sweden and southern Finland. By 1.8Ma this new crust had become consolidated and the Baltic Shield began to be subject to deformation along major N-S and NW-SE trending strike-slip shear zones cut through the

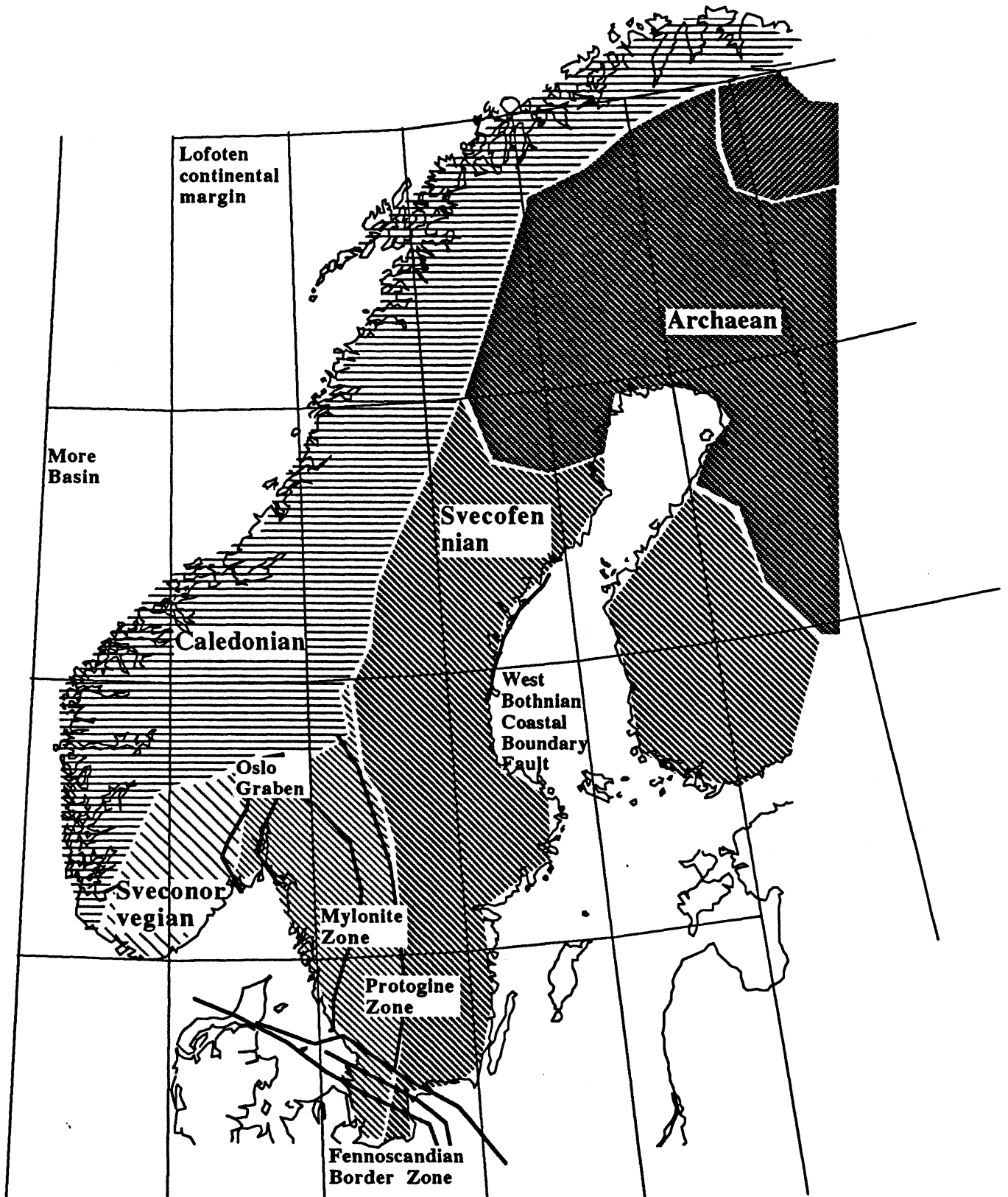


Figure 2-1: Tectonic units of the Baltic Shield.



thick continental crust (Berthelsen and Marker, 1986).

In southern Sweden, the continental crust continued to be accreted to the west within further Gothian orogenic episodes between ca 1.76 and 1.5 Ga, which also involved the reworking of the margins of the Svecofennian crust (Gorbatshev, 1980). This was the last major episode of orogenesis in southern Sweden in which considerable crustal thickening and magmatism, accompanied widespread crustal deformation. Following this period there were continuing phases of metamorphism and plutonism at around 1400 and 1200Ma, while, on the western margins further orogenesis continued between 1200 and 900Ma in the Sveconorwegian phase that culminated in an orogeny correlated with that of the Grenvillian in eastern Canada.

The last orogenic phase was that of the Caledonian which involved the reworking of the whole western margin of the shield with overthrusting and nappe tectonics involving transport towards the east of earlier continental fragments and rifts, with very significant crustal shortening. A separate NW-SE trending Caledonian arm also passed to the south of the Baltic Shield, its northern boundary forming the Fennoscandian Border Zone.

## 2.2

### CRUSTAL AND LITHOSPHERIC THICKNESS

The crust of the Baltic Shield shows some pronounced thickness variations (from 55-30km), the thickest crust being located under central western Finland (see Figure 2-2, compiled from Kinck et al, 1991 for south-western Fennoscandia and Meissner et al, 1987 for the remainder of the region). The lithosphere also shows significant thickness variations from less than 70km in southwest Norway to more than 160km around the Gulf of Bothnia (Babuska et al, 1988), see Figure 2-5. The lithosphere has been defined both seismically and from regional heatflow (Pasquale et al, 1991). To the north of Finland very low heat flows imply a lithosphere more than 200 km thick (see also Section 7). The heatflow observations suggest a sharp decrease in the thickness of the lithosphere in passing to the south along the central Swedish

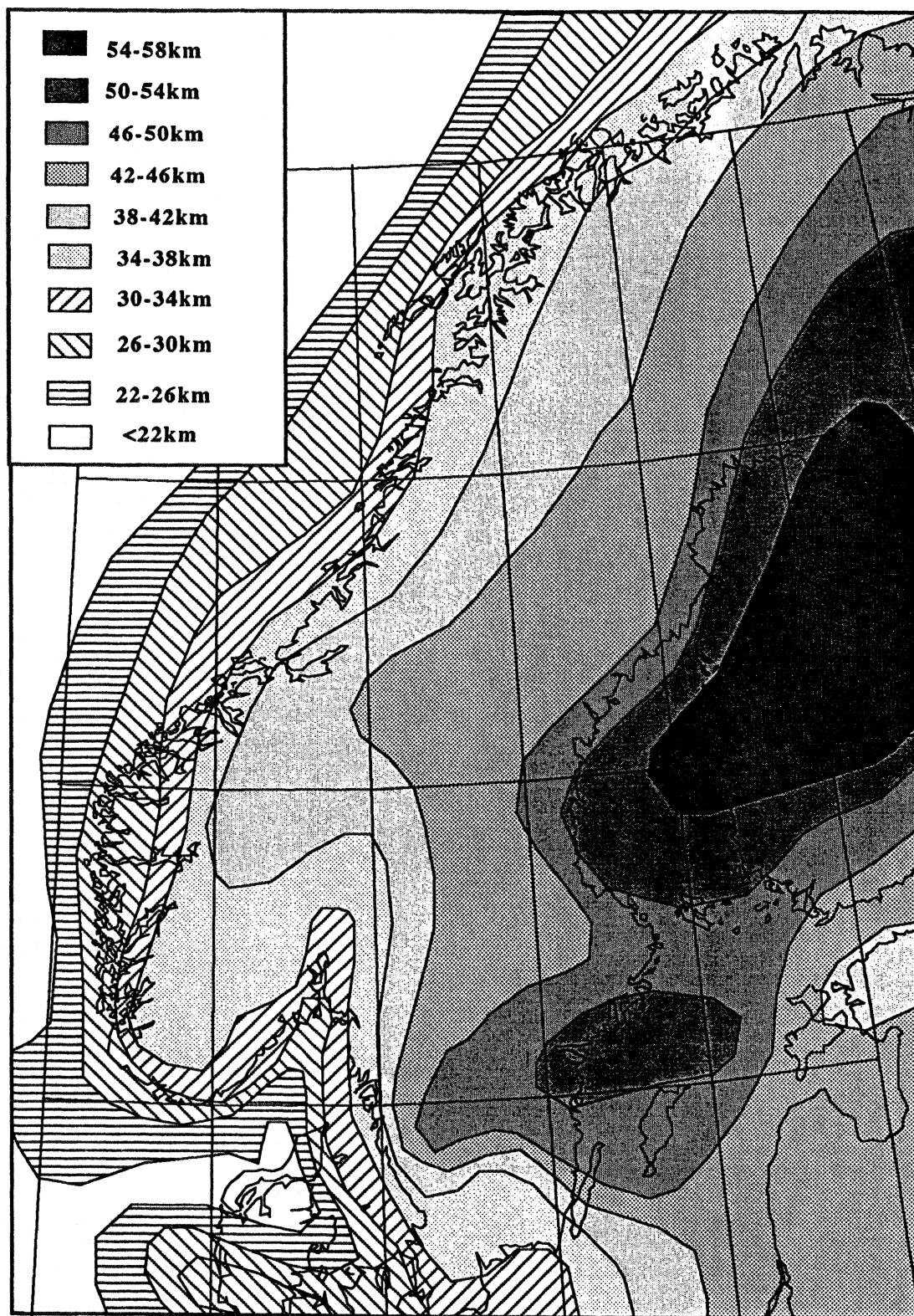


**Figure 2-2: Fennoscandian crustal thickness (compiled from Kinck et al., 1991 & Meissner et al., 1987).**

east coast. The thickest lithosphere and crust are both found in the centre of the shield, and approximately correspond to the more asymmetric distribution of orogenic provinces. There is also a strong relationship between crustal thickness and age: the older crust having the greater thickness (see Kinck et al, 1991) as is typical of other continental shields (Meissner, 1986).

The sub-Moho seismic velocities across the shield indicate low velocity mantle underlying the uplifted mountains of western Norway and northern Norway, consistent with some replacement of the older lithosphere with hotter asthenosphere during the Tertiary opening of the Norwegian Sea (Bannister et al, 1991). The most marked gradient of crustal thickness is found across the Fennoscandian Border Zone, where, in a distance of about 160km, the thickness decreases by 20km (Gregersen et al, 1991). The steepest gradient is found paralleling the NNW-SSE Swedish coast to the south of Lake Vanern where it decreases by 10 km in less than 50km.

### 2.3 MAJOR TECTONIC ZONES IN SWEDEN

The Baltic Shield is crossed by many fault zones formed in the numerous phases of strong crustal deformation that occurred during the consolidation of the shield. The largest of these are the suture zones, faults with many tens of kilometres of displacement that mark the boundaries between crustal units. Some of these sutures have continued to be zones of pronounced crustal weakness repeatedly reactivated; others have become annealed and deformed in later episodes of deformation.

There are two great Sveofennian suture zones in southern Sweden: the Protogine Zone and the Mylonite Zone to the east. The Protogine Zone appears to follow an old pre-1700 Ma suture (Gorbatshev, 1980) and has subsequently acted as a locus of pronounced deformation; to the south it is the frontal edge of the Sveconorwegian province. The Mylonite Zone is also a major composite tectonic fault complex, primarily steeply dipping to the north but passing into a westerly dipping thrust complex to the south.

The southern edge of the shield is demarcated by a major continental suture - the Tornquist or Fennoscandian Border Zone, beyond which lies the thinner and younger middle European crust. In contrast to the Protogine Zone and the Mylonite Zone this border zone has continued to act as a prominent suture zone concentrating many kilometres of displacement through the past few hundred million years.

## 2.4 POST-OROGENIC RIFTING

Following the accretion and consolidation of the shield, the region has maintained a cratonic character. A number of episodes of relatively minor rifting can however be identified within the shield, each of which led to the deposition of an unmetamorphosed sedimentary succession. Around the margins of the shield there are larger sedimentary basins all of which have been intensively studied through seismic reflection surveys, that allow the style and age of different tectonic episodes through the past few hundred million years to be discerned.

### 2.4.1 Late Pre-Cambrian Rifting

The most important phases of rifting occurred in the late Pre-Cambrian (ca. 1000-600 Ma). Up to 1km of Middle and Upper Rhiphaean age sediments are found around the Gulf of Bothnia and Baltic (Floden, 1980 and Wannas, 1989), and some of the bounding faults have displacements of up to 1000m. These include the coastal fault zone to the west of the Gulf of Bothnia (Axberg, 1980) and the Landsort-Kappelshamn line to the north of Gotland (Floden, 1980). Part of a narrow NW-SE rift associated with the Upper Rhiphaean graben passes on land in Finland close to Oulu. In the central Baltic, a series of narrow NNE-SSW trending narrow graben structures, with vertical displacements in excess of 500 m, are of possible Upper Rhiphaean or Vendian age (Ulmishek, 1991) and up to 1km of late Rhiphaean - early Vendian rift subsidence occurred in the Lake Vattern area (Vidal, 1984). Other Rhiphaean - Vendian sedimentary successions are known to underlie the Caledonian deformation front.

## 2.4.2

**Palaeozoic Basins**

In the Baltic Basin the late Pre-Cambrian rift structures had no influence on either sedimentation or tectonics through the Lower Palaeozoic, and thereafter (Ulmishek, 1991). The Lower Palaeozoic succession in the basin probably developed as a result of thermal sag following rifting and a few hundred metres of Early Palaeozoic sediments survive across much of the Baltic and Gulf of Bothnia. The sedimentary sequence is complete from the late Vendian, Early Cambrian, through to the Lower Devonian, reaching thicknesses in excess of 4km in the deepest southern part of the basin. However the Lower Devonian and sometimes the entire Upper Silurian section have been eroded from the crests of a series of E-W and NE-SW trending arches controlled by high angle reverse faults passing in a chain from Latvia to northern Poland. The maximum vertical offset seen on these faults is 300-350 m, although most faults and associated monoclines have amplitudes between 100-150 m.

By analogy with the Baltic, it is probable that the displacement of a complex of NNE-SSW - E-W faults, known to affect the sub-Cambrian peneplain and overlying remnants of Lower Palaeozoic sediments in southern central Sweden (Ahlin, 1982, 1987) and the Gulf of Bothnia, may chiefly be of Caledonian (Mid Devonian) age. These faults have displacements typically of 40-60 m, rising to 200-300 m for the West Bothnian coastal boundary fault north of Gavle. This is the last significant tectonic episode recorded from the Baltic basin. Hercynian (Late Devonian to Carboniferous) sedimentation distributed across the truncated Caledonian sedimentary sequence in the southern and eastern Baltic is almost entirely undeformed.

At the end of the Palaeozoic, the Oslo Graben formed as a result of rifting probably associated with underlying mantle diapirism, as there was significant accompanying volcanic activity. The major graben boundary faults have displacements of 2-3 km, and formed in response to E-W extension, probably on the site of a pre-existing continental fracture zone (Ramberg and Spjeldnaes, 1978). It is possible that some of the faulting seen in and

around the Lake Vanern area also moved at this period.

#### 2.4.3

#### Mesozoic and Tertiary Tectonics

While there is little conclusive evidence for any deformation in the Baltic shield through the Mesozoic this is not the case within and to the south of the Fennoscandian Border Zone. Even within the Mesozoic, horizontal and vertical displacements on faults within the zone can be measured in kilometres (see for example Sivhed, 1991). A major phase of uplift and igneous activity occurred along the Border Zone in the mid-Jurassic (Kimmerian) (Norling, 1984), associated with sinistral transcurrent faulting, to be replaced by dextral transcurrent faulting and further major inversion in the late Cretaceous - early Tertiary (Kumpas, 1984).

The Norwegian continental margin also remained the site of pronounced rifting and extension through the Upper Palaeozoic and Early Mesozoic, creating the Norwegian continental margin basins and the North Sea. The opening of the North Atlantic finally occurred in the early Tertiary. From the Early Cretaceous intermittent phases of transpressional tectonics have prevailed across parts of these sedimentary basins, and dominated the tectonics of the mid- and northern Norway continental margin in the Neogene (see Figure 2-3). The eastern margin of the Tertiary uplifted region of northern Norway is a NNE-SSW trending mountain scarp, that parallels the boundary of the Caledonian mountain front (Strand and Kulling, 1972). The highest summits in this region (see Figure 2-4) are not found in the centre of the dome, as in western Norway but on its eastern limit (in Sweden), suggesting the partial influence of a tectonic origin perhaps related to the compressional reactivation of Caledonian structures. No evidence has however been found to demonstrate a Tertiary phase of reactivation on any of these Caledonian structures.

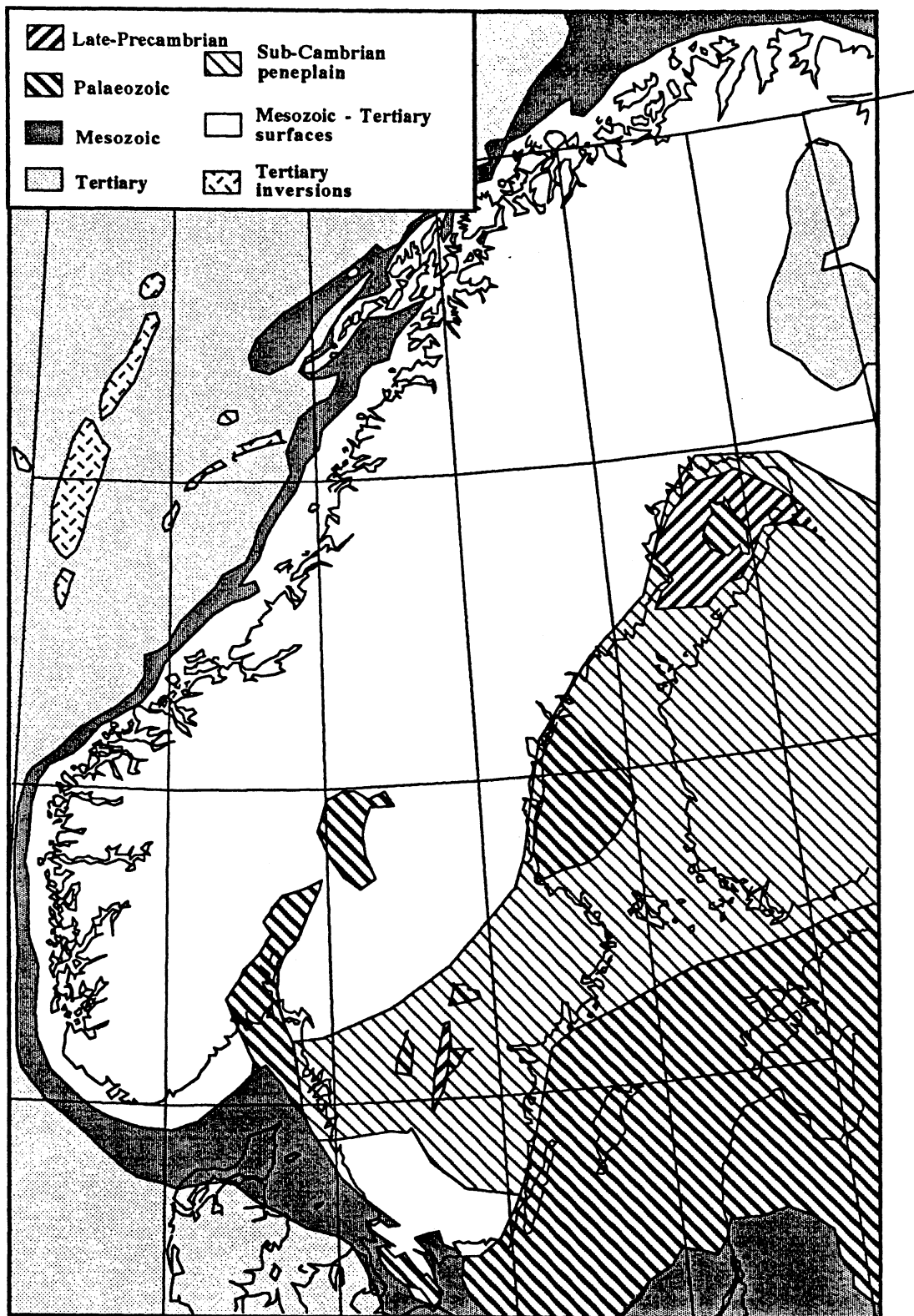


**Figure 2.3: Sedimentary cover and erosion surfaces on and around Fennoscandia.**

#### 2.4.4 Neogene Tectonics

Throughout this period, away from the Fennoscandian Border Zone, Sweden appears to have remained geologically stable, a true continental shield, unaffected by the major phases of extension that dominated the tectonics of northern Europe through much of the Mesozoic. Although the reactivation of some of the pre-existing fault-zones within the shield is not improbable, during the most important tectonic episodes, the movements have always been very minor in comparison with those encountered around the margins of the shield. This is because the surrounding basins provided zones of thinner, hotter (and hence weaker) crust and lithosphere (see Figure 2-5), that have absorbed phases of extension and compression. No evidence is known to substantiate models of significant transcurrent fault movements passing through the shield in the Neogene (as proposed by Talbot and Slunga, 1989), and in respect of the considerable rheological differences between the crust of the shield and its surroundings such models appear highly unlikely.

The latest phase of deformation to affect the shield appears to reflect the passive doming of western Scandinavia, centred over western central Norway, and northern Norway at various periods during the Tertiary, apparently as a result of the easterly streaming of lighter mantle material as identified from tomographic studies of sub-crustal seismic velocities (Bannister et al, 1991). There are no Tertiary sediments known from anywhere in Sweden although scattered deposits of both Palaeogene marine and Neogene freshwater microfossils are regionally distributed in north-eastern Finland (Tynni, 1982), across topography rising to 260 m. These indicate that the influence of mid-Tertiary uplift has extended over to the east of the shield.

#### 2.5

#### **SUMMARY OF PLIO-QUATERNARY TECTONICS**

There are three regions where crustal movement has been seen (generally on hydrocarbon industry seismic reflection profiles) around Scandinavia that could reflect Plio-Quaternary tectonics.



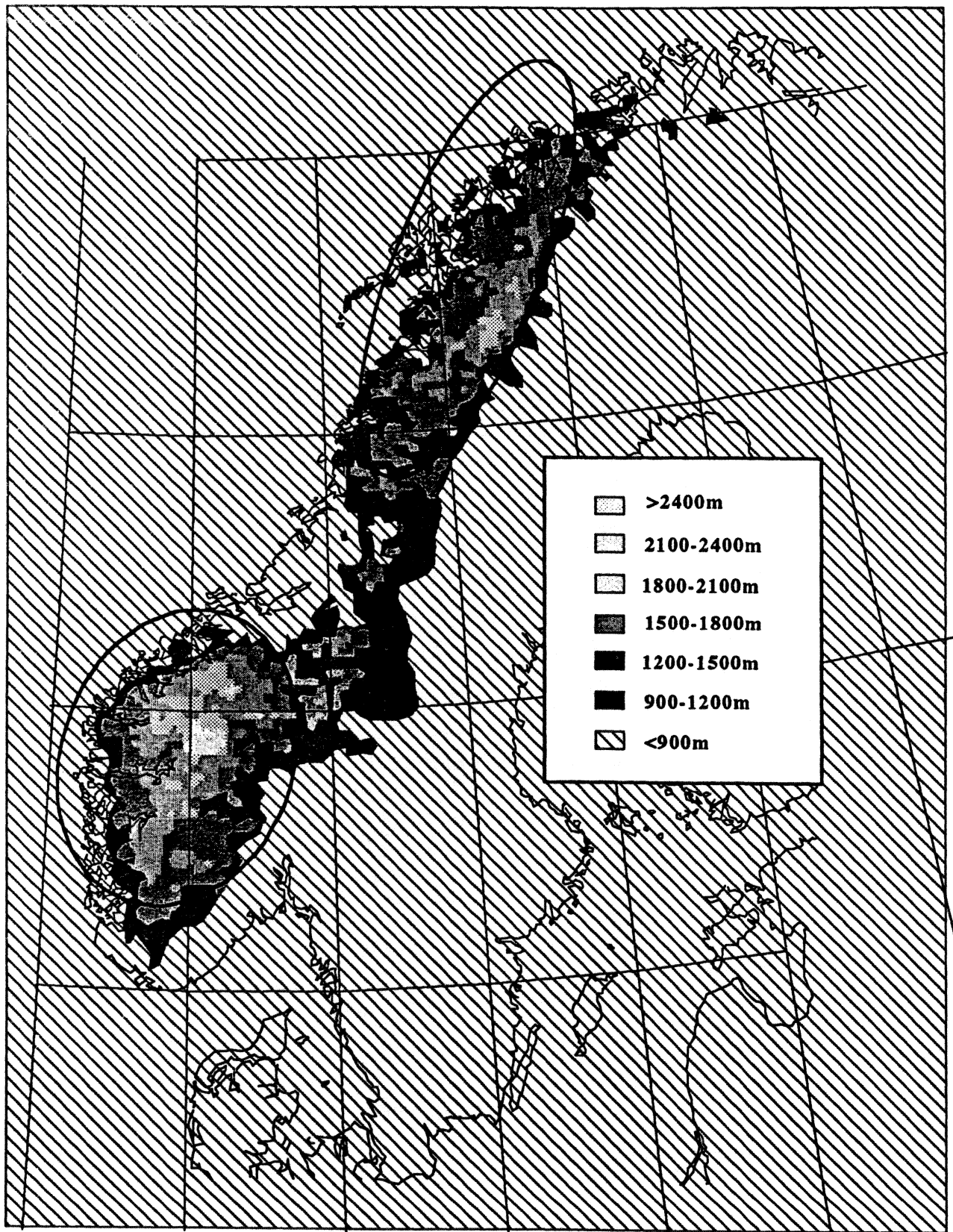


**Figure 2-4: Summit surfaces above 900m in Fennoscandia, contoured over 10km x 10km grid, with centres of Tertiary uplift ringed.**

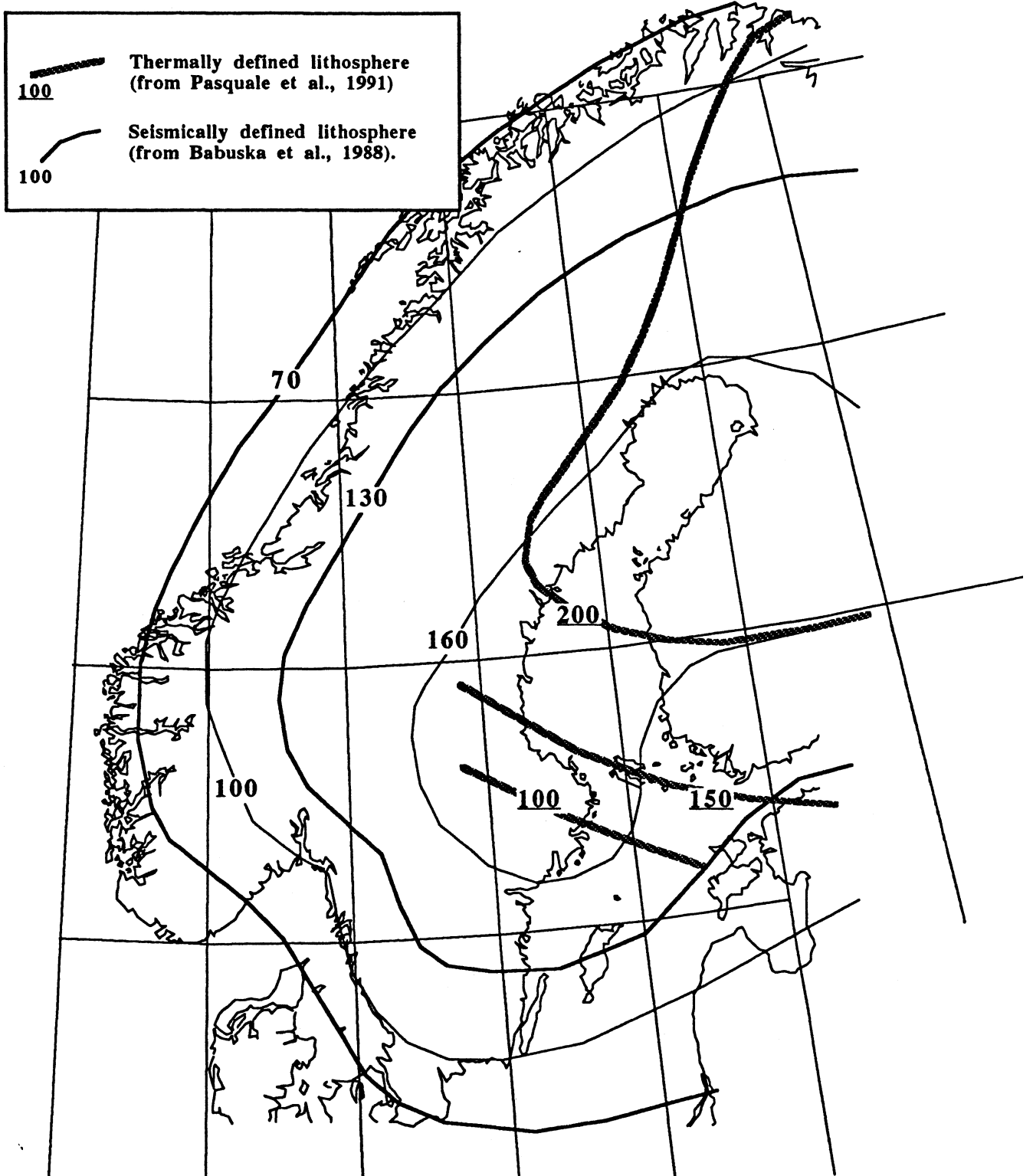


**Figure 2-5 Lithospheric thickness.**

- Extension along the Fennoscandian Border Zone between Denmark and Sweden, as suggested by some neotectonic evidence from this region (see Sections 3.2.1 and 3.2.2, Lykke Andersen, 1987), would correspond with rifting accompanying uplift seen on NW-SE faults of the Lower Rhine Graben. Elsewhere in Scandinavia the absence of any evidence of rifting accompanying late Tertiary uplift is to be predicted with regard to the thickness and temperature regime of the lithosphere (Kusznir and Park, 1987).
- Deformation around the margins of the subsiding More Basin, offshore mid-Norway. The More Basin has undergone very rapid (>1000 m) Upper Pliocene and Quaternary (presumed thermal) subsidence, which may affect marginal deformation.
- Along the mid-Norway continental margin compressional deformation associated with large anticlinal inversion structures can be seen to have ended in the Early Pliocene. However along the Lofoten continental margin it is not possible to date the end of this episode and there is some indication (from continuing mud diapirism) that uplift and associated compressional deformation may have continued into the Quaternary (see Mutter, 1984).

### NEOTECTONICS

Neotectonics is the study of recent geological deformation. The time-scale over which neotectonics is held to persist defies universal definition: most usefully it can be considered to cover the locally calibrated time period over which observations of crustal deformation are directly comparable to those prevailing today. The subject of Neotectonics is also commonly considered to encompass land-level changes and palaeoseismicity, as well as surface faulting. The first of these is ubiquitous throughout Scandinavia and is considered under a separate discussion of land-level changes (see Section 4). In this report palaeoseismicity is discussed under Seismology (see Section 6). The account that follows concentrates solely on the phenomenon of surface faulting.

#### 3.1

#### **MAKING A SCIENCE OF NEOTECTONICS**

Neotectonic studies in slowly deforming continental regions are problematic. Young sediments are often poorly preserved, and those of continental origin are very difficult to date. Because any account of neotectonics excites interest and controversy it becomes relatively easy to publish scientific papers claiming neotectonics. Many of these claims are incomplete and inferential, not properly weighing alternative, less exciting, explanations for the phenomena. Once published it is often extremely difficult to refute neotectonic claims, in particular when the required exposures are inaccessible. In Scandinavia there are around twenty primary papers which claim to describe neotectonic phenomena.

In attempting to assess these claims it is important to avoid a simple argument of certainty, fought in terms of right and wrong. In many cases the available evidence (at least what has been published) is insufficient to settle the dispute one way or the other. The most useful outcome of any review would be to establish what additional observations would need to be collected to clarify whether a fault had, or had not, suffered a recent surface displacement. However as many authors have

been content to allow their observations to become a published inference, without undertaking the investigations that would be necessary to resolve interpretational uncertainties it becomes necessary to establish some system of grading by which these claims can be evaluated. To achieve this it is first necessary to consider the most important characteristics of surface fault ruptures.

### 3.1.1 Earthquake Geology

Scientific studies of faulting and surface deformation, collected in the immediate aftermath of around one hundred major earthquakes over the past century, provide the most useful resource for evaluating the range of neotectonic phenomena. These studies have shown that the most important characteristics of surface fault ruptures are their length, displacement and the consistent overall sense of movement (viz. Bonilla et al, 1984).

### 3.1.2 Demonstrating Offset

Most neotectonic claims are founded on the apparent displacement of some surface or material formerly considered to be unbroken. Most disputes centre around this problem. For example, elevated river terraces, and lake or sea shorelines, are difficult to characterise except for their elevation above a river or the sea. The pattern of alluvial or marine erosion can easily remove certain terraces for different stretches of a valley or shoreline. The survival of different sections of terraces could resemble a displacement. Clearly this ambiguity could be resolved, where a terrace/shoreline is uniquely identified or dated, where more than one terrace/shoreline shows an identical apparent offset, or where the fault presumed to offset the terraces/shorelines can be exposed.

As another example, a number of authors have employed observations of horizontally offset stream channels as a demonstration of lateral neotectonic displacement along a fault, finding analogies with the well-documented examples along the central San Andreas Fault (see Davenport et al, 1989). However

in older rocks, streams commonly follow some pre-existing zone of weakness, such as a fracture. Hence the apparent offset may not be of the stream but of the fracture, that could have originated, or even have been offset, hundreds of millions of years earlier.

Such situations exist in many other potential neotectonic environments. For example a step in bedrock at a fault could simply be an erosional cliff, formed where different rocks are juxtaposed. The resolution of a neotectonic, rather than an erosional interpretation, depends on dating the rock surface and the material overlying it, on either side of the fault, and showing that the offset postdates the overlying material.

### 3.1.3 Superficial Faulting

A further problem concerns differentiating the outcrop of a seismogenic fault-break from faulting of a superficial origin. Normal faulting of a superficial origin forms under the influence of gravity through mass movement into some space, that could be the base of a topographic slope, a natural or artificial cavern or the void left by the melting of ice or the dissolution of salt. Rarely horizontal driving forces acting at the surface may produce shallow reverse faulting as at the toe of a landslide or in the advance of an icesheet bulldozing into a pile of unconsolidated sediments.

The diagnostics of superficial faulting are: the shallow base of deformation; the curved outline of fault traces; their short length, and the identification of a local superficial cause. Some superficial disturbances do however develop in conjunction with the surface trace of major fault scarps and at such time a distinction between the two types of movement may become more difficult.

### 3.1.4 Neotectonic Diagnostics

In order to attempt to discriminate neotectonic surface faulting from other unrelated phenomena the following criteria can be applied.

- (a) The surface or material that appears to be offset has to have originally formed a continuous unbroken unit. Can the surface or material be dated? Is it the same age?
- (b) Can the apparent evidence of an offset be shown to relate directly to a fault?
- (c) Is the ratio of displacement to overall length of the feature less than 1/1000? For most faults this ratio, a function of the strength of the rock prior to fault rupture, is between 1/10,000 and 1/100,000 (Scholz, 1990).
- (d) Is the displacement reasonably consistent along the length of the feature?
- (e) Can the movement be shown to be synchronous along its length?

#### 3.1.5 Grading Neotectonic Claims

In the review that follows, claims of neotectonic surface fault rupture have been judged as falling into five grades:

- (A) Almost certainly neotectonics
- (B) Probably neotectonics
- (C) Possibly neotectonics
- (D) Probably not neotectonics
- (E) Very unlikely to be neotectonics.

These assessments, based on the published information, are of course a matter of judgement, following the set of principles for identifying neotectonic evidence of surface fault rupture, as set out in Section 3.1.4. These judgments may of course change in the future as results of additional investigations along these features, in particular trenches exposing the presumed fault itself, become available. Such results should resolve a fault's status, having the potential to prove one way or the other, whether the feature is, or is not, a product of surface fault displacement.

### 3.2 SCANDINAVIAN NEOTECTONICS

The principal claims of neotectonic surface faulting in Scandinavia, identified on Figure 3-1, have been assessed in Table 3-1 according to the principles established in Section 3.1 above. A number of other claims also exist for which the degree of documentation is generally so poor as to prevent any useful discussion. By far the most important of the neotectonic observations relating to surface faulting in Scandinavia are those of the Lapland post-glacial fault province.

### 3.3 THE LAPLAND POST-GLACIAL FAULT PROVINCE

Faults of the Lapland post-glacial fault province are found in a diamond shaped region about 300 km E-W and 500 km N-S, in northern Sweden, northern Finland and Finnmark, Norway. The province comprises a series of reverse fault scarps, the longest of them the Parvie Fault, that stretches almost unbroken for 165km (see Figure 3-3). The faults in Sweden were first announced by Lundquist and Lagerbäck (1976) and Lagerbäck (1979), those in Finland by Kujansuu (1964), and in Norway by Olesen (1988). Further detailed descriptions of the Swedish faults can be found in Lagerbäck and Witschard (1983). From their morphology alone many of the Lapland late-glacial faults can be clearly identified as the surface scarps of major fault ruptures. In particular this is demonstrated by their continuity and consistency of both displacement and trend. Further evidence obtained in trenching the Lansjarv Fault scarp in Sweden (Lagerbäck, 1990), has confirmed an origin in a sudden episode of fault displacement.

#### 3.3.1 Orientation

All but two of the faults (the easternmost faults in Finland) trend close to SSW-NNE, although there are some variations in the line of a number of the faults, apparently reflecting the transfer of displacement onto available faults. All major faults involve the uplift of the eastern block relative to the west. The only exceptions to this are shorter faults that lie a few kilometres to the



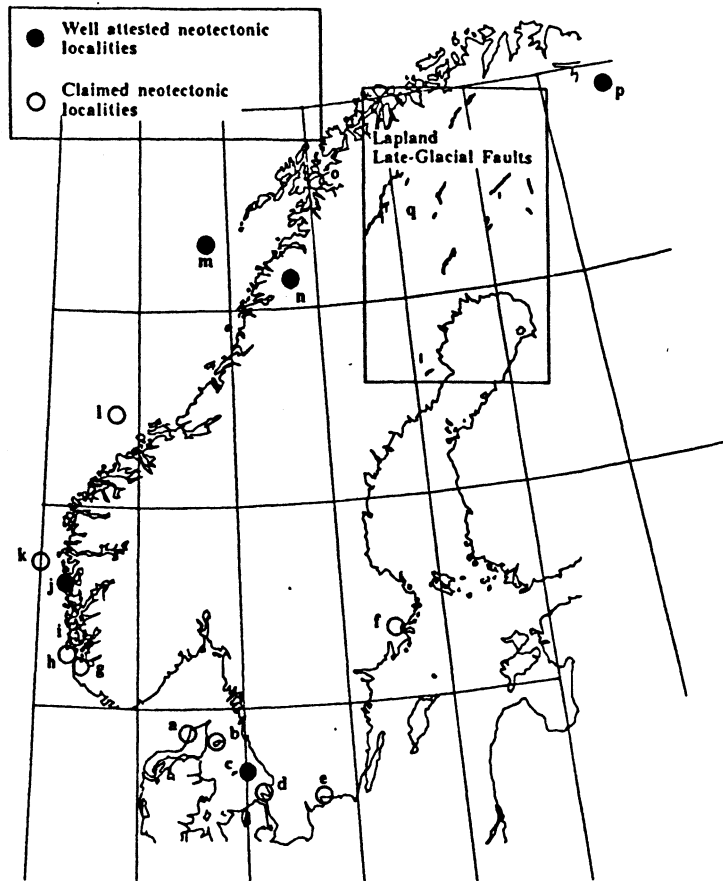


Figure 3-1: Key-map for reports of Fennoscandian neotectonics.

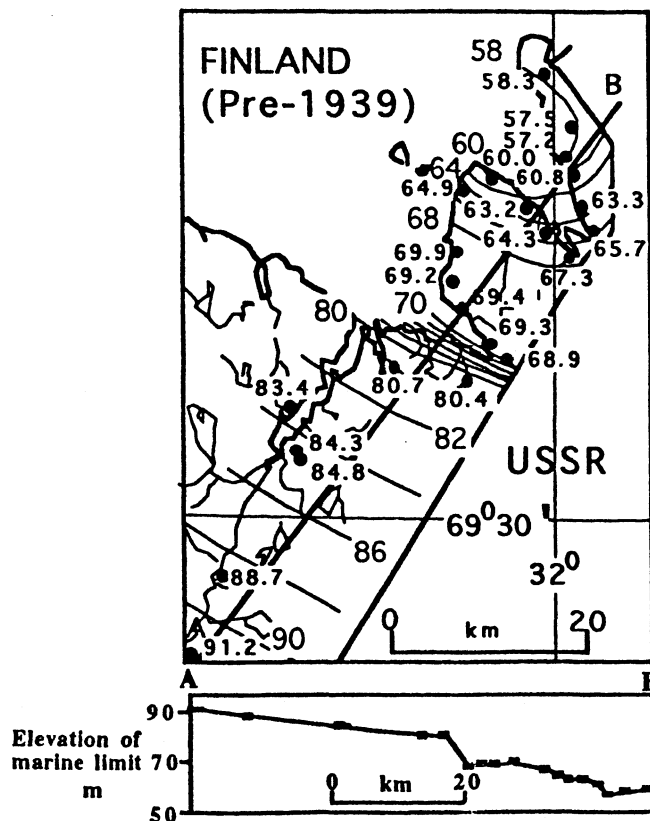


Figure 3-2: Observation points and contours of the marine limit around the Fiskarhalvon Peninsula, Russian Kola (redrawn from Tanner, 1930).

east, and hence within the hangingwall, of the major faults. Projecting these faults to depth shows them to be antithetic faults, emerging from the master faults within the crust (Muir Wood, 1989a). The two faults on the north-east edge of the fault province in Finland trend NW-SE to N-S, and involve the uplift of the south-western block.

### 3.3.2 Fault Groups

The faults can be considered to lie in three groups: (i) a lowland group that is found close to the 200m contour, from close to the coast west of Skelleftea in the south, and which includes most of those in Finland to the north. The lowland faults tend to be shorter and more irregular in geometry than the higher elevation faults. The highland group of faults (ii) comprises the two longest faults: the Parvie Fault and the 80 km Stuoraggura Fault which are typically located at around 500 m. Between these two groups there is a third central group (iii) of two faults (the Merasjarvi and Lainio Suijavaara) which appear to have the largest vertical displacements.

### 3.3.3 Age

The faults all demonstrably formed in association with deglaciation. The Lansjarv Fault formed at the time of the highest post-glacial sea-level and hence within a few years, or at most decades, of being uncovered by the ice-sheet (Lagerbäck, 1988a). Stagnant ice still lay in hollows to the north of the fault. The Parvie Fault developed while ice still covered some part of the fault's trace (Lagerbäck and Witschard, 1983). The northern part of the Lainio Suijavaara fault also may have moved beneath the ice-sheet, while further to the south, the Merasjarvi Fault postdates the ice-melting (Lagerbäck and Witschard, 1983). As the ice-sheet retreated into the upland areas away from the Gulf of Bothnia it is certain that the lowland faults moved first. However the exact sequence of the remaining faults is not known. The final deglaciation of this area may have taken a few hundred years, and involved a series of isolated stagnant ice-masses.

	LOCATION	OBSERVATION	REFERENCE	COMMENT	GRADE
a	Lonstrup Klint, Vendsyssel, north-west Jutland	Southerly downthrow of fault exposed cutting glacial and late glacial sediments intensely deformed by glaciotectionic activity.	Lykke Andersen (1981)	Such extension could simply reflect slumping associated with the removal of the advancing ice, or with the formation of a kettle-hole above melting stagnant ice. However, some support for a tectonic explanation is given by the observation that the latest normal fault is approximately in line with a major basement fault, known to have had important extensional and reverse activity through the Mesozoic and early Tertiary.	C
b	Laeso Island, Kattegat.	The island comprises an almost horizontal interglacial-late-glacial wave-cut platform, comprising differential dips of shore terraces. Along the island's southwestern margin a 4m jump in the platform's surface forms a prominent sea-cliff and appeared related to one of the faults of the Fennoscandian Border Zone.	Hansen, (1980).	The location gives credence to such a proposal, but no account has been published of the fault, or of exposures of offset sediments surfaces etc., by which this inference can be properly judged.	C
c	Kattegat.	Narrow NE-SW trending Quaternary filled basins in the Kattegat, appear to be defined by faults of the Fennoscandian border zone. The base of the Quaternary includes rocks of Cretaceous, Jurassic and pre-Cambrian age.	Lykke Andersen (1987)	The pattern of depressions does not accord with a simple erosional origin and a tectonic explanation seems probable.	B
d	Fennoscandian Border Zone. Southern Sweden.	Faults bounding Mt Kullen, were indicated "according to studies" as younger than Late Weichselian. No data were provided in support of this conclusion. "Stratigraphical evidence" was also claimed for a rather large Late Weichselian vertical displacement of the horst Romekrasen in southwest Skane.	Lagerlund (1977)	No evidence was provided in support of these conclusions. The relief of this region is very striking, but also the difference in erosibility of the pre-Cambrian and Mesozoic makes for marked contrasts, likely to promote strong topography.	D
e	Morrumsan river valley, Blekinge province, south east Sweden.	A difference in altitude of approximately 5m between the levels of the highest postglacial shoreline was claimed across a NNW-SSE trending gneiss - granitoid bedrock boundary, but not proved, to be a fault.	Bjorckman and Trøgardh (1982)	The range of heights of the washed/unwashed till boundary on the granite was found to vary by more than 6m. This work followed work by Bjorck (1979) that appeared to show a very sudden change in shoreline elevation now explained as a result of a sudden emptying of the ice-dammed Baltic Lake at that time.	D
f	Stockholm.	Seven sets of rock scarps found in the Stockholm region that were claimed to be fresh late- or post-glacial fault scarps. The length of the features ranged from 50-250m, the displacements from 1-3m.	Mörner et al (1989)	These scarps are irregular in orientation, and often composed of a series of individual structures. None have been shown to correspond with any fault structure. Displacement to length ratios are about three orders of magnitude higher than genuine fault scarps. All the published details of these rock scarps suggest a superficial erosional origin.	E

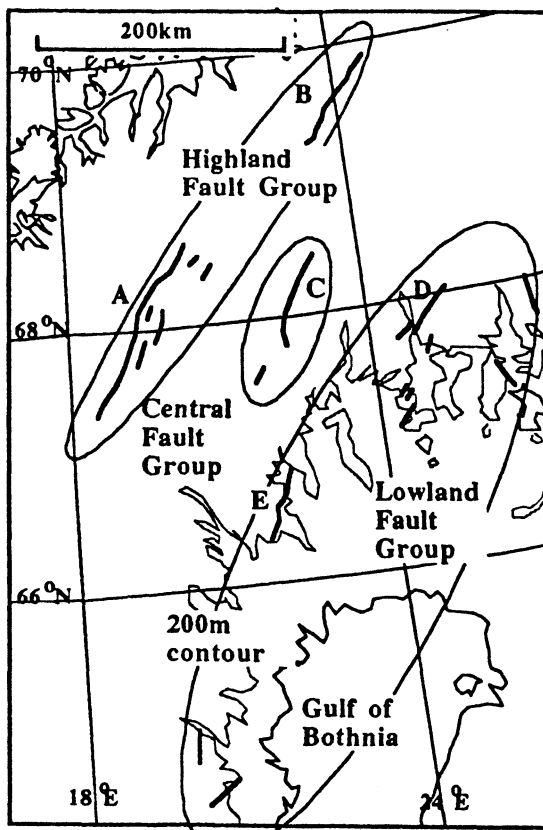
Table 3-1: Assessment of Claims of Neotectonic Surface Faulting in Fennoscandia (Sheet 1 of 3)

	LOCATION	OBSERVATION	REFERENCE	COMMENT	GRADE
g	Sandnes, SW Norway.	At an abandoned clay pit at about 10-30m asl at Gann, on the western side of Sandnes Harbour, subsurface boreholes revealed a NE-SW trending boundary, steeper than about 60 degrees, between mostly marine clay to the west and sand to the east. The clay is overlain by Weichselian till.	(Feyling-Hansen, 1966)	No attempt was made to trench the contact to establish whether it reflects an erosional or faulted boundary. If faulted it could still have a superficial origin.	D
h	Karmsundet Basin, 20km NW of Stavanger.	The Karmsundet Basin is a small halfgraben bounded to the east by the major Kvitsoy Fault and filled with sediments of assumed Jurassic age. Overlying Quaternary sediments show plentiful evidence of instability including slump scars, rotated sediment units and superficial fault structures.	Boe et al., (1992)	The majority of these superficial features do not correspond with underlying faults and hence cannot be considered as direct evidence of outcropping fault-rupture. Deformation accompanying glacial readvance cannot be discounted.	C
i	Western end of Yrkjefjorden, SW Norway.	In a study of the marine isolation of eight basins the complex pattern of transgression, associated with the Younger Dryas, appeared consistent for all but two of the basins. The most anomalous basin, located about 2km to the south of the main sets, appeared to have an elevation about 13m higher than was predicted for the age of marine isolation. This basin lay between two NNE-SSW, NE-SW faults, claimed to have caused the anomaly.	Anurdsen (1980)	No further work was undertaken employing other suitable lake basins in this area, and no attempt has been made to study evidence for postglacial displacement along the faults themselves. From a very limited set of dates and cores the fault explanation for the apparent variation in isolation levels, is not unique.	C
j	Hjeltefjord, 30km NW of Bergen.	At the northern end of Hjeltefjorden a boomer seismic survey was undertaken in the mid 80's for a potential tunnel crossing. Several E-W lines between Seloy and Uttoska, appeared to show a consistent offset of the superficial sediments in the floor of the fjord, along a MNW-SSE trending dislocation, involving down to the west displacement of 5-10m.	Unpublished commercial report from NGI/MORSAR.	The observation appears relatively convincing but awaits publication and further scientific scrutiny.	B
k	Oygarden Fault (north).	The northern half of the N-S trending Oygarden Fault (between 61° and 61°45'N) runs parallel with the coast of western Norway to the north of Bergen and marks a very significant change in the depth of the bedrock surface beneath the thick Quaternary sedimentary cover. The major scarp that has developed along the fault has some of the appearance of a fault-scarp (with a vertical offset of up to 150m), and although offsets have not been observed in the overlying sedimentary section itself, sediments onlap the scarp, with some suggestion of dips steepening towards the fault.	Rokoengen and Ronningsland (1983), Muir Wood and Forsberg, (1987)	The fault now bounds crystalline basement in the east from relatively soft Cretaceous sediments in the west. The key to the origin of this scarp remains the age of the basal sequence above the unconformity. If, as claimed, this comprises marine sands of probable Pliocene age then a faulted origin for the scarp is preferred. However, if the basal sediments formed immediately following intense glacial scouring then an erosional origin is indicated; as is strongly suggested by the southern section of the Oygarden Fault, which has no scarp where similar lithologies of Cretaceous and Jurassic sediments are juxtaposed.	D

Table 3-1: Assessment of Claims of Neotectonic Surface Faulting in Fennoscandia (Sheet 2 of 3)

	LOCATION	OBSERVATION	REFERENCE	COMMENT	GRADE
l	Southern end of the Kristiansund - Bodo Fault Zone, about 100km to the west of Hitteren island.	On a NE-SW regional seismic reflection profile a faulted offset of Tertiary reflectors appears to pass up through the youngest base Quaternary (?) reflector. The fault involves downward displacement to the west and the reflector offset is several tens of metres. The underlying fault appears to be near vertical in dip and probably trends approximately N-S.	Muir Wood and Forsberg (1987)	The displacement does not affect the sea-bed, and the quality of the regional seismic line on which the offset is observed makes it impossible to observe any detailed structure in the uppermost part of the sedimentary section. Quaternary displacements have not been observed further to the north along the Kristiansund-Bodo Fault Zone.	C
m	Rost Fault, NW of the island of Rost.	About 1.2km beyond the steep boundary separating the crystalline basement from deformed sedimentary sequences, the seafloor shows a marked ca. 10m down to the west displacement along what appears to be a significant fault structure as observed on a shallow seismic reflection section.	Rokoengen and Saettem (1983)	On the original seismic lines with their considerable vertical to horizontal exaggeration, true scarp dip could not be resolved. The scarp appears to be related to the north-east flank of a large anticlinal structure, probably related to the mid-Tertiary compressional inversion of the continental margin.	B
n	The mountain ridge of Gratahaugen, Kvass Haugen and Monsfjellet between Beiardalen and Gratadalen, about 50km to the south of Bodo.	A 2km long series of deep en echelon fissures, trend NNW-SSE and dip steeply to the west. The displacement along them appears to reflect the upward and outward extensional movement by about 5m of the western side of the ridge.	Johnsen (1981)	The surface traces are most readily explained as the head of a very large rockslide along the lithological boundary of the limestones that follows the mountain ridge.	A but probably superficial
o	Tjeldsundet, Ofoten, South Troms.	An offset of about 2m (down to the west) was identified on the interpolated elevation of the marine limit, although lower shorelines appeared to be unbroken.	Gronlie (1922)	No attempt appears to have been made to follow up this claim, or identify where the apparent displacement was localised. The similarity with the observations at Fiskarhalvon is particularly interesting.	C
p	Fiskarhalvon Peninsula, Russia (part of Finland pre-War)	The elevation of the postglacial marine limit through northern Finland shows a gradual decline towards the north-east, but is interrupted by a sudden step down by about 10m onto the Fiskarhalvon Peninsula (see Figure 3-2). On the peninsula itself the marine limit is relatively irregular appearing to form an anticline-syncline pair. Tanner was unable to follow the form of these level changes on the eastern side of the peninsula into Russia.	Tanner (1930)	The step in the level of the marine limit, is the sharpest change of this kind noted anywhere in Scandinavia, and is very suggestive of faulting at some time during deglaciation.	B
q	Lapland post glacial faults.	Major fault-scarps traceable for long distances, cutting glaciated features.	Lagerbäck (1979)	See Section 3.3	A

Table 3-1: Assessment of Claims of Neotectonic Surface Faulting in Fennoscandia (Sheet 3 of 3)



**Principal Faults**

Name	Length	Max. Displacement
A - Parvie Fault	165km	13m
B - Stuoragurra Fault	80km	7m
C - Lainio - Suljavaara Fault	55km	30m
D - Suasselka Fault	48km	5m
E - Lansjarv	50km	22m

Figure 3-3: The Lapland post-glacial fault province.

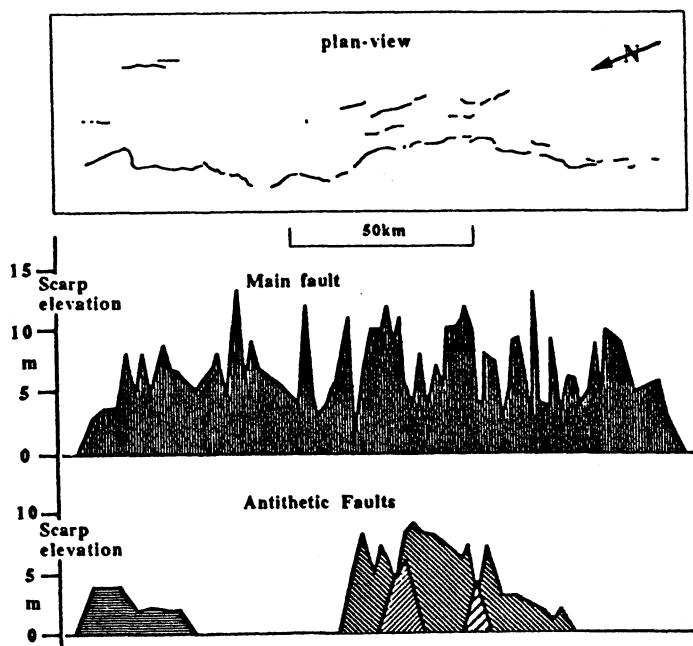


Figure 3.4: Displacement along the Parvie Fault and related structures.

### 3.3.4 Fault Reactivation

Wherever observed in detail, both in outcrop and from geophysical investigations, the line of surface displacement appears to follow pre-existing fault-zones (Paananen, 1987; Vuorela et al, 1987; Kuivamaki et al, 1988; Kukkonen and Kuivamaki, 1986; Lagerbäck and Witschard, 1983; Lagerbäck, 1988a & Olesen et al, 1991). However there is a great range in the character of these faults: from major long-lived continental fracture zones, as followed by the Stuuragurra Fault in Finnmark, to relatively minor faults, as observed on trenches on sections of the Lansjarv Fault, along which the displacement has clearly been expedient in following available fractures, tracking a range of fault orientations.

### 3.3.5 Fault Families

- (i) *Parvie Fault.* A series of shorter faults run parallel with the main Parvie Fault, located within 15km to the east in the hangingwall of the fault. These faults are clearly geometrically inter-related, forming a family of parallel structures (see Figure 3-4). Two alternative sub-surface geometries of these faults have been proposed (see Figure 3-5). Models that demand a steepening of dip with depth (see for example Talbot, 1986) would generate antithetic normal faults (as have been observed in a number of recent reverse fault earthquakes, most notably that of El Asnam, Algeria, M7.2, in 1980: Yielding et al, 1981). In contrast a shallowing of dip with depth (as proposed by Muir Wood, 1989) allows a large horizontal component at depth to pass into a smaller horizontal component distributed over a set of synthetic and antithetic reverse faults close to the surface. All the antithetic faults of the Parvie Fault family appear to have a reverse displacement, hence lending support to the second model. An analogous fault geometry was observed in the 1896 M7+ North Honshu reverse fault earthquake, Japan (see Matsuda et al, 1980; and Figure 3-8).

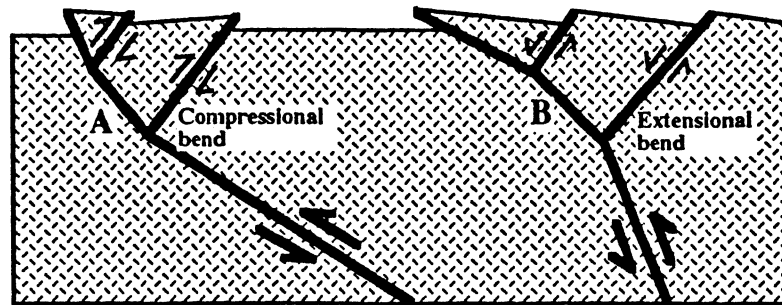
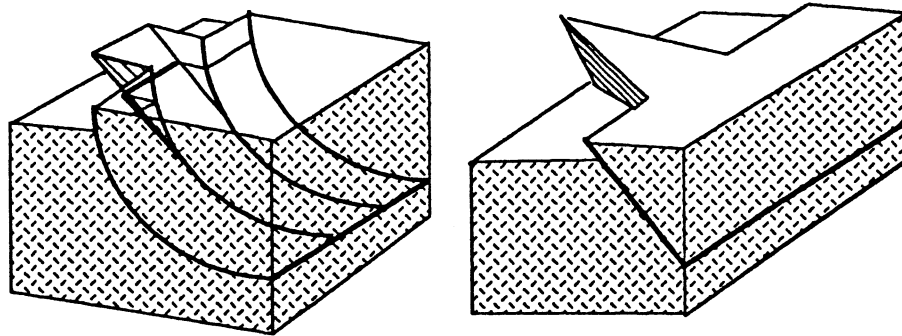


**Figure 3-5: Alternative subsurface geometries of the Parvie Fault family: A) Fault shallowing dip with depth, and B) fault steepening with depth.**



**Model 1: Rotation on a listric fault trace.**

**Model 2: Wedging between two high angle converging side-wall faults.**

**Figure 3-6: Alternative models for the amplification of vertical displacement on a frontal thrust**



- (ii) *Lansjarv Fault.* Short sections of antithetic faults are also observed in the hangingwall of a number of other faults in the province. Along the Lansjarv Fault the Molberget trench section is remarkable for showing that the vertical component of fault displacement emerges along a vertical fault (Lagerbäck, 1990). On this segment of the fault the horizontal component of crustal shortening appears to emerge at the surface on a hangingwall backthrust that outcrops 2-3 km to the east. Again this demands a shallowing of fault dip with depth.
- (iii) *Stuorogarra Fault.* The southern end of the Stuorogarra Fault comprises a pair of parallel faults both dipping to the east, separated by 2-3km. From field inspection rock outcrop is found only along the eastern fault of the pair, suggesting that this has the steeper dip, and that these faults meet at depth. Multiple synthetic (parallel dipping) faults have been seen forming in a number of recent reverse fault earthquakes, most notably the M7.8 event at Tabas, Iran in 1978 (Berberian, 1979).

### 3.3.6 Frontal Thrusts

Two of the faults, those of the Lansjarv and Lainio-Suijavaara, have frontal thrusts located 1-3 km in advance of the main fault trace, with vertical displacements significantly higher than those found elsewhere along the fault. Such amplification has not been observed in other well documented cases of recent surface reverse faulting.

There are two simple geometrical explanations for such amplification (see Figure 3-6). In the first there has been wedging whereby the reverse displacement has become channelled along two converging side-wall faults. This appears to be the cause of the amplification of displacement along the Ristrask salient of the Lansjarv Fault, where the highest displacement is encountered at the tip of the salient.

A second explanation, in which the frontal thrust has become rotated along a circular fault plane, was proposed by Muir Wood (1989) and may be the cause of the amplification on the Lainio Suijavaara Fault. A major spring emerges from beneath the frontal thrust of this fault consistent with the existence of a void-space within the frontal thrust, as required by this model.

### 3.3.7 Analogies to Other Reverse Fault Scarps

In Figure 3-7 the outcrop trace of a number of the PGFs is shown alongside the surface scarps of a number of recent continental reverse fault earthquakes: 1896 Rikuu northern Honshu, Japan M7+ (Matsuda et al, 1980); 1969 Meckering, Australia M6.8; 1979 Cadoux, Australia M6.0; 1988 Tennant Creek M6.8 (Denham, 1988) and 1989 Ungava, Canada M6.3 (Adams et al, 1991). The events in Canada and Australia are both closely comparable in terms of the regional cratonic environment to the crust of northern Fennoscandia. However it will be seen that while the Lansjarv Fault is not dissimilar in outline to the longest Australian fault scarps, the Parvie Fault is three to four times the length of any of these recent intra-continental reverse fault scarps.

The displacement to length ratios of the Lapland post-glacial faults show some significant variation across the province. A plot of  $\log d$  vs  $\log L$  (see Figure 3-8) shows values for the Highland faults that are comparable to other reverse fault earthquakes. However the displacement to length ratios of some of the other faults of the Lowland and Central fault groups are consistently higher than observed in recent earthquakes.

There are a number of possible explanations for these anomalous values:

- The length of the faults mapped from their surface traces, underestimates the true length of the faults at depth.

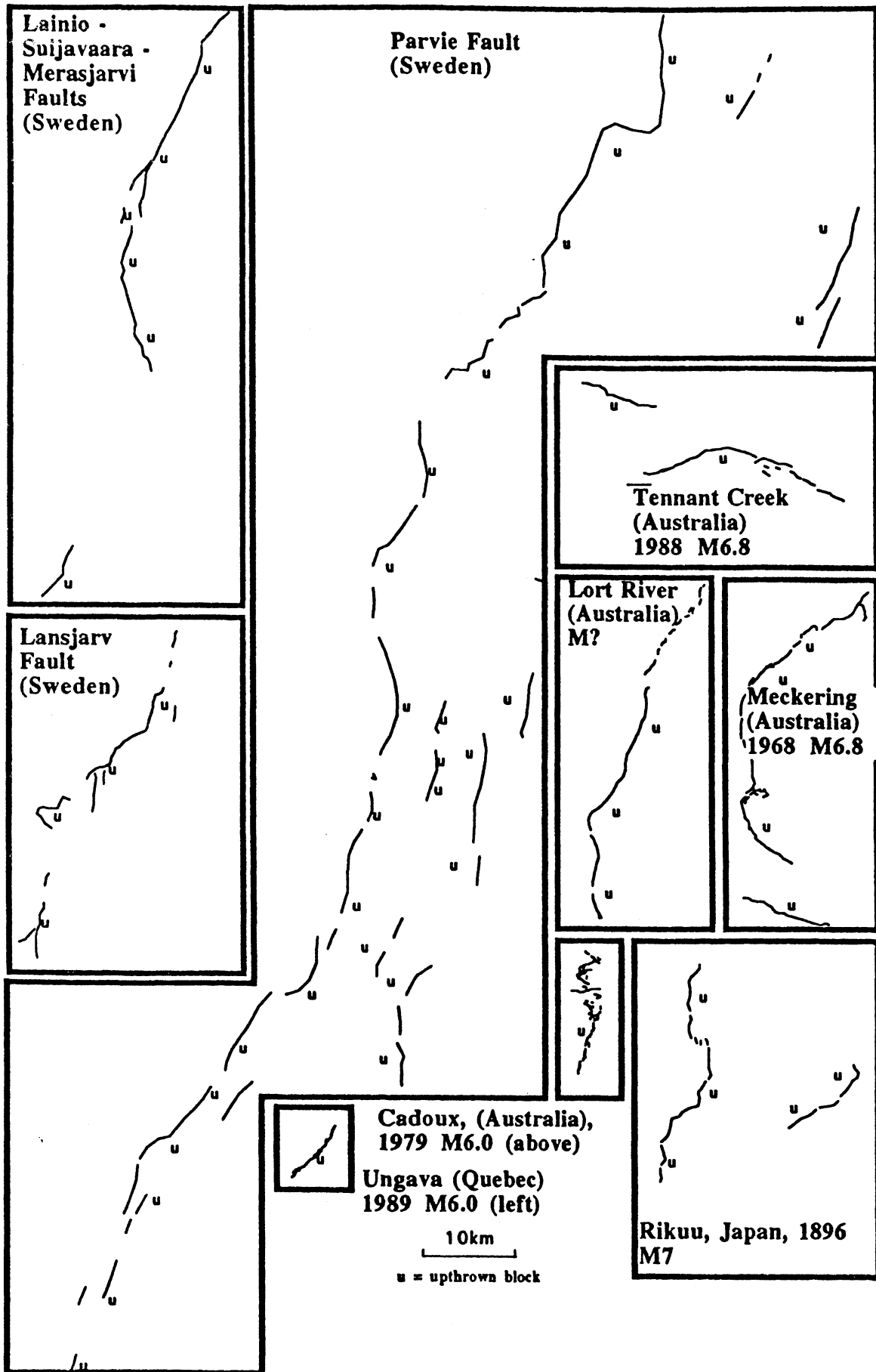


**Figure 3-7: Comparison of the surface traces of the Lapland post-glacial faults with recent reverse fault scarps.**

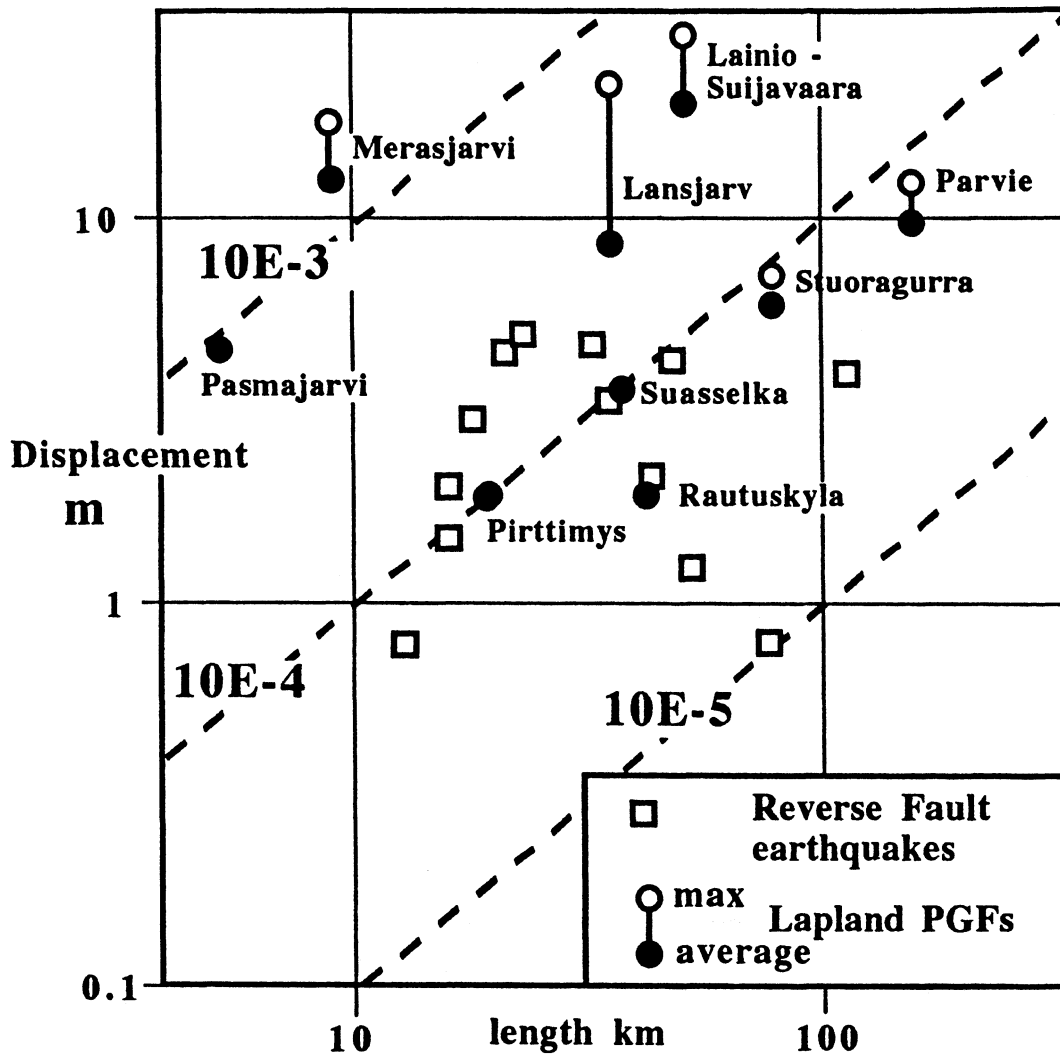


Figure 3-8: Log. fault length vs Log. displacement for Lapland post-glacial faults and other recent reverse fault scarps.

- Those faults with high displacement to length ratios have suffered more than one displacement.
- The faults ruptured to deeper levels than are typical of continental earthquakes, and hence the length of the fault does not possess the same relationship to fault area as is typical of most high angle continental fault ruptures.
- The crust in the vicinity of these faults was particularly strong and required higher levels of angular strain before rupturing than are typical. This could be because the crust is unusually cold and strong in the region of these faults (in comparison with areas of active tectonics). It might imply that the main crustal fault that broke, or at least part of the fault, was new, and simply followed pre-existing faults of other orientations in passing towards the surface.

#### 3.3.8 Fault Spacing

The separation between one major active crustal fault and another is an important indicator of the rheological behaviour of the seismogenic, or brittle, crust. In most regions of active continental tectonics, as for example in the Utah, Montana, Idaho region of western North America (see for example Eddington et al, 1987) this separation is typically 15-30 km and reflects the volume of crust within which strain can be relieved by a single central fault. This in turn is determined by fault dip and fault depth. Across the centre of the PGF province this spacing is about 80km, lending further support to a continuation of these faults to lower, and even sub-crustal, depths.

#### 3.3.9 Accompanying Earthquakes

The seismic moment of an earthquake is defined (from Kasahara, 1981) as:

$$M_0 = \mu AU \quad (3-1)$$

The rigidity modulus  $\mu$  is taken as 30 GPa, A is the fault area and U the average displacement. The displacement and length of the post-glacial faults can be directly measured. That of the Lansjarv Fault is taken as an average of 8 m displacement on a 50 km long fault; the Parvie Fault is assigned an average displacement of 10 m along a fault 165 km long. Only the fault width cannot be measured directly. However for the reasons discussed in Sections 3.3.8 and 3.3.7 above, this is likely to be high: and is conservatively taken as 40 km for both the Lansjarv Fault and Parvie Faults. From these figures the seismic moment for the Lansjarv Fault earthquake is estimated to have been  $5 \times 10^{20}$  Nm; that of the Parvie Fault earthquake  $2 \times 10^{21}$  Nm.

From seismic moment, a moment magnitude ( $M_w = 0.667 \log(M_0) - 10.7$ ) can be calculated. This would give an  $M_w$  for these two faults of 7.8 and 8.2 respectively. Magnitudes  $M_w$  in excess of 7 are suggested for another five of these faults. As all these faults appear to have ruptured within a few centuries of one another, the seismicity of this part of Lapland must have been very high immediately following deglaciation, comparable to that of a similar area of a continental plate boundary, such as present-day Iran (Muir Wood, 1989).

## LAND MOVEMENTS

Land-level changes across Scandinavia have been explored over four time-periods: an instrumental period of geodetic surveys and tide-gauges that started in the late 19th Century; a historical-scientific period, dependent on written contemporary observations; a pre-scientific period, dependent on circumstantial acts of recollection and human construction, and a Holocene period dependent on the record preserved in marine and lacustrine sediments. All of these observations can only provide a record relative to some water-level, that in almost all cases is that of the sea.

### 4.1

#### **GEODETICS**

Information on changes in vertical elevation in Fennoscandia has been collected from releveled geodetic surveys, and long-term observations of water-level changes, chiefly those at marine tide gauges, but also from the ends of some long lakes in Sweden and Finland. Both geodetic surveys and lake observations can provide only relative changes in level, that have to be adjusted to some primary reference surface through marine tide-gauge observations. These in turn can only be referenced to some geoidal datum through knowledge of the eustatic change in sea-levels.

In the different countries of Scandinavia these regional data sources are heterogeneous, in terms of the time-spans over which data has been collected, the treatment of errors, and the manner in which they have been adjusted to a common datum. Hence it is as yet impossible to provide a uniformly treated dataset of continuing land-level changes for the whole Fennoscandian region (although it is understood that an attempt to create this unified and coherent geodetic data-set is now in progress: Sjöberg personal communication). In order to find to what extent the available geodetic and tide gauge information can provide a primary resource for investigating regional variations in crustal deformation, it is necessary to explore the different data-sources.

#### 4.1.1 Relevelling

Geodetic relevelling has been undertaken in all the countries of Scandinavia. Both Sweden and Finland are currently engaged in a third levelling survey, while in Norway the second levelling programme is underway. For Denmark, Sweden and Finland a fairly full treatment of the methods of surveying and survey errors has been published, but the data for Norway is very partial and preliminary and does not allow a full investigation of errors and reliabilities.

The network of relevelled geodetic lines has a spacing of only 100-200 km in Jutland, south-east Norway, Denmark, southern Sweden and southern Finland, but across the whole of northern Fennoscandia the lines are very widely spaced, comprising a coastal ring around the Gulf of Bothnia and a few radiating spokes that follow some of the principal routes across to the Norwegian coast (see Figure 4-1). Where the data coverage is relatively dense it has been possible to explore directly the errors found in survey loop misclosures. However errors on the radiating survey lines, along with all other lines linked only at one end (including almost all those undertaken in Norway) are impossible to calibrate.

The time-spans over which relevelling observations have been collected are very variable, see Table 4-1.

Location	1st Levelling	2nd Levelling
Jutland	1885 - 1894	1943 - 1953
Finland	1892 - 1910	1935 - 1975
Sweden	1886 - 1905	1951 - 1967
Norway (Berg�en-Voss railway)	1913 - 1915	1974 - 1975
Eastern Norway	1926 - 1931	1961 - 1967

Table 4-1 : Periods of Relevelling Observations



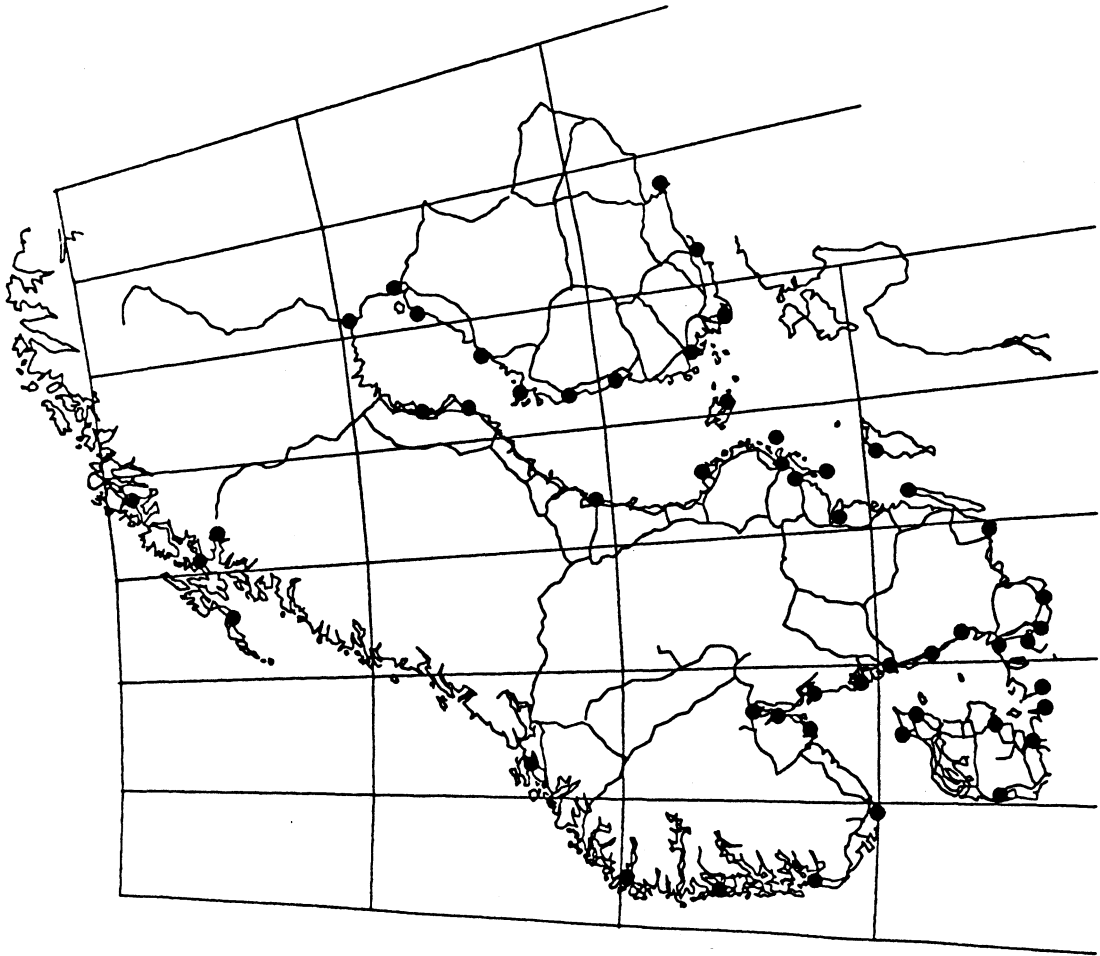


Fig 4-1 Geodetic leveling lines and tide-gauges with more than 30 years data

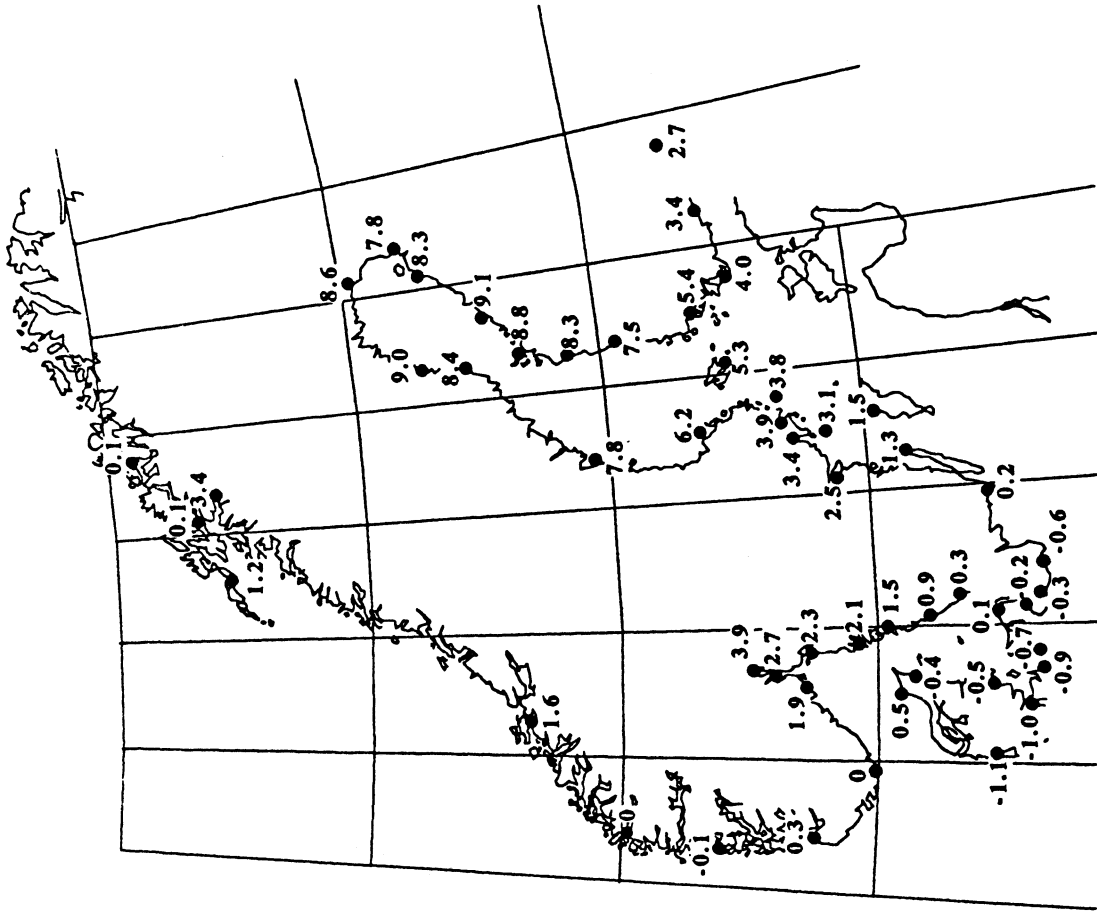


Figure 4-2: Change in sea-level (mm/yr) at Fennoscandian tide-gauges: positive = fall in sea-level.

As can be seen, Norwegian data has been obtained over a period 55-70% of that in other Scandinavian countries, inevitably affecting the precision by which land-level changes can be mapped.

Intrinsic releveling standard errors, found from survey loops, have been explored in some detail within data from Sweden (see Ussiso, 1977), and are  $4.4 \text{ mm. (km)}^{1/2}$  (Ekman et al, 1982) in the 1st levelling survey, and  $1.6 \text{ mm. (km)}^{1/2}$  in the 2nd levelling survey. Ussiso reduced the data for the two surveys to epoch 1892.0 and 1960.0, and found that for a 100 km survey line the standard error was equivalent to 0.7mm/yr. Across the whole 1500 km length of Sweden the standard error would be more than 2.5mm/yr. To avoid such accumulated errors, Ussiso adjusted the geodetic survey at each tide gauge (see below). Problems of error estimation become exacerbated in comparing one country's observations with another, as inevitably the surveys have different base levels. Hence it is not possible to present Fennoscandian releveling results on their own.

#### 4.1.2 Tide Gauge Observations

Mechanical tide gauges have been operated in Scandinavia since the mid 19th Century, although the individual records are commonly discontinuous. Tide gauges for which more than 30 years of data are available (up to the early 1980s) are shown in Figure 4-1.

There are a number of different ways in which the land-level changes can be extracted from the tide-gauge records. Each tide gauge can be treated independently and the yearly means and the overall regression lines calculated, although the mean errors for such a procedure can be fairly large. Apparent changes in sea-level obtained from tide gauges have to be assessed from the same time-period, if eustatic changes are to be excluded (these are likely to have varied with time). For the same general region, variations in sea-level associated with climatic, oceanographic, or long-term tidal factors are likely to correlate, and hence some of the least noisy results have been obtained by the direct comparison of the readings

from one tide gauge with its neighbour, or with a regional standard (for Finland the standard is the Hanko tide gauge, Kaariainen, 1975). A survey of differences between neighbouring tide-gauges for Finland shows significant variation according to the time-interval over which the comparison is made. Lastly the whole data-set can be utilised by exploring the deviations in the yearly means from the regression lines. This method helps reduce some of the errors.

In combining published land-level changes obtained from Scandinavian tide gauges it is to be noted that values given for Finland have had 0.8mm/yr added to them in order to attempt to compensate for an assumed eustatic change in sea-level. Any attempt to gain 'absolute' uplift figures from the changes in sea-level will need to add some amount believed to best represent the eustatic rise in sea-level through this period (that of course may not itself be a linear quantity) in addition to some additional compensation for the geoidal rise in sea-level that follows the reduction in surface gravity consequent on the land-level rise. This additional rise of sea-level is about 8-10% of the rate of land uplift (Ekman, 1977, Sjöberg, 1983).

The best estimate values for annual average sea-level rise around Scandinavia at tide gauges for which there is at least 30 years of data are shown in Figure 4-2. Changes in sea-level obtained independently from tide-gauge observations were reported by Ekman (1986a) for twenty sea-level stations in Sweden, a number of stations having produced almost a century of data. Sea-level changes for Norwegian tide-gauges are taken from the results published by Emery and Aubrey (1991). The earliest tide-gauge in Norway, still in operation today, is that at Oscarsborg, installed in 1872. However all the pre-1940 tide gauges have discontinuous records, and the longest run of information, for the Oslo station was reported as only 52 years. Information for Denmark is also taken from Emery and Aubrey (1991), a number of stations having been operated continuously from the late 1880s and 1890s.

#### 4.1.3 Calibrated Geodetic Observations

Through the tide-gauge observations it is possible to attempt to convert the land-level changes found from the geodetic releveling, to a common datum surface. Finnish data assumes a eustatic sea-level rise of 0.8mm/yr (Suutarinen, 1983), which has to be deducted from the reported figures (see above). Norwegian data close to Trondheim is tied to the Heimsjø tide gauge and originally assumed a sea-level fall at this location of 1.2mm/yr, but which has been calculated to be 2.0 mm/yr from a longer time-series of tidal data (Emery and Aubrey, 1991). Danish data is set on the Aarhus tide gauge that shows a submergence of 0.5mm/yr (Emery and Aubrey, 1991). These calibrations have to be compensated for in attempting to adjust the data from the different countries to a comparable sea-level datum.

The existence of independent geodetic releveling data and tide-gauge observations offers a possibility to compare alternative sources of data on land-level changes. However because of the errors in the land-level surveys this possibility is relatively restricted. Sjöberg L.E. (1987) compared the releveling differences with those of the tide-gauge observations themselves and found a significant disparity with an error of -0.97mm/yr RMS from neighbouring tide-gauge differences and 1.25 mm/yr RMS for the unreduced tide-gauge readings, taken individually. For nine comparisons the maximum errors were 1.84 and 1.97 mm/yr respectively. It is for this reason that Ussiso simply interpolated the geodetic errors along the survey lines between the tide gauges (hence approximately halving the level of errors found by Sjöberg down to  $\pm 0.5$ mm/yr) relative to a tide-gauge error as low as  $\pm 0.1$ mm/yr. Clearly where survey lines do not link tide-gauges, their errors become even less constrained, and for long survey lines, linked at only one end to the remainder of the survey, could well exceed 1mm/yr.

In order to accommodate unconstrained errors Ussiso was forced to make some ad hoc adjustments. He increased the rate of land uplift on the Swedish east coast at latitude 56.7N from 0 to 1 mm/yr, to obtain a better fit with a nearby tide-gauge

('justified' by the size of the error in the adjacent levelling loop encountered in the 1st survey) and also 'modified' values in order to obtain a closer match with results across the Finnish frontier.

In Finland geodetic and tide-gauge observations have been considered independently. The difference between the releveling and tide gauge land-level changes was found to be in almost all cases better than 0.5mm/yr, the most anomalous instance being the Oulu tide-gauge which gave an uplift rate about 0.8mm/yr less than indicated geodetically. There appears to be no published work on the exploration of errors in the limited amount of regional geodetic data for Norway, but the absence of circuit loops and the relatively short period over which releveling was attempted suggests that the lines through eastern Norway, connecting Oslo to Trondheim are likely to be relatively poorly constrained, with errors even larger than those encountered in Sweden and Finland.

On Figure 4-3 the results of the releveling surveys, tied to the tide gauges and adjusted to a common sea-level datum, are shown in the form of intersections with integral mm/yr uplift rates. These have then been contoured in order to give a generalised picture of the uplift surface. Releveling information to be found on this map is taken from: Nesje and Dahl (1990) as adapted from Sorenson et al (1987) for Norway; Andersen et al, (1974) for Jutland, Denmark; Ussiso (1977) for Sweden and Suutarinen (1983) for Finland. No further resolution is justified from the level of inherent errors, and within central Norway, it is likely that even this level of sampling overestimates the reliability of the data. Errors could be expressed on a map in the form of the width of a contour, or the range of possible level changes at a given location.

The high density of tide gauges and the long time period over which observations have been collected, in particular along the Baltic coasts of Scandinavia, provides great consistency to the picture of land uplift. However there is a significant difference in the available knowledge of uplift along the coasts of the Baltic and Gulf

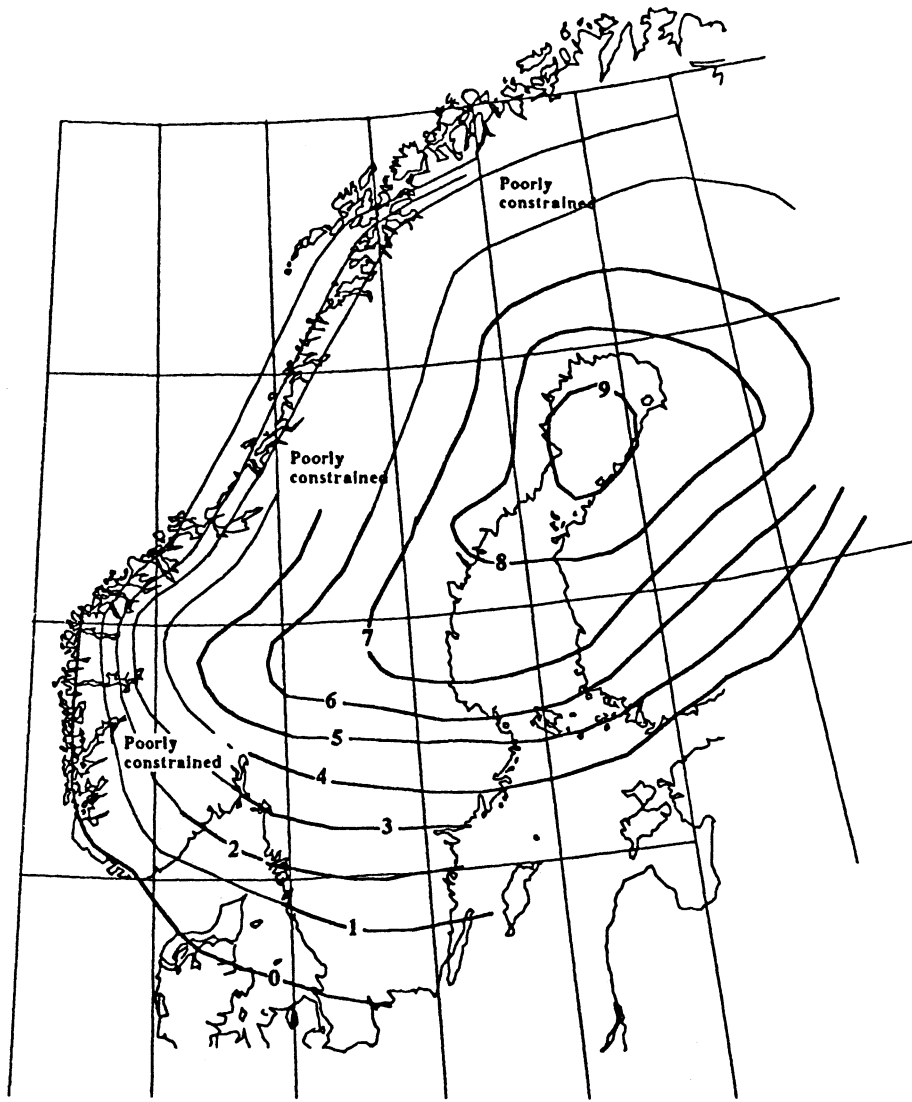


Figure 4-3 Contoured Fennoscandian land-level changes (mm/yr).

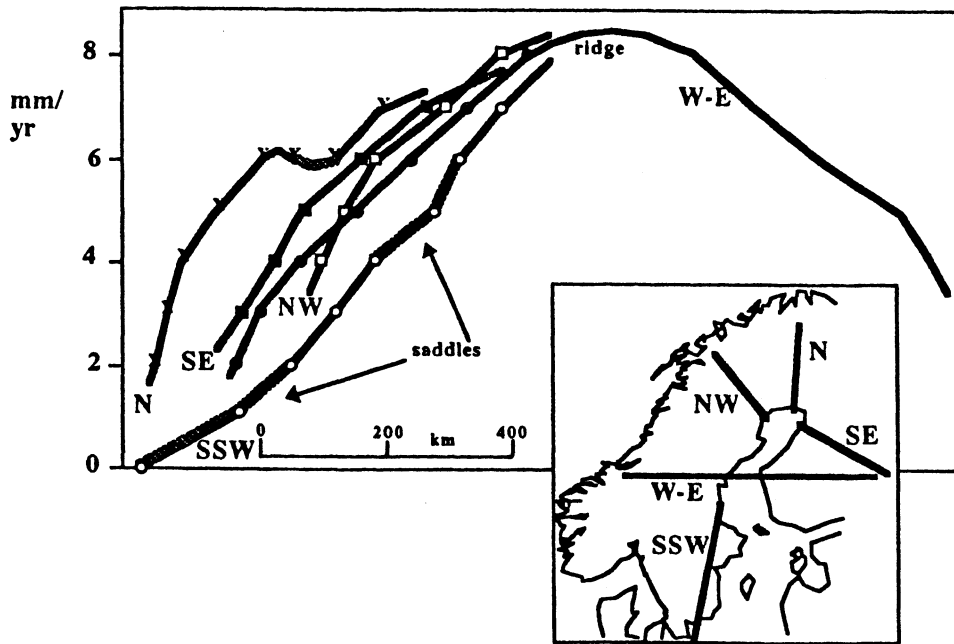


Figure 4-4: Uplift profiles along the principal geodetic survey lines radiating from the centre of rebound.

of Bothnia, with that across much of northern and western Scandinavia.

Interpolating contours between the survey lines (as in Figure 4-3) is inevitably of lower precision than that of drawing profiles of uplift along the line of the principal geodetic survey routes that radiate from the centre of uplift (see Figure 4-4). From these profiles it can be seen that the regional gradient of uplift varies by a factor of about five along the flanks of the rebound dome. Although the geodetic profiles provide a relatively skeletal coverage to the west and north of the rebound dome, it appears that the flank of the rebound dome is consistently convex on approaching the Atlantic coast, the gradient increasing over the watershed. Only to the north is there some suggestion that the gradient must once again become concave before reaching the coast. The rebound profile also appears to be generally convex in passing to the east and southeast across Finland, increasing in gradient towards southern Finland where there appear to be some flexures. However to the south through Sweden there is no simple convexity, the profiles indicating a generally linear decrease in elevation, that itself appears (probably within the error of the observations) to be composed of both convex and concave profiles.

As the regional gradients indicated by the survey lines are likely to be more reliable than the individual numerical values of uplift, so it is possible to identify variations in gradient of the uplift surface along the survey lines (see Figure 4-5). Of particular interest are those locations where the gradient is found to change, as these (if real) inevitably demand some deformation within the crust. In Figure 4-6 these regional gradient changes have been identified along the survey lines (sampling over a distance of 100 km). Even from this very coarse sampling it is evident that regional gradient changes are commonly in excess of  $5 \times 10^{-9}$  radians/yr. In Figure 4-7, a simple model of crustal flexure is shown to illustrate how these gradient changes could be used to provide some estimate of horizontal strain. To within an order of magnitude the result is fairly insensitive to the depth of the neutral surface used in the model, here taken to be 20 km (approximately half the

average thickness of the Fennoscandian crust). As a result of the coarse sampling of gradient changes this horizontal strain should be considered a lower bound estimate of the actual strains encountered in the uplifting region.

#### 4.1.4 Third Relevelling Surveys

A third relevelling survey should offer the possibility to explore how land level changes vary with time. A third relevelling survey began in southern Finland in 1978, and while variations in the apparent rate of uplift of around 0.5mm/yr (relative to the velocities calculated between the earlier two surveys) were found across southern Finland, the accuracy of this third levelling was found to be inferior to that of the second levelling and similar to that of the first. Differences in apparent uplift rates found from comparing the earlier relevelling (2nd -1st) lie within the range of statistical uncertainty (Kakkuri and Vermeer, 1985). A third motorised levelling survey is at present underway in Sweden, but its accuracy is known to be inferior to that of the second survey (see for example Becker et al, 1988) and the way in which the data is being collected means that the full results will not be available for comparison with earlier surveys, until the conclusion of the survey after 1997. A major programme of relevelling in Norway, of approximately 13,000 km of survey lines, was planned to start in 1986 and to take 25-30 years to complete (Bakkelid, 1986).

#### 4.1.5 Reducing the Spatio-Temporal Scale of Observation

Through looking at the observations of level changes on a smaller scale, both spatially and temporally, it has sometimes proved possible to see evidence for more detail in the information on land-level changes. Over long time-periods and large distance scales, the Fennoscandian rebound dome appears smooth. Over shorter distance scales and time periods, some graininess can be found.



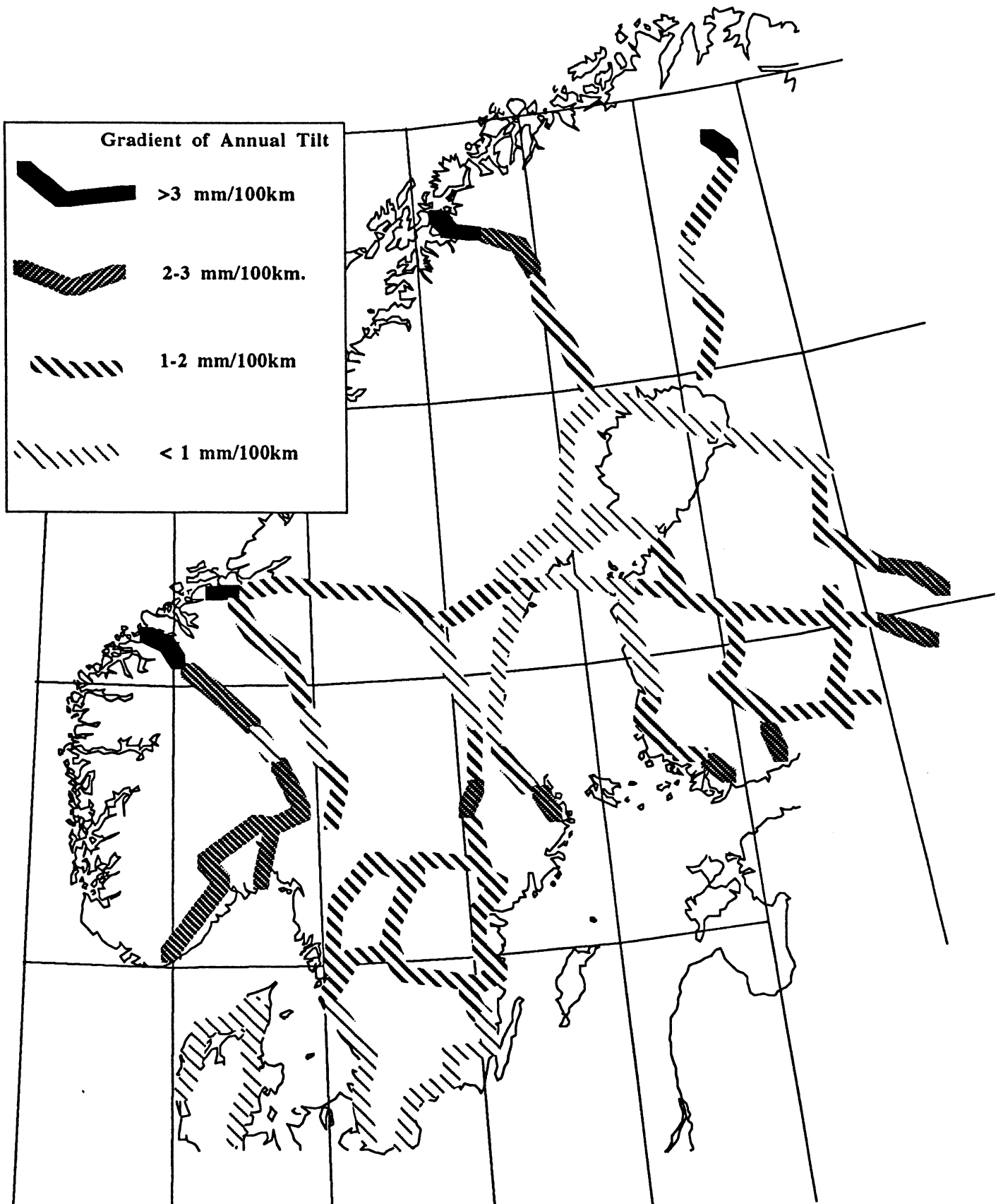
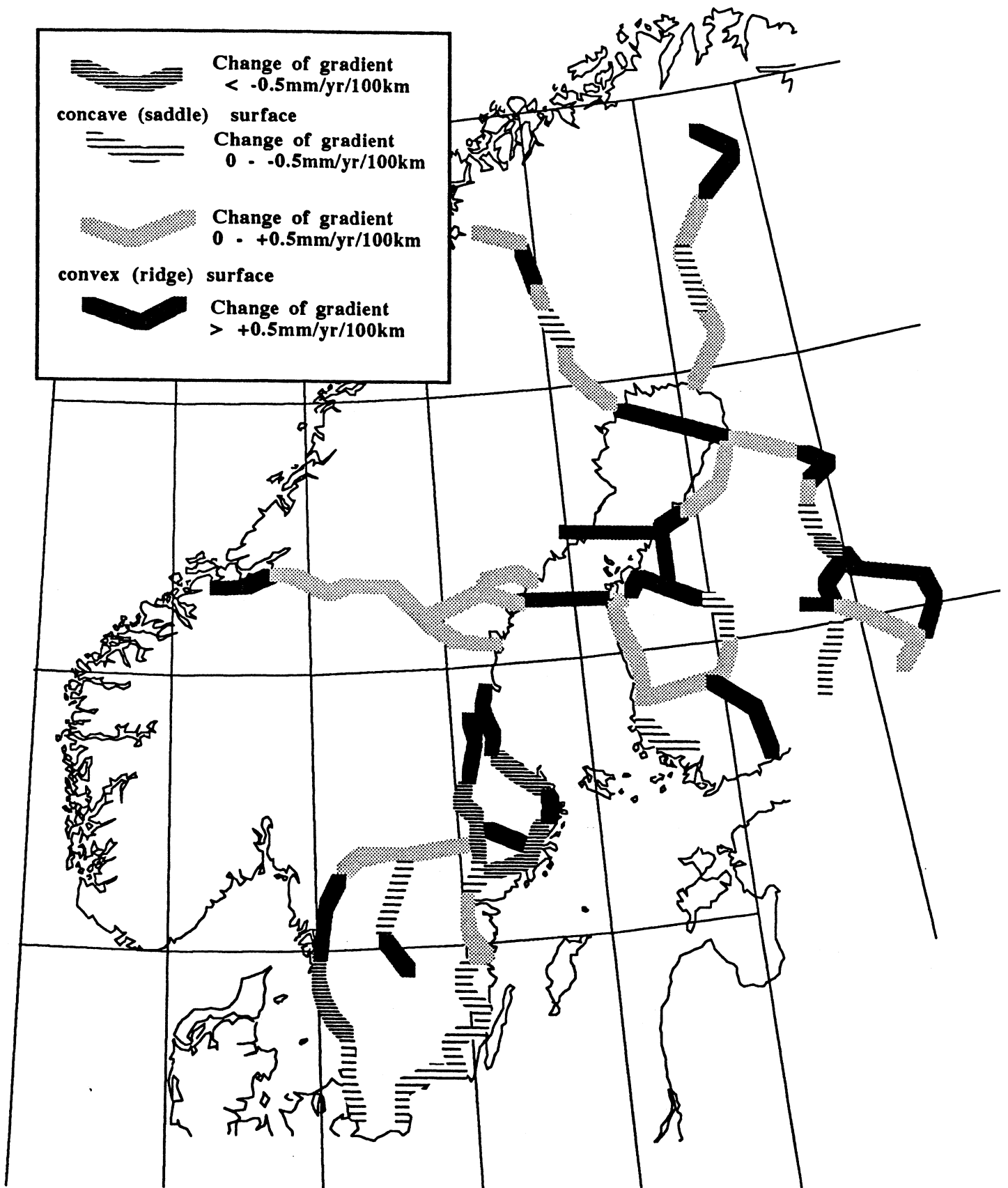
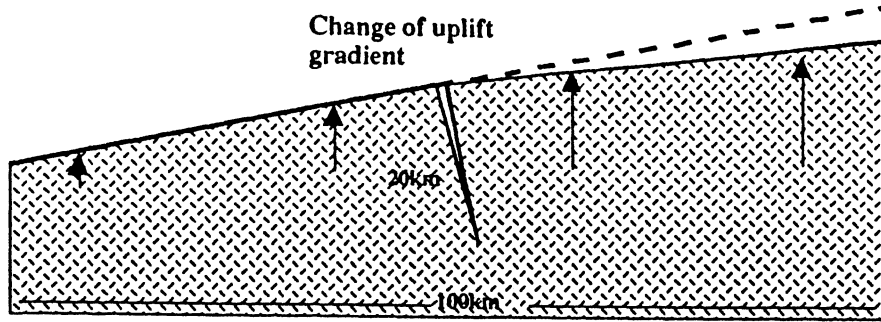


Figure 4-5: Gradients of uplift from geodetic leveling data.



**Figure 4-6: Changes of gradient in the uplift surface from geodetic releveling data.**



A reduction in gradient of 0.5mm/100km/yr distributed over 100km is equivalent to an extensional crack to 20km with a surface separation of 0.1mm = a horizontal fibre strain of  $10E-9$ .

Figure 4-7: A modelled conversion of uplift gradient changes into near-surface horizontal fibre strain.

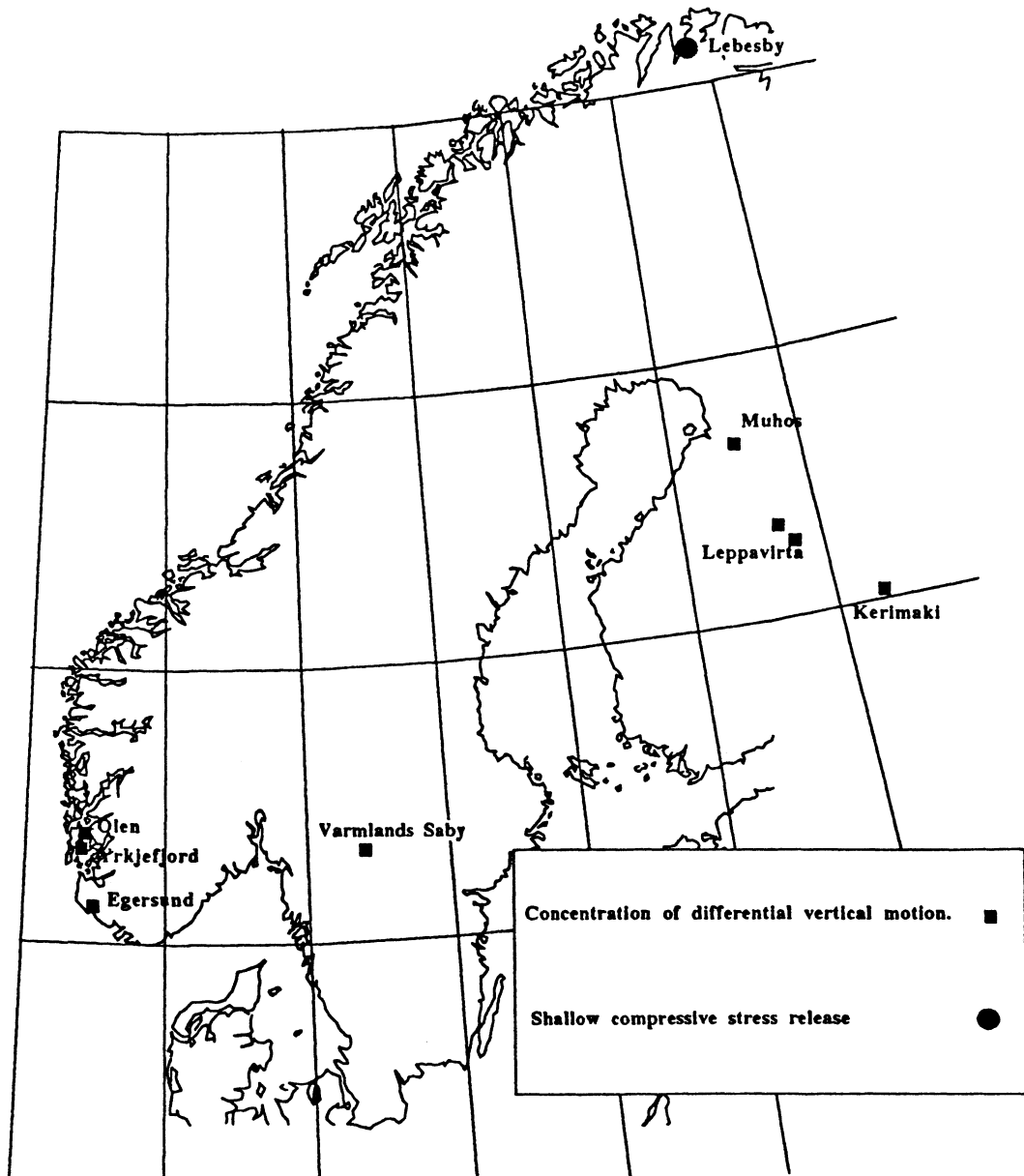


Figure 4-8: Observations of strain localisation in Fennoscandia

A regional releveling survey is such a major undertaking in terms of manpower, time and expense that it cannot hope to be undertaken more often than about twice every century. In the future GPS observations will assist in reducing this time-scale (Talbot, 1990a), although, at least in the short-term, these may not have the level of accuracy, or density of coverage to provide an alternative overview. Reductions of spatial scale have been possible in the geodetic data where observations are repeated over a small distance range, generally across some geological feature suspected as having an influence on land-level changes, or else along some geodetic survey line on which an anomalous change in level was previously noted. Local releveling surveys have been fairly widespread in Finland and in the 1980s have been undertaken across a few features in the southwestern corner of Norway. A number of observations were also collected from Sweden in the 1970s.

The advantage of a local survey is that errors can be contained, and hence after a few years repeated observations may have the potential to reveal land-level changes, where these are concentrated. Verio (1987) reported observations of land-level changes found from releveling along survey lines crossing parts of the Main Sulphide Ore Belt that runs NW-SE across central Finland. At four locations significant level changes of around 0.5 mm/yr were found, over time-intervals of about 18 - 60 years, over distances of a few kilometres. The highest rate of elevation change was 0.8mm/yr. The most northwesterly of these steep gradients was located around Muhos and Oulu on the coast of the Gulf of Bothnia, close to structures that define a deep fault-bounded Jotnian-age sedimentary basin. Verio (1990) summarised observations obtained from 42 special survey lines installed across known faults and fractures, which had been relevelled after some time interval in excess of nine years. Of these lines 13 (30%) had shown some statistically significant elevation change totalling between 8-13 mm. Of the ten survey lines straddling faults or fractures that had been resurveyed three or more times, half indicated contrary 'seesawing' motions.

In the period 1974-6 repeated annual observations were undertaken at four locations in Sweden: Bastad, Vastervik, Varmlands Saby and Kil (Ekman, 1976). Significant land-level changes were only detected at Varmlands Saby (located on the north-eastern edge of Lake Vanern). A tilting uplift (to the east) was mapped over the distance of about 3 km, in two releveling surveys, equivalent to 0.42 mm/km per year between the first two surveys, with an additional rise of the eastern end of the line found in the third survey suggesting an overall change after two years of 0.23 mm/km per year. The results of a fourth levelling survey revealed a land-level change in the opposite direction, but somewhat typically for the discovery of information contrary to an earlier published hypothesis, these were not published (Ekman personal communication). No further releveling was attempted.

In southwestern Norway, repeated geodetic observations were undertaken by Anundsen (Anundsen, 1989). These have been concentrated across some N-S and NE-SW fault-zones close to Yrkjefjorden in an area that appeared to show evidence of differential uplift through the Holocene. A traverse originally surveyed in 1965 was resurveyed in 1988, and revealed a tilting towards the east reaching about 6 mm close to the fault, with apparent uplift immediately to the east of the fault of about 12 mm, although the subsequent survey point was little changed in elevation. The maximum gradient of elevation change was therefore 0.8 mm/yr. From survey points installed across the projected lines of the faults in the early 1980s Anundsen found a rise of 0.3 mm/yr along one feature, and an apparent 1 mm of shortening that was followed by some widening. On three survey traverses across the nearby Skjoldafjord Fault, in two observations the eastern side had risen (by ca 0.1 and 0.33 mm/yr), while at the third it had sunk by 0.2 mm/yr.

Observations from survey points in rock around the town of Egersund have also indicated some apparent localised displacement. Inland from the town, relevelings along the railway line have indicated a NW-SE trending broad zone of subsidence oriented parallel with the coast (Bakkelid and Skjothaug,

1985). However within the town itself a relative land-level rise of 1.2-1.4 mm/yr was determined from around the harbour and along the fjord to the south. Along the railway within 2 km to the northwest of Egersund, this has fallen to -0.3 mm/yr, itself a value more typical of the surrounding region. Hence the high values in the town appear to be the anomaly. A number of N-S and NNE-SSW trending faults are believed to run in the vicinity of these observation points, although any potential fault control remains elusive.

Locations in Fennoscandia at which land-level changes appear, as a result of repeated geodetic observations, to have been concentrated over a narrow zone are shown in Figure 4-8. At only one location (Lebesby, Finnmark) has evidence been found of reverse displacement along a fault as a result of unloading associated with the excavation of a road-cutting (Roberts, 1991).

#### 4.1.6 Horizontal Component of Deformation

Almost all the geodetic data collected in Fennoscandia has only been employed for determining vertical level changes. However one attempt has recently been made to use triangulation and trilateration data in Finland for ascertaining horizontal changes in the crust (Chen, 1991). Although the Finnish data has large inherent errors (the triangulation network was neither installed nor resurveyed with this purpose in mind), some significant results were obtained in this study. Values of horizontal movement appeared to be of the same order as vertical rates of uplift, but with far greater regional variability. Horizontal extension of up to  $21.8 \pm 10.4$  mm/yr was found along a 140 km line passing across the Raahe Ladoga zone close to the Bothnian coast (ie a strain per year of  $1.6 \pm 0.8 \times 10^{-7}$ ). Maximum rates of shortening were measured as  $-7.3 \pm 6.3$  mm/yr along a line 131 km long in the south of the country, although the error is almost as large as the reported signal. Because of the size of the errors it is difficult to employ the results in a quantitative form.

Perhaps the greatest significance of this work in Finland was the discovery that the rates of extensional strain were higher than compressional

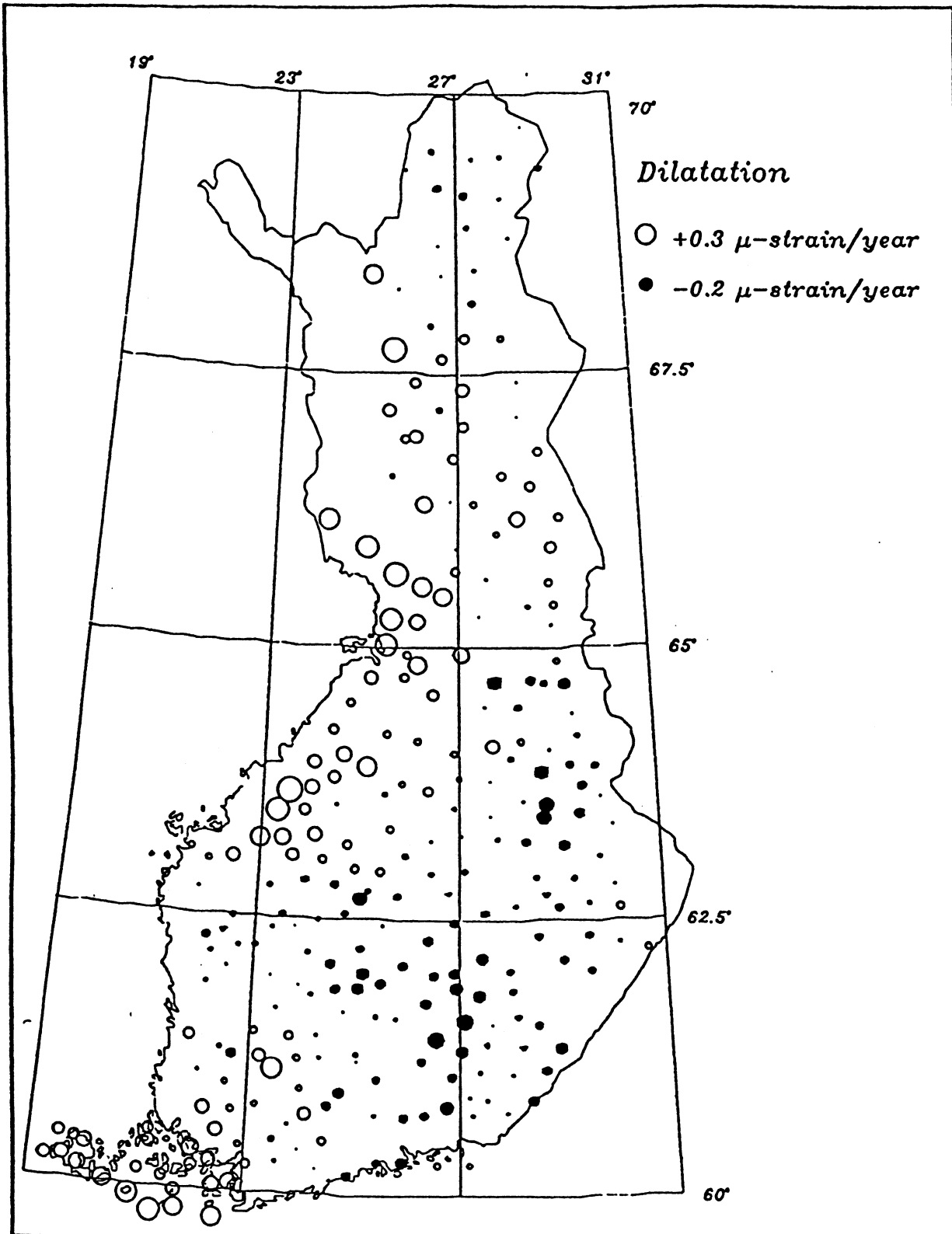


Figure 4-9 Observed dilatation distribution in Finland (from Chen, 1991).

strain, and covered more of the country (see Figure 4-9). Extensional strain was found over almost all of the west and north of Finland while compressional strain was restricted to the east. Although areas of extension and compression were similar, extensional strain was of larger magnitude and appears to dominate.

In the future, by employing GPS (Global Positioning System) stations across the Scandinavian rebound dome it is to be anticipated that primary information on the horizontal component of the strain field may also become available for Sweden (Talbot, 1990a). For the present this horizontal component can only be inferred from the vertical component and from models of the rebound process (see Section 8.1.2).

#### 4.2 HISTORIC OBSERVATIONS OF UPLIFT

Before the era of instrumental tide-gauges, there are a number of types of historical observation available, that may extend the overall picture of rebound, although these are all relatively scattered, and inevitably less precise than those discussed above. A number of water-level marks were cut in rock along the coast of Sweden in the mid 18th Century, and a set of detailed sea-level observations was kept at Stockholm. In analysing this time-series, compensating for some changes in datum point, Ekman (1986b) identified a decrease in the rate of sea-level rise from  $4.93 \pm 0.23$  mm/yr for the period 1774-1884 and  $3.92 \pm 0.19$  mm/yr for the period 1885-1984, which he ascribed to a significant increase in the eustatic rise in sea-level at the end of the Little Ice Age in the early 19th Century. Other infrequent observations of two mid 18th Century water marks further to the north along the Swedish coast of the Gulf of Bothnia, were reported by Sjöberg (1986), who found no evidence for a significant change in uplift rate through the record.

Before marks were cut into rocks, measurements have to rely on human recollection of features, such as rocks that were previously invisible, and constructions that either depended on the adjacent sea-level, such as a causeway or doorway, or came



into existence as a result of uplift. Most notable among the latter is the foundation of a town at Stockholm when the rise of a submerged rock sill blocked the passage of boats from the sea into the extensive navigation routes through the Malaren Lakes, forcing cargo to be disembarked and transported over a rocky island. In the 17th Century, to preserve the level of the inland lake, that was in danger of draining too low to allow access to all the lake-shore towns and villages, a sluice had to be constructed in Stockholm (Ekman, 1986b).

#### 4.3 HOLOCENE UPLIFT

Holocene uplift data has been collected in two distinct forms, that are in some ways analogous to the contrasting geodetic releveling and tide-gauge style observations. Individual shorelines, reflecting a contemporaneous sea-level, have been mapped across much of southern Sweden and around the Baltic. Where correlation is unambiguous, they provide the opportunity to date the cumulative uplift since some formerly near-horizontal datum surface was created.

In contrast, studies of the dates at which a staircase of lakes or ponds became isolated from the sea can provide an estimate of the changing rates of land-movement relative to sea-level for a region that is sufficiently small as to be considered a point on the map. Such studies require detailed field work, coring, diatom analysis and radiocarbon dating and for each region can reflect several years of intensive research. For two regions, western Norway and southern Sweden, sufficient of these 'staircase lake-isolation dating' studies have been undertaken to allow the changing pattern of uplift through the earliest millennia of post-glacial rebound to be mapped in some detail. For example for fifteen lakes situated between 129 m asl and 91 m asl close to Hunneberg at the south-western end of Lake Vanern, western Sweden, a regression gradient has been obtained from 12,200 to 10,200 BP, with the steepest fall in sea-level of about 3.3 m/100 years, an order of magnitude faster than for the same region today (Bjorck and Digerfeldt, 1982). A

compilation of all the lake-isolation studies undertaken in southern Sweden is provided by Bjorck (1989).

In employing data from these lake isolation studies it is important to be aware of a number of inherent sources of error. The date at which a lake or pond ceases to be influenced by the ingress of salt water will be critically dependent on the size of waves likely to impact against a particular coast, and could vary by 5-10 m in elevation according to the degree of exposure. A separate series of errors arises in selecting and dating the oldest freshwater or youngest marine deposits. Hence every point on a shorelevel displacement curve should be represented as an area, reflecting both the uncertainties in the elevation relative to the sea for full isolation, and the inherent difficulty of dating the exact date when isolation was completed. Fortunately, in the period around deglaciation, the rates of land level changes have been sufficiently rapid as to make these errors of lesser consequence.

Other problems arise when sedimentary deposits are employed to indicate the contemporary sea-level. For example some authors consider ice marginal delta surfaces to reveal the sea-surface from the proximal surface, others by the distal surface, while others consider the whole delta surface to have been submerged several metres (Fernlund, 1988). The upper limit of wave-washed till has also been used as an upper bound sea-level marker, but wave washing up to 6 m higher than sea-level and exceptionally up to 15 m higher than sea-level has been reported.

Many published attempts exist to correlate a whole range of isolated shorelines (see for example Mörner, 1969), but correlation often has to assume parallelism rather than be internally calibrated by dates of the shorelines themselves. Shores may form as a result of local rather than regional influence, and hence never have existed as a single contemporary sea-level indicator, but rather reflect a whole range of local dates of formation. The errors in multiple shoreline tracing are generally too great to be admissible as a primary source of information on changing patterns of

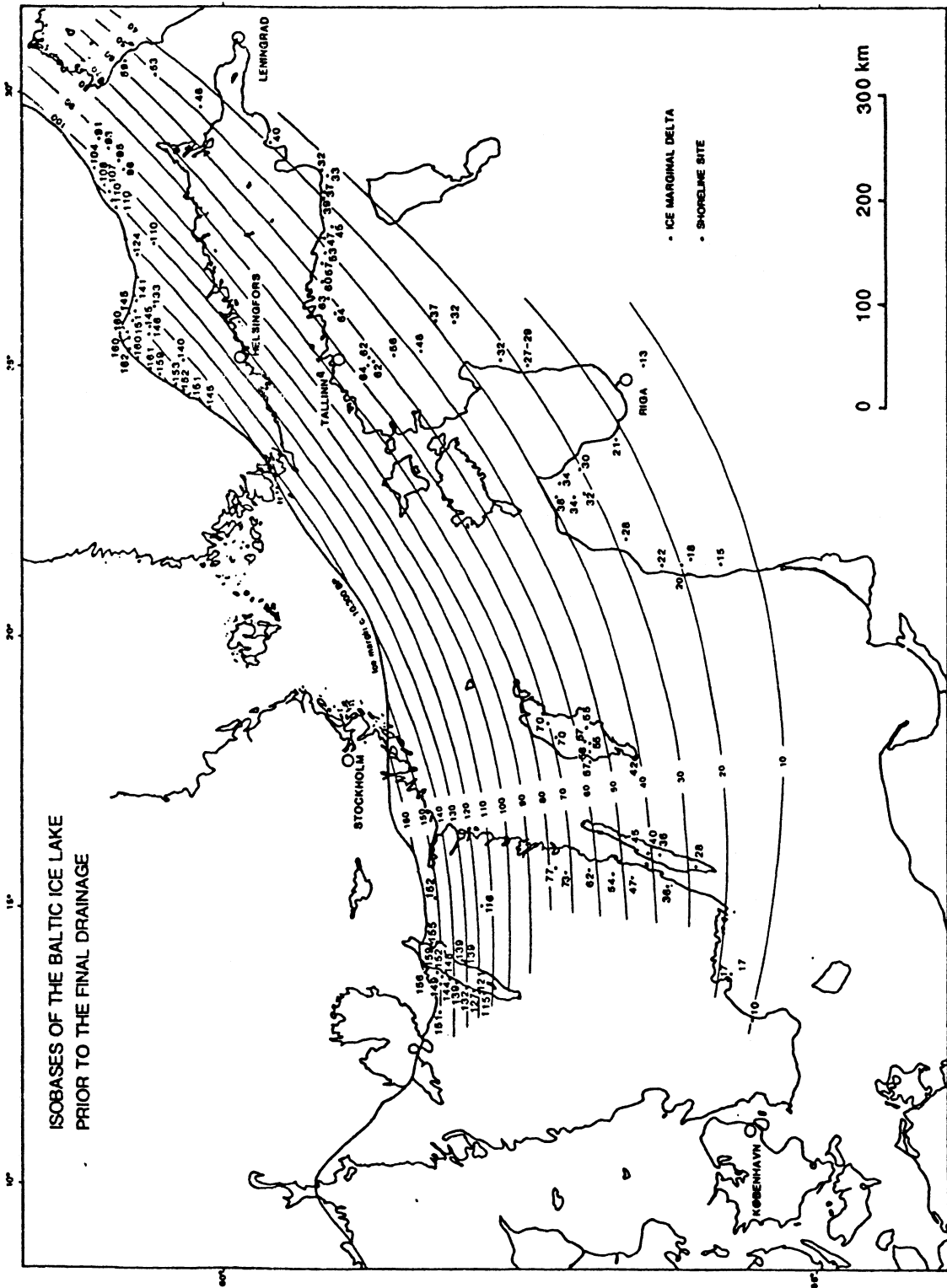


Figure 4-10 Elevation of Ancylus Lake shoreline in southern Fennoscandia (from Svensson, 1991).

uplift. A good critical review of the problems of multiple shoreline correlation is to be found in Donner (1980), who disputed his own earlier claims for correlation in southern Finland and noted that a scatter of elevations of shorelines is more likely simply to reflect a continued fall in sea-levels rather than a series of distinct and separately identifiable contemporary beach deposits.

One of the few shorelines in southern Fennoscandia that is demonstrably datable is that of the Baltic Ice Lake shoreline. The formation of the shoreline was followed by a rapid ca. 25 m decrease in water-level as the lake suddenly drained out to the west, and this has prevented the shoreline suffering the degradation and smearing that is common to most regressing marine beach deposits. A regional study of the elevation of this shoreline has been undertaken by Svensson (1991), see Figure 4-10, and provides the best datum surface for comparison with subsequent uplift in southern Fennoscandia.

5

**SEISMICITY**

Earthquake ground motion in Sweden has been recorded over three broad time-bands: the instrumental period (approximately from 1950), the historic period (from around 1400/1600AD) and the prehistoric (palaeoseismic) period which almost inevitably begins at the time of deglaciation 13,000-8,500 BP. In each case the nature of the recording medium preserves information on different levels of ground shaking. In effect the amplitude necessary to trigger a record has shown a stepped series of falls from the prehistoric through to the current instrumental period.

5.1

**QUALITY CONTROL**

For historical and instrumental data, individual quality criteria of uncertainty can be developed (chiefly from the number and consistency of individual data sources) for estimates of the earthquake's size, maximum intensity and felt area. Epicentral location has an uncertainty that may be based on both the number and reliability of individual data sources while an accurate hypocentral depth can only be achieved through calibrated velocity models of the crust. From palaeoseismic observations only crude estimates of earthquake intensity and epicentral location are ever possible.

Assessing the geographical distribution of seismicity or the population of events of different sizes, requires complete datasets for which it becomes necessary to explore the size threshold for any region above which the earthquakes can be certain to have been recorded.

5.2

**HISTORICAL SEISMICITY**

The earliest record of an earthquake in Sweden is an event in 1375, known from Gotland, and possibly Denmark (Kjellen, 1910). This compares with earliest earthquakes ca. 800 AD in Belgium and Germany, 900 AD in England, 1073 in Denmark and 1570 in Norway. As in all these countries the first earthquakes reported from Sweden are known in too

little detail to be mapped. It can only be assumed that from the late Middle Ages, if a major damaging earthquake had occurred in Sweden, with significant loss of life, then reports of this event would probably have found their way into other surviving sources of historical information in Germany or Britain.

Early events in Sweden are (as with most other European countries) non-specific about the area affected. The significance of the early record is no more than to confirm that there has probably been a recurrence of events reaching intensity VI around the coast of south-western Sweden of about one per century. It is only from the middle of the 17th Century, with the rise of literacy and centres of documentation, that the catalogue of earthquakes begins to rise. However, with the exception of the 1657 earthquake around Oslofjord (Muir Wood and Woo, 1987), it remains impossible to map the felt effects of any of the Swedish events known from this period. However for a number of events it is possible to identify at least part of the area affected.

#### 5.2.1 Historiography

In order to explore to what degree, and over what area, the surviving record represents a reasonable picture of contemporary seismicity, it is necessary to know the geographical distribution of centres of literacy and record keeping. One simple manifestation of this process is to compare the known distribution of earthquake reports (or where sufficiently detailed, earthquake macrocentres) with the locations of continuously published Scandinavia newspapers. Figure 5.1 (a, b and c) illustrates this relationship from the end of the 17th Century through to the mid 19th Century.

At the end of the 17th Century there was only one newspaper published in the region, at Stockholm. For the previous fifty years knowledge of earthquakes in the region is almost all restricted to southern Sweden and the extreme south-east corner of Norway and Denmark, although two events have also been reported from the important cathedral city of Trondheim. By 1749 there were

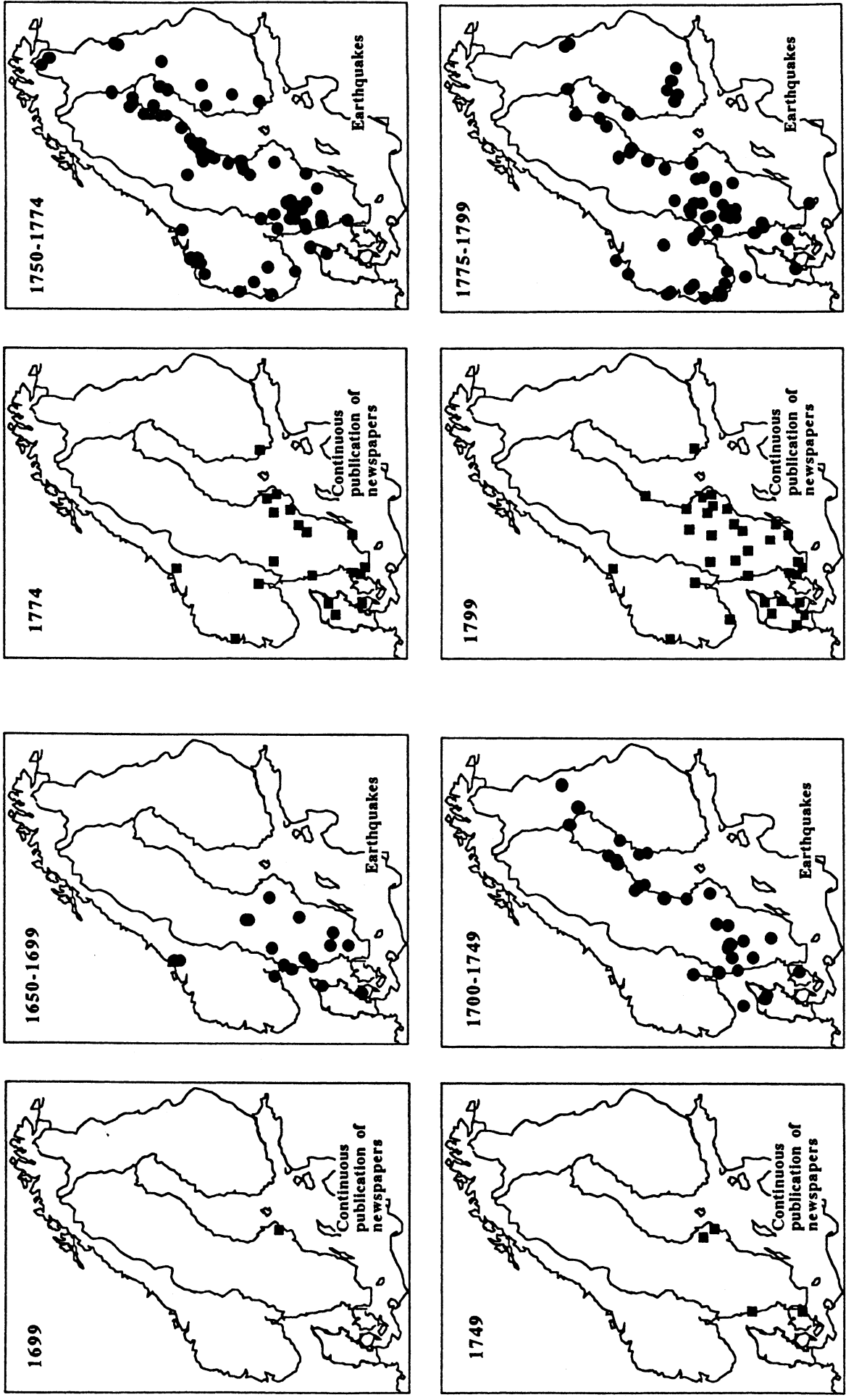


Figure 5-1a: Comparison of newspaper production with reported earthquakes 1650-1749

Figure 5-1b: Comparison of newspaper production with reported earthquakes 1750-1799.

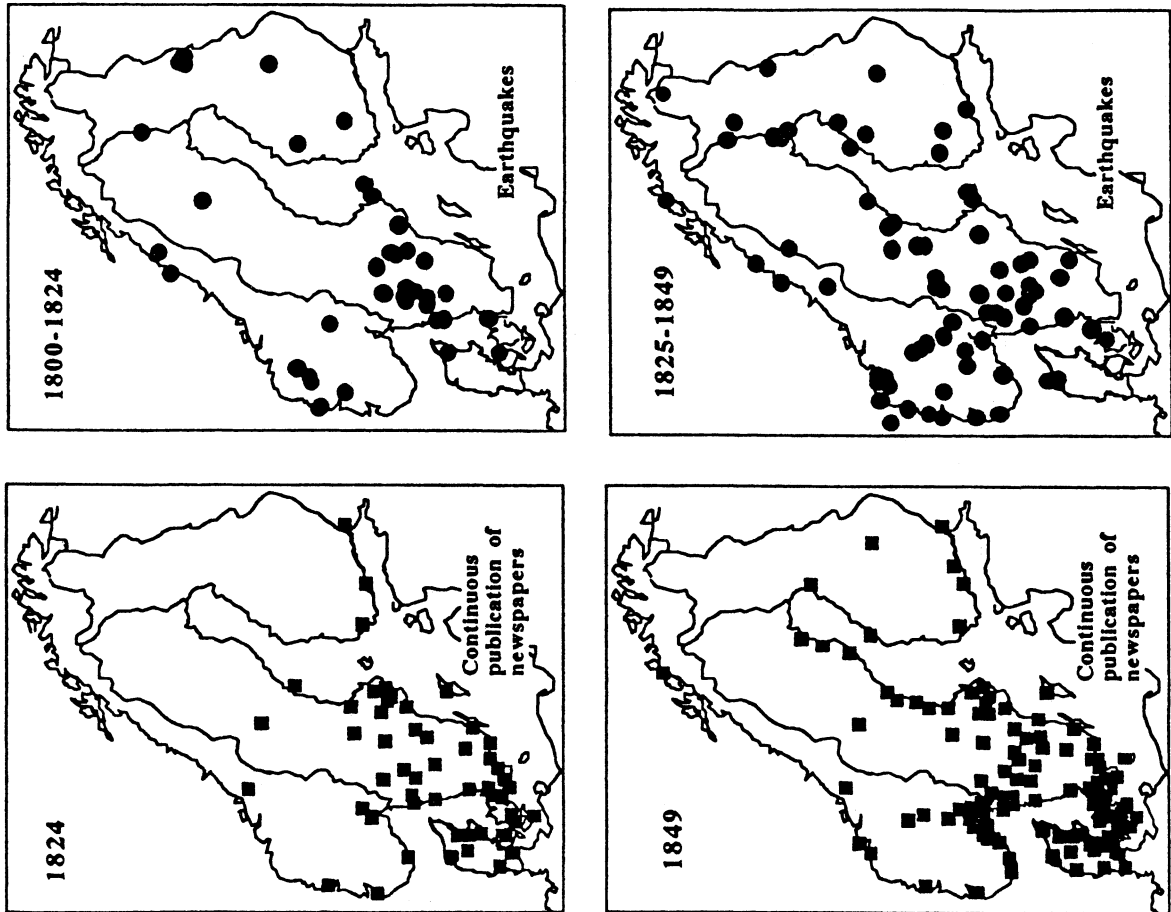


Figure 5-1c: Comparison of newspaper production with reported earthquakes 1800-1849.

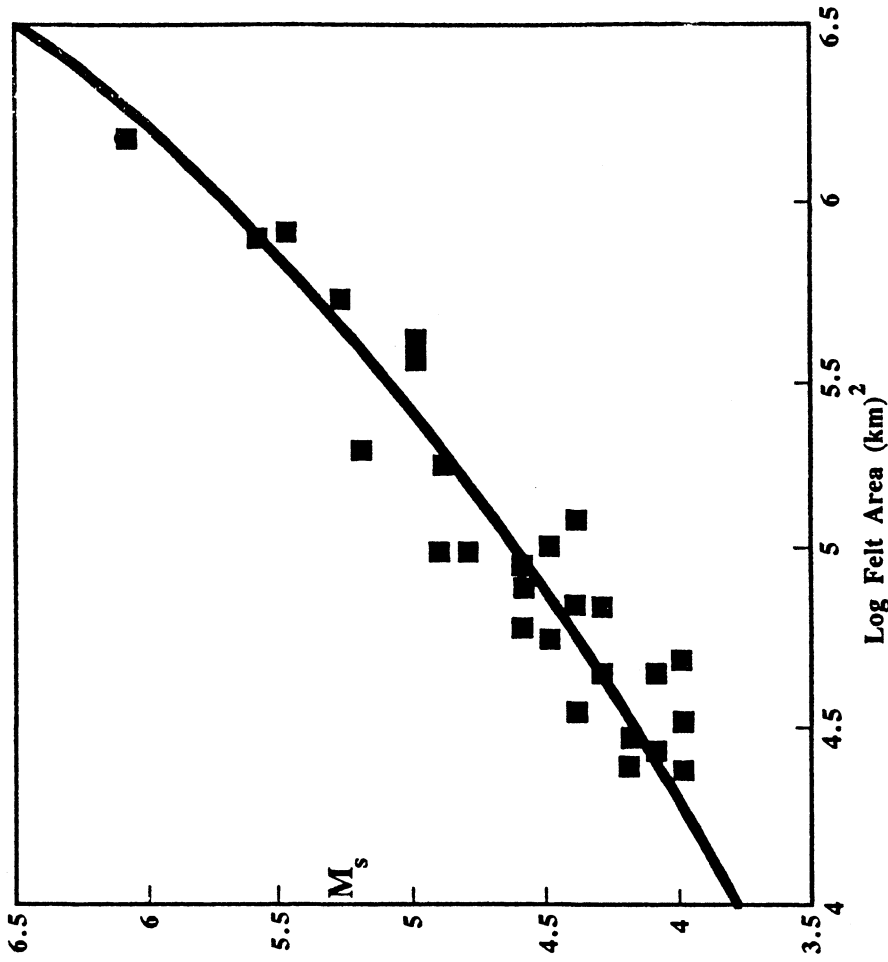


Figure 5-2: Magnitude  $M_s$  vs Felt Area correlation for North-West Europe, from Muir Wood and Woo (1987).



four newspapers published in southern Sweden and Denmark and knowledge of earthquakes has extended around the Gulf of Bothnia, reflecting increased communication through this region. By 1774 when the first newspapers had appeared on the west coast of Norway, for the first time there were also earthquakes known from the region. Little had changed by the end of the century, with no events known from anywhere in northern Scandinavia. It was not until the last of these periods that a newspaper was founded in northern Norway, and the recording of earthquakes from this region all postdates 1800.

Throughout all these panels the number of earthquakes reported from Sweden appears to be significantly greater than that of western Norway, and only for the last period to be comparable with that of Norway. However even at this mid 19th Century period, the density of newspaper publication in south-east Norway, southern Sweden and Denmark is an order of magnitude higher than that of western Norway, reflecting the different population densities, and the difficulty of communication through the western fjords. For all of these periods up to 1850 the effect of under-reporting of events to the west ensures that it is impossible to have an accurate picture of the relative levels of seismicity, even across southern Scandinavia.

### 5.2.2 Macroseismic Monitoring

From 1883 Gumaelius in Sweden revived the collection of contemporary macroseismic accounts of Swedish earthquakes (Gumaelius, 1883), although the procedure of sending out questionnaires following an initial report was only undertaken continuously after 1890. Such practice had started in Norway in 1887. In both Norway and Sweden this active request for information has continued uninterrupted up to the present, although in both countries there was a decline in the pursuit of such information in the period from around 1930-1950. The effect of actively collecting earthquake data in both Norway and Sweden was dramatic: the number of reported earthquakes significantly increased, and for many of the smaller events it became possible to plot an

intensity map. Since this time the macroseismic record of earthquakes is good, although potentially incomplete for the smaller events in the more remote parts of inland northern Sweden until the early or mid 20th Century.

### 5.2.3 Macroseismic Interpretation

Historical reports of earthquakes arrive in the form of descriptions of the effects of the shaking on objects and individuals as well as mention of where an observer was (ie outside, in a car, upstairs etc.) when the event was felt. All these descriptors can help in defining the intensity perceived at that location. In this study the MSK (Medvedev - Sponheuer - Karnik) intensity scale has been followed, in accord with earlier studies in Norway and Sweden, and with ongoing intensity mapping activities for current earthquakes in both countries.

The degree to which an intensity can be defined is determined by the detail that is available in the description. Faced with the minimal descriptions contained within felt reports for the large majority of Swedish historical earthquakes before 1850 it is hard to discriminate better than to within a range of III to V (ie. probably IV) for mention that an earthquake was "felt". Only a very small number of earthquakes in Sweden have generated reports that are without doubt intensity V or higher.

For some of the larger pre-1880 earthquakes, intensities have been assessed and mapped according to well established procedures of modal intensity assessment (for a range of descriptions at a single location) and contouring (running intensity isoseismals through individual intensity points). However the number of earthquakes from this period worthy of detailed intensity mapping is very small. The largest event with a macrocentre in Sweden is that of November 24th 1823 (with a felt area radius of around 250km). Throughout history the largest regional earthquakes have all been located to the west of Sweden, notably the events of 21 December 1759 Kattegat earthquake (Ms 5.6), 31 August 1819 Luroy earthquake (Ms 5.8) (Muir Wood, 1989b) and

the 23 October 1904 Oslofjord earthquake (Ms 5.4).

Through the detailed contemporary collection of macroseismic data, revised in Bath's extensive work, felt earthquakes for the past century have been well analysed and mapped. It is only earthquakes from before 1880 that can significantly benefit from fresh research. However any major research effort on early Swedish earthquakes, although likely to reveal new events, is unlikely to be very rewarding: firstly because of the strong research-work that was performed on this topic towards the end of the 19th Century (Kjellen, 1910); secondly as a result of the small number of earthquakes sufficiently large to generate widespread reports; but chiefly because of the generally meagre information concerning earthquakes that is known from these earlier periods.

Kjellen's (1910) pre-1890 record of earthquakes has recently been researched by Wahlström (1990) who returned to many of the original sources. Wahlström's revised catalogue of information has been a very useful source in preparing a list of historical earthquakes within this present study, although for some events, as a result of re-visiting the primary information in this study, small changes have been made in the estimated felt areas and locations relative to those interpreted by Wahlstrom.

#### 5.2.4 Locational Accuracy

Earthquakes can be defined in terms of a location in space (the epicentre being the point on the surface immediately above where the earthquake was initiated), the hypocentre including the depth of the focus, and a size expressed in terms of a magnitude or seismic moment. All of these parameters have their inherent uncertainties reflecting the way in which the information has been recorded.

For example, the resolution implicit in historical data is that of the grid of towns or villages at which the event was reported. Site effects, that cause variations in perceived intensity, further limit the degree to which this information can be

used to identify an earthquake's epicentral location. The centre of the felt area, the macrocentre, is rarely identical with the epicentre. Even in the most populated regions of Europe, with the most detailed historical information, epicentres cannot be resolved better than to within a radius of uncertainty of about 5km. In areas of low population, as apply to much of Sweden, and for earthquakes that have relatively flat intensity variations, as are typical for this region, the uncertainty is commonly no better than to within a radius of 20km. This limitation generally prevents macroseismic earthquakes being associated with a specific surface mapped geological fault: the event could occur anywhere within a crustal volume typically in excess of 10,000 km<sup>3</sup>.

#### 5.2.5 Depth Estimates

From the rate at which the intensity decays from the centre of the felt area to its margins, it may be possible to obtain an approximate estimate of depth. However all such estimates are uncertain, in particular as a result of variations in intensity from site effects. At best the intensity distribution of crustal earthquakes can be used to suggest one of a series of overlapping depth bands: such as shallow (0-10km), middle (5-15km) or lower (10-25km) or deep (20-40km) crust. For the majority of poorly known historical earthquakes, depth remains unconstrained.

#### 5.2.6 Regional Magnitude Scales

In order to achieve consistency between the historical and instrumental periods of seismicity it is necessary to establish consistent methods of determining the size of earthquakes. This is not straightforward. Several different instrumental magnitude scales have been in use in Fennoscandia that have tended to prevent a simple comparison between event sizes and seismicity levels in the different countries and over different time-periods.

Recently a new local magnitude scale was adopted in Norway. This scale like many others is based on Richter's original Wood-Anderson scale (Alsaker et al, 1991). The Wood Anderson scale is defined as:

$$M_L = \log A - \log A_0 + S \quad (5-1)$$

where

A - measured amplitude  
 $A_0$  - reference amplitude at 100 km  
 S - correction term.

Further,

$$-\log A_0 = a \log(R/100) + b(R-100) + 3.0 \quad (5-2)$$

where

a - geometrical spreading  
 b - anelastic attenuation  
 R - hypocentral distance.

The Norwegian dataset consisted of earthquakes covering both continental paths and oceanic paths. The attenuation was found to be slightly lower for the continental paths than for the whole dataset, making an average difference of 0.1 magnitude units between the two sets when the same correction terms were used.

The new  $M_L$  scale (hereafter denoted  $M_{LN}$ ) is related to Båth's et al (1976) scale ( $M_{LB}$ ), which previously was used in Norway, as

$$M_{LN} = 0.96M_{LB} - 0.04 \quad (5-3)$$

$M_{LB}$  is related to the  $M_L$ (UPP) scale (Wahlström and Ahjos, 1984; here denoted  $M_{LW}$ ), which is currently used in Finland and Sweden, as (Wahlström, 1978)

$$M_{LB} = M_{LW} - 0.07 \quad (5-4)$$

Thus

$$M_{LN} = 0.96M_{LW} - 0.11 \quad (5-5)$$

The  $M_{LB}$  and  $M_{LW}$  scales are based on data from analog seismographs with peak response around 1 Hz,

whereas the  $M_{LN}$  magnitude scale is based on digital data from instruments with peak response up to 5 to 10 Hz.

Within this project an attempt has been made to see whether it would be possible to ascertain surface wave magnitudes,  $M_S$ , for Swedish earthquakes. Records from long-period seismo-graphs in Sweden and Finland have been checked for surface waves. It was found however that for events below magnitude 4.5 no clearly visible surface wave was observed. The only two events for which surface waves were observed are: 15 June 1985, Kattegat earthquake,  $M_{LW} = 4.6$ , and 14 July 1986, Skövde earthquake,  $M_{LW} = 4.5$ . The corresponding  $M_S$  values computed according to Vanek et al (1962) are 3.8 (from four readings) and 3.1 (from three readings) respectively.

The big difference in  $M_S$  in spite of similar  $M_{LW}$  values can be explained by the different focal depths. The 1985 earthquake had a depth of about 10-15 km (see Arvidsson et al, 1991) and the 1986 earthquake about 30-35 km (Arvidsson et al, 1992). A discrepancy in depth of 20 km corresponds to a magnitude difference of about 0.4 according to Panza et al (1989).

Different ways to obtain  $M_S$  from regional magnitude have been suggested by Norwegian seismologists. The most recent relationship is from Alsaker et al (1991).

$$M_S = 0.83M_{LN} + 1.09 \quad (5-6)$$

and with the above formulas in mind we obtain

$$M_S = 0.80M_{LW} + 1.0 \quad (5-7)$$

This would make  $M_S$  for the 15 June 1985 and 14 July 1986 events, 4.7 and 4.6 respectively.

The results from the two methods to compute  $M_S$  are very different. The reason for this remains to be investigated.

### 5.2.7 Calibrating Macroseismic Information for Magnitude

In order to achieve a catalogue that spans from the historical into the instrumental period it is necessary to have some method of converting historical macroseismic data into magnitudes consistent with the instrumental record. There are two approaches to this problem that can be found within research on Scandinavian seismicity through the 1980s.

(i) The  $M_L$  (UPP) calibration.

A calibration between  $M_L$ (UPP) was derived by Wahlström and Ahjos (1984) from 76 earthquakes in Sweden, Finland and the Kola peninsula of Russia for which both macroseismic and instrumental data were available in the period 1960-1979. The formula used is:

$$M_L(\text{UPP}) = 0.38[\pm 0.25] + 1.14[\pm 0.18]\log(R) + 0.23[\pm 0.07]I_0 \quad (5-8)$$

where  $R$  is the felt-areas radius (assumed  $R_{III}$ ) and  $I_0$  is the peak intensity.

This relationship is based on equations proposed by Gutenberg and Richter (1942), relating magnitude to energy release. It has the advantage of being derived from a relatively large body of data that extends to the smallest size of felt earthquakes local to Sweden. However as a result of the comparatively short duration of the observational period, this data has to be extrapolated to the largest regional historical earthquakes. The magnitude scale cannot also readily be compared with other regions. However perhaps the greatest disadvantage with the method is that the scale requires knowledge of peak intensity, and this is commonly unavailable for the incomplete picture that can be gained from the historical earthquakes.

(ii) The surface wave magnitude correlation.

The alternative approach to the assessment of historical earthquake magnitudes, as developed by Ambraseys (1985a), has now been widely applied to many regions of the world, including Britain, the

North Sea, Norway, Denmark and the Norwegian continental shelf (Ambraseys, 1985b, Muir Wood and Woo, 1987). The method involves a calibration of surface wave magnitude  $M_S$  with the radius of some outer isoseismal of the earthquake. The felt area of an event is in general easier to reconstruct from incomplete historical data than the peak intensity. Unlike  $M_L$  data, that is in general only available for the past 30 years, surface wave magnitudes can be established for events dating back to around 1900 and as the magnitude scale is a global standard, the sample of suitable calibration events can be further expanded by testing the correlation over a broad area (having shown that there are no significant variations in seismic attenuation across the region). The surface wave magnitude  $M_S$  felt area relationship, established for Britain, Norway, North Sea and the Norwegian continental shelf, is illustrated in Figure 5-2 (Muir Wood and Woo, 1987).

This relationship has continued to be refined by NORSAR who derived the following correlation relating felt area (A) to surface wave magnitude:

$$M_{SA} = 0.95 + 0.69 \log(A_{III}) + 6 \times 10^{-7} A_{III} \quad (5-9)$$

(Bungum et al, 1991).

Although significant variations with western Norway are not predicted, the disadvantage with using an  $M_S$  - felt area relationship for Swedish earthquakes is that there are very few events in, or adjacent, to Sweden by which the correlation can locally be correlated. The surface wave magnitude scale cannot be applied to events below about  $M_S 4$ , and in contrast to western Norway, North Sea, Denmark and UK (where earthquakes are largely restricted to the top 20 km of the crust), some Swedish earthquakes have had depths down to 40 km (see Section 5.3.4 below). Increasing depth reduces the amplitude of surface waves relative to body waves. This may be the explanation for the low surface wave magnitude obtained for at least one of the two recent Swedish earthquakes (see Section 5.2.6 above).

In mapping the magnitudes of historical earthquakes for the present study the surface wave magnitude



correlation has been employed, chiefly because it does not require unavailable peak intensity data. In effect a magnitude scale has been used that is solely dependent on the earthquake's felt area ( $M_{SA}$  scale). Within this present study the purpose of assigning magnitudes has principally been to allow a comparison of data across Scandinavia. Close attention would have to be given to refining and adapting these historical - instrumental magnitude correlations for deriving detailed magnitude recurrence statistics, as would be needed for a full seismic hazard investigation in Sweden.

In the present study approximate energy equivalents for earthquakes have been derived using the formula (Bath, 1978):

$$\text{Log } E = 12.3 + 1.27M_L \quad (5-10)$$

The cumulative energy release within a designated zone is obtained by converting the  $M_L$  value for each event to an equivalent energy value, summing the corresponding energy values, and then converting the total energy back to an equivalent value of  $M_L$ .

#### 5.2.8 Seismicity Statistics

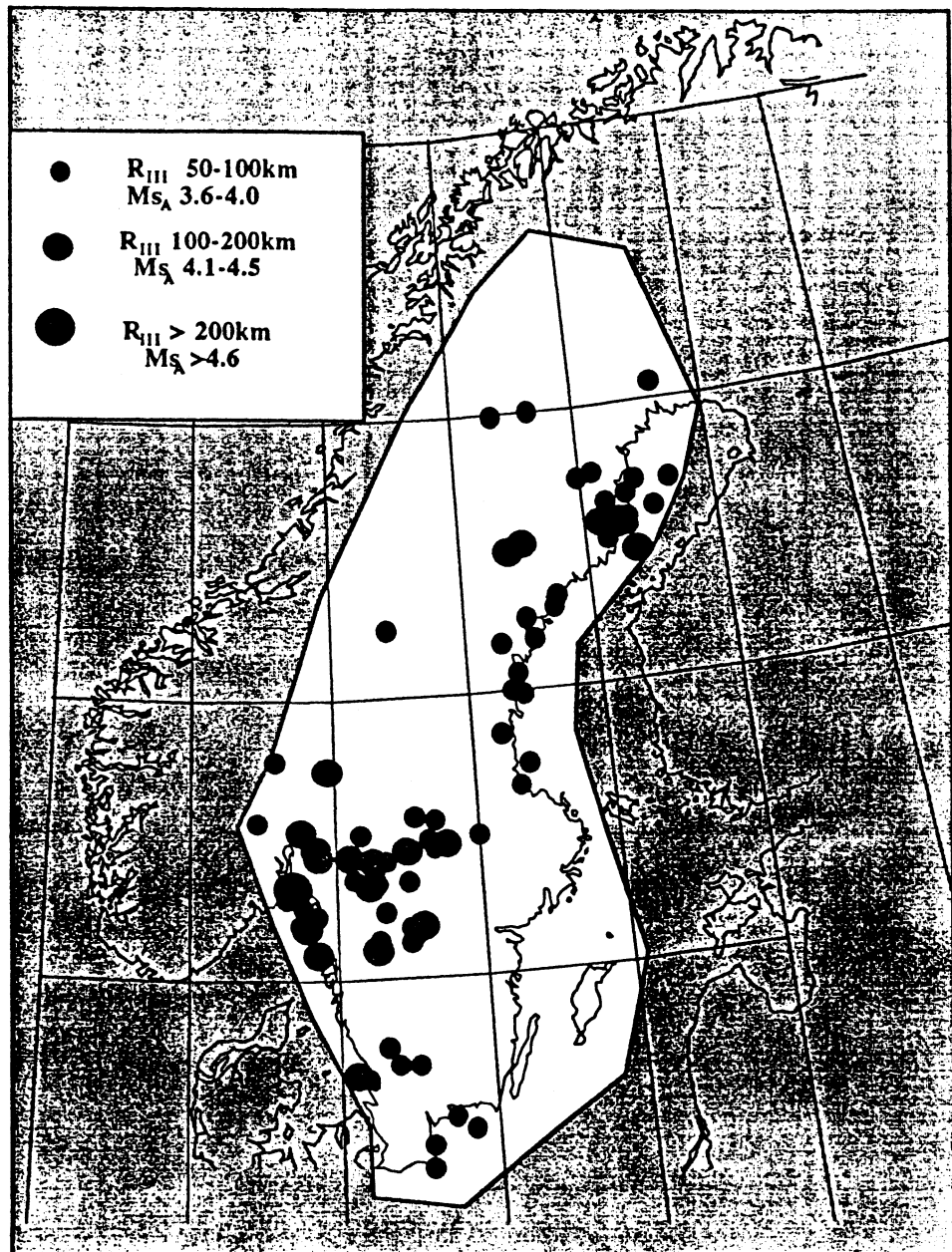
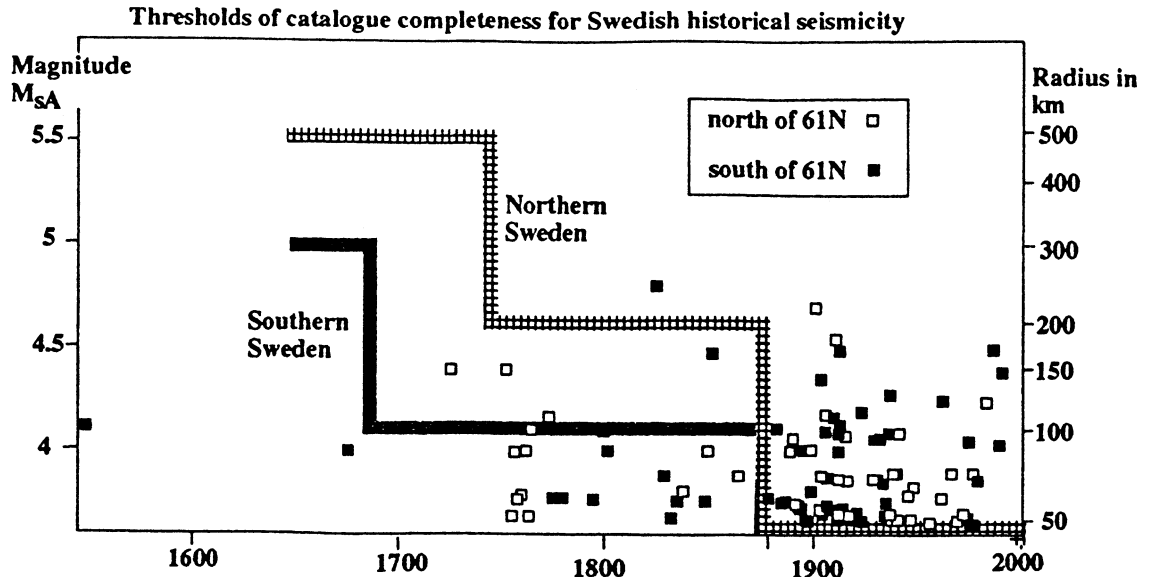
In order to obtain information as to the geographical distribution of seismicity, or variations in seismic energy release through time, it is vital only to employ data-sets that are complete. Any method of recording earthquakes will only obtain a complete record above some size threshold. Many events will be known below that threshold, because of their fortuitous location (such as beneath an important town) or timing (such as at a period when a local natural historian kept detailed records). However other events of comparable size will have escaped recording, having occurred at inauspicious times or locations. No catalogue of earthquakes can be properly comprehended unless thresholds of catalogue completeness are defined. These thresholds vary from region to region and from age to age.

Thresholds can be explored in two separate ways. In the first, catalogue completeness is found by

plotting the annual number, or recurrence-rate of events above some size, in order to find from what date the frequency is comparable to that found in recent decades. This however assumes that the rate of seismicity is constant through time. In the second a historiographic study is undertaken of the sources of earthquake records to find out their sensitivity (ie. what intensity would be guaranteed to be documented), as well as the separation of recording centres (perhaps locations such as major cities, where people recorded observations of natural phenomena). The procedure is no different for historical information as for instrumental information, defining the maximum size of an event at different historical periods that could have fallen through the net of recording centres and hence remain unknown. The largest size of this lost event defines the threshold of catalogue completeness.

A historiographic study of Sweden shows that the record for inland northern Sweden is unlikely to be complete even for moderate magnitude events, with felt area radii in excess of 100km, until the early part of the 20th Century. The spacing of towns and the cultural activity and literacy of southern Sweden might suggest that the record ought to be complete for events with a felt area of 50km or greater since the mid 18th Century. However from the plot of the felt areas of earthquakes (with felt area radii of 50km or greater) through time (see Figure 5-3) it appears that the record is deficient in events between 50 - 100km felt area radius for the whole period preceding 1890, when the active collection of data was initiated. This deficiency is far larger in northern Sweden than in the south, but even in the south there is an obvious lack of earthquakes.

There seems little reason to believe that the level of seismicity has coincidentally changed at the time that active research was initiated to collect macroseismic data. There remain two possible causes for this deficiency: either the felt area of many events has been consistently underestimated as a result of incomplete reporting, or a number of moderate size events have been missed. It is probable that both factors are significant with the first being dominant. Many of the smaller events



before 1890 are known from a single location, allowing only the minimum size of the felt area to be gauged. Not unreasonably Wahlström (1990) uses a convention of giving an event reported from a single location a felt area radius of 10km. In general this is probably closer to a minimum felt area, than a best estimate, although there is unlikely to be any additional surviving information for almost all of these 'single-location' events that could improve this situation.

This problem of incomplete data means that it is impossible to develop useful or accurate seismicity statistics for Sweden for any of the data-sets prior to 1890 except for the larger magnitude events (with felt radii in excess of ca. 150km), for which the record is likely to be complete for southern Sweden at least back to around 1750. A map of the macro-seismic earthquakes for Sweden and south-east Norway in the period and magnitude ranges in which the record is considered near complete is shown in Figure 5-4.

### 5.3 INSTRUMENTAL SEISMOLOGICAL DATA

#### 5.3.1 Introduction

The scope of the present work is to give (1) threshold magnitudes for earthquakes in Sweden and Fennoscandia; (2) an idea of uncertainties in location (epicentre and focal depth) for Swedish earthquakes; (3) focal mechanisms for Swedish earthquakes.

The results come from compilations of information given in various studies and enclose the time period of modern seismic instrumental recording, ie. approximately the last 30 years. Figure 5-5 shows the seismicity in Sweden for the period 1963-1989.

#### 5.3.2 Seismic Instrumentation and Threshold Magnitudes

##### (a) Sweden

For the period since 1963 the instrumentation of the permanent Swedish Seismograph Station Network

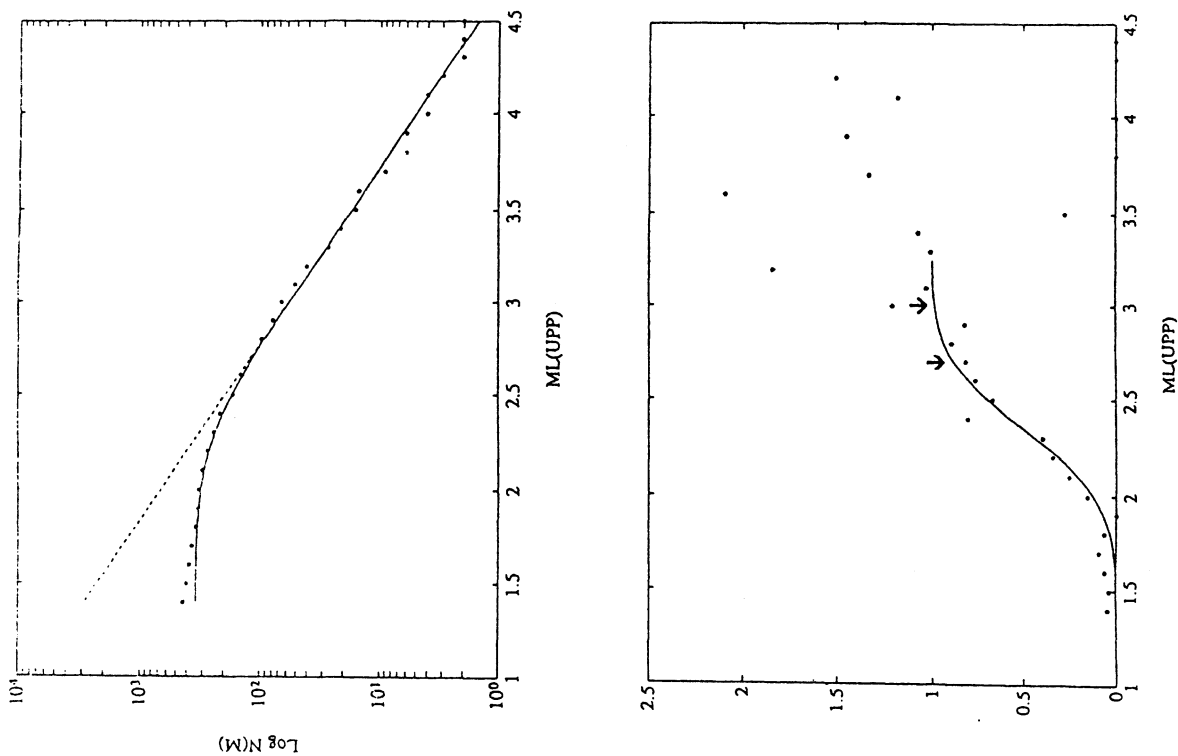


Figure 5-6 Observed cumulative number of Swedish earthquakes in 1963-1989; and ratio between the number of observed earthquakes to the number predicted from the ideal Gutenberg-Richter distribution. The solid line represents the fitted cumulative normal distribution. The arrows show the location threshold magnitudes at 90% (left) and 99% (right) probability levels.

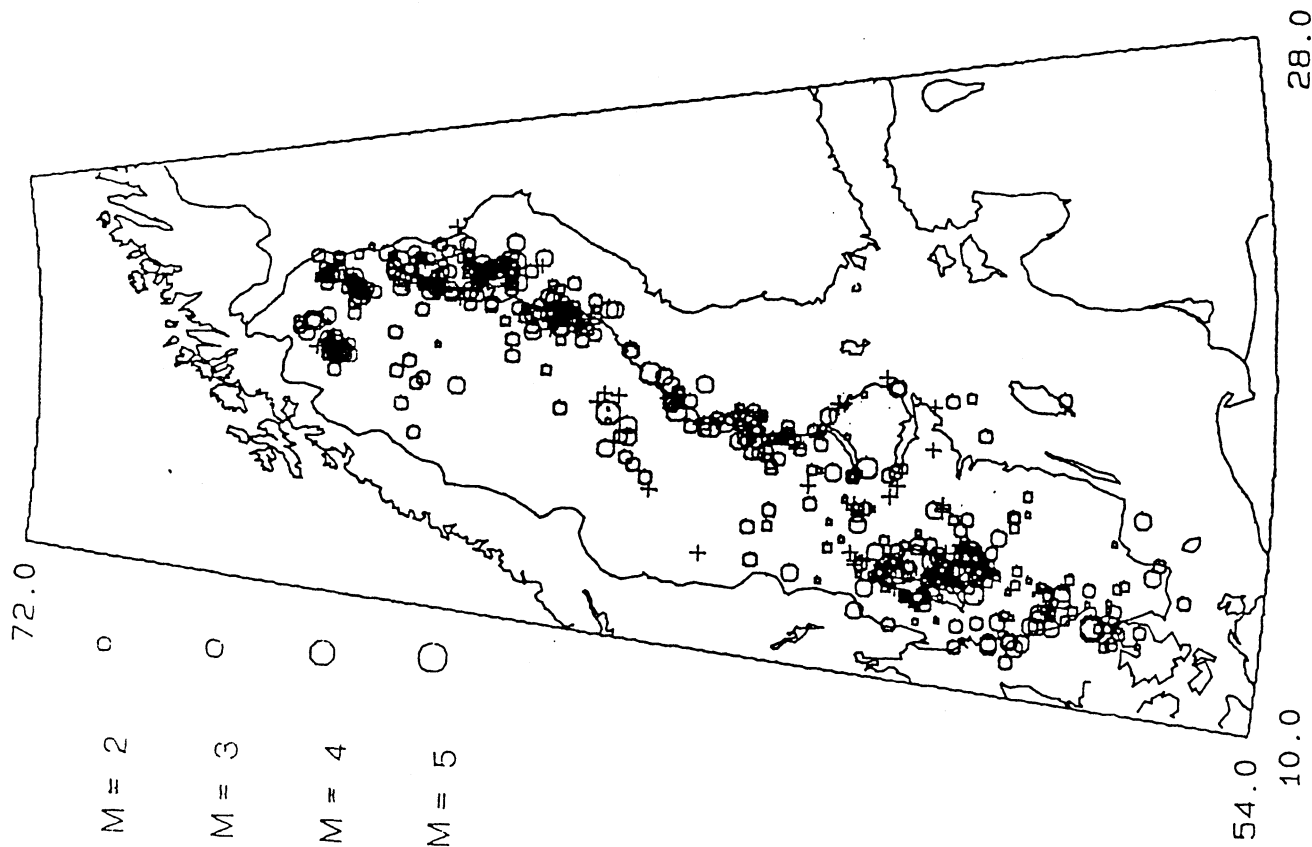


Figure 5-5 Seismicity of Sweden in the years 1963-1989 (+ indicates magnitude not determined).

Network/ array	Station	Location	Operation time		
SSSN	KIR	67.840	20.417 1951-		
	UPP	59.858	17.627 1955-		
	SKA	63.580	12.280 1957-1981		
	UME	63.815	20.237 1960-		
	GOT	57.698	11.978 1958-1968		
	KLS	56.165	15.592 1961-1968		
	UDD	60.090	13.607 1966-		
	DEL	56.470	13.870 1968-		
	MYV	62.942	14.347 1981-		
	*)Hagfors	HFS	60.134	13.696 1969-	
		SKI	+) HRN	60.250	16.486 1979-
			+) KTB	61.066	16.284 1979-
			+) NYK	58.924	17.091 1979-
+) VIM			57.788	16.002 1979-	
+) ALR			56.995	15.918 1979-	
+) VNY			59.904	12.482 1979-1988	
GBD			59.457	14.554 1979-1988	
BHU			57.428	16.559 1986-1988	
VUM			57.328	15.488 1986-1988	
SGA			57.304	18.473 1979-1987	
HVK			60.009	18.566 1979-1986	
ORK			56.268	13.262 1979-1985	
VEB	55.599		13.516 1979-1985		
OLO	56.308	14.470 1979-1985			
HEB	58.680	11.788 1979-1984			
MRD	58.617	13.746 1979-1984			
ABB	57.845	12.786 1979-1984			
BYD	57.059	13.163 1979-1984			
TNU	57.638	14.269 1979-1984			
MUG	67.462	22.045 1987-1989			
LJV	66.665	22.182 1987-1989			
HAK	66.925	21.560 1987-1989			
KLX	66.067	23.031 1987-1989			
KRP	66.755	22.905 1987-1989			
VMK	65.680	21.587 1987-1989			
Finland	NUR	60.509	24.651 1958-		
	KJN	64.085	27.713 1959-		
	KJF	64.199	27.715 1970-		
	SOD	67.371	26.629 1956-		
	SO	67.420	26.394 1973-		
	KEV	69.755	27.007 1961-		
	PKK	60.005	24.517 1964-		
	PRV	60.357	25.558 1964-		
	PR	60.387	25.680 1979-		
	PRF	60.386	25.681 1968-		
	KAF	62.113	26.306 1977-		
	KEF	62.166	24.871 1977-		
	JOE	62.650	29.685 1960-		
SUF	62.719	26.151 1977-			
JOF	62.918	31.312 1981-			
OUL	65.085	25.896 1963-			
MA	65.911	29.044 1970-			
VAF	63.0422	22.6715 1989-			
FIAO	61.4436	26.0771 1989-			
BER	60.383	5.334 1960-			
KON	59.649	9.598 1960-			
TRO	69.633	18.928 1962-			
LHN	61.05	10.88 1963-1969			
KRK	69.724	30.062 1964-1969			
NAO	60.8237	10.8324 1971-			
NRS	60.7353	11.5414 1985-			
EVJ	58.583	7.960 1980-1983			
DRA	59.104	9.097 1980-1983			
SJD	59.556	8.614 1980-1983			
SPG	59.353	11.339 1980-1983			
SRU	60.063	11.257 1980-1983			
NFJ	60.379	9.561 1980-1983			
RGS	63.021	10.435 1984-			
HVA	61.166	6.187 1984-			
ASK	60.483	5.195 1983-			
ODD	59.950	6.667 1984-			
SUE	61.057	4.761 1984-			
BLS	59.294	6.927 1985-			
KMY	59.212	5.247 1984-			
FRO	61.757	4.882 1983-			
FOO	61.598	5.044 1983-			
ARAO	69.535	25.506 1987-			
KTK	69.010	23.236 1987-			
LOF	68.131	13.542 1987-			
MOR	66.237	14.767 1987-			
MOL	62.570	7.548 1987-			
NSS	64.530	11.967 1987-			

\*) Array: a larger number of densely spaced sensors.

+) Presently run to supplement the Hagfors array stations.  
The table is not necessarily complete.

Table 5-1 Developments of modern Fennoscandian seismograph stations.

(SSSN) operated by the Seismological Department, Uppsala University (SDU), has been more or less consistent. The minor changes made during the past three decades have been: substitution of the stations KLS and GOT by DEL and UDD in the late 1960s and SKA by MYV 1981. These changes do not cause any significant difference in the detection capability of the network (see Table 5-1 where also the general development of Fennoscandian seismograph stations is shown).

The National Swedish Defence Research Institute (FOA) has operated the Hagfors array over a small area in Western Sweden since the late 1960s. The main purpose is to monitor nuclear explosions, but the detectability of local earthquakes in the area is also enhanced. Due to the proximity to the Uddeholm seismic station, and its intended target of nuclear explosions, it has not much significance for lowering the general threshold for Sweden.

Some temporary networks have also been in operation during this period, especially during its later part.

Installed in 1979 and operated fully by FOA until 1984, the Southern Sweden SKI network consisted of some 15-20 stations. Five stations are still operating, mainly as an aid to the Hagfors array, and not directly aimed at regional events, although they somewhat lower the threshold.

From 1987 to 1989 a network of six stations for recording local events in Swedish Lapland was operated by FOA. The estimated threshold was 1.0 (Slunga, personal communication).

Since 1982, a mobile network with digital and analog recording facilities is available at SDU. The purpose is for quick deployment to record aftershock series of Swedish earthquakes, and for microearthquake surveys of areas of seismological interest. The two longest recording periods were during the summers 1987 and 1988, to record microseismicity in the Lansjärv region, Swedish Lapland. The strict temporal and spatial limitations of the operation of this network make its contribution to the detectability minor, even though the occurrence in Sweden of very small

quakes, with negative magnitudes, is indicated.

The threshold magnitude for Sweden was firstly calculated on the basis of single station detection of the SSSN (Shapira et al, 1979). A threshold of 2.0 was derived for 90% detection probability at any one station of the network (time period 1963-1976). The results of Shapira et al (1979) have been extended to calculate the detection at at least three stations in order to derive a location threshold. The estimate is 2.6 and 90% probability. Networks outside Sweden have been disregarded, ie. the estimate may be conservative. Magnitudes given in the present study refer to the regional scale used in Sweden and Finland (Wahlström and Ahjos, 1984).

The b-value from the Gutenberg-Richter relation is used in determining the location threshold in the Shapira et al (1979) study. For Norway, the complete Gutenberg-Richter frequency-magnitude distribution, not only b, was used for estimating the 90% detection threshold for a single station (Bungum and Husebye, 1974). The Gutenberg-Richter relation was also used for a network by just checking the point at lower frequencies where the curve starts to deviate from the linear trend, and taking that point as the threshold (eg see Bungum et al, 1986, Engell-Sørensen and Havskov, 1987).

In the present work the following procedure is applied to Swedish earthquakes 1963-1989:

- 1 Find the Gutenberg-Richter distribution from the maximum-likelihood estimate (Aki, 1965).
- 2 Calculate the ratio between the actual number of earthquakes and the ideal Gutenberg-Richter relation stepwise for a specified magnitude interval. The fall-off towards lower frequencies approximates the threshold.
- 3 The fall-off towards lower magnitudes is assumed to be normally distributed. The cumulative normal distribution curve is, in an interactive way, fitted to the curve obtained in step 2. Thresholds for different probability levels are thus given once the curve is established.



- 4 As a check that the result in 3 is valid, the Gutenberg-Richter distribution is corrected with the derived normal distribution and compared with the actual data.

Figure 5-6 shows that the threshold magnitude for all Sweden at a 90% probability level is about 2.7 and at a 99% probability level about 3.0. As indicated above there are certain problems with the applied procedure. Uncertainty in the slope of the Gutenberg-Richter distribution will affect the results and non-stationarity may be reflected as a time dependent variation of the b-value (Skordas and Kulhanek, 1991). Thus, even though it is considered that the results are fairly reliable, the 90% and 99% probability thresholds should be taken only as estimates. The seismicity maps for the 90% and 99% probabilities are shown in Figures 5-7 and 5-8.

For Swedish earthquakes south of 61°N and the period 1980-1984, when the FOA network was in operation, the derived thresholds were about 2.0 and 2.3 at 90% and 99% probabilities, respectively (Figure 5-9). However, the short time period may have introduced large uncertainties.

#### (b) Fennoscandia

Deployment of seismograph stations in Fennoscandia began in 1904 and 1905 when Wiechert seismographs were installed in Uppsala and Bergen, respectively. The first seismograph in Finland was a Mainka in 1924. The Uppsala Wiechert is still in operation.

Modern instrumentation started to be introduced in the national networks in the 1950s and the modernisation has continued with deployment of arrays, digital stations and local networks. The instrumental network capability in both Finland and Norway is today no doubt superior to that in Sweden. A brief summary of the development in Finland and Norway follows (see Table 5-1).

Seismograph installation at Sodankylä (SOD) in 1956 and Nurmijärvi (NUR) in 1958 commenced the era of modern seismograph recording in Finland. In the mid 1960s seven stations were in operation. The

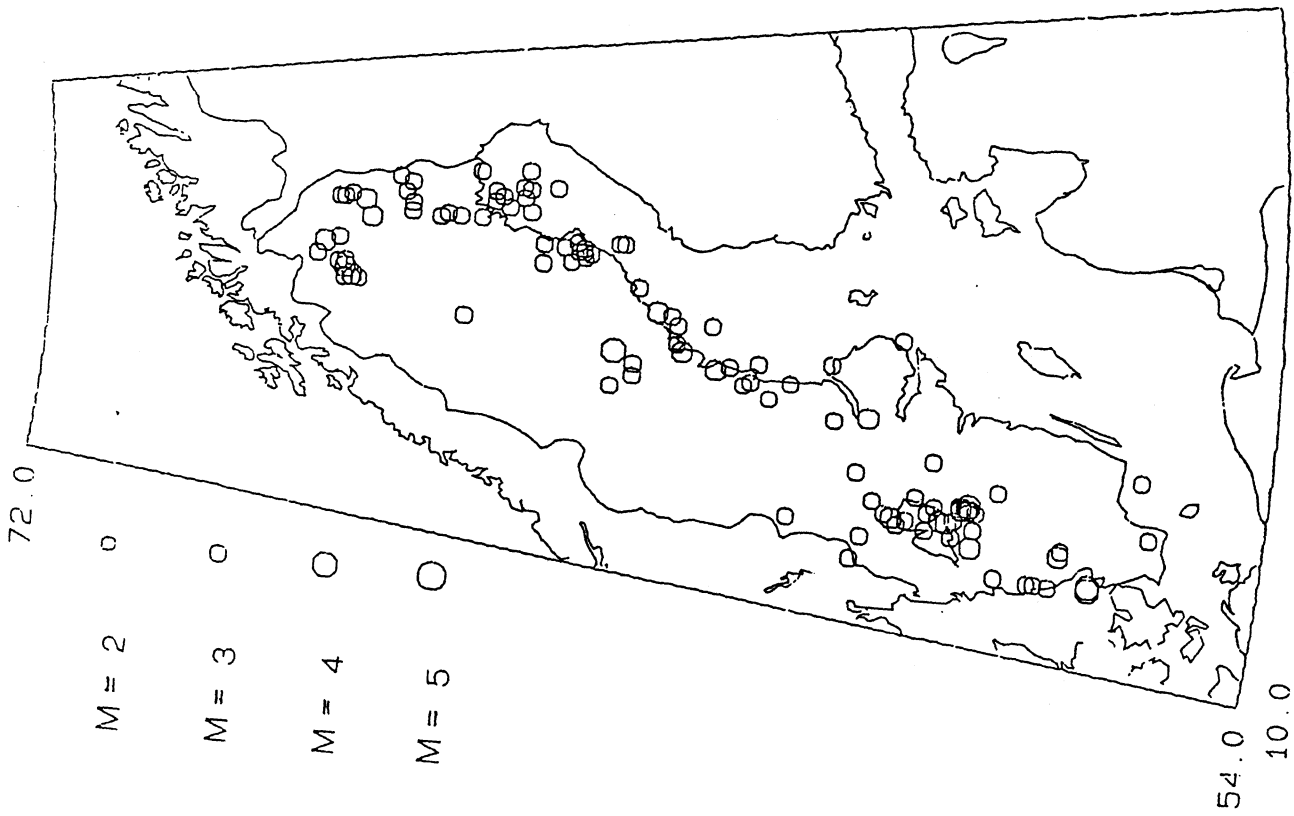


Figure 5-7 Seismicity of Sweden for earthquakes in 1963-1989 above the 90% threshold of  $M_{2.7}$ . 28.0

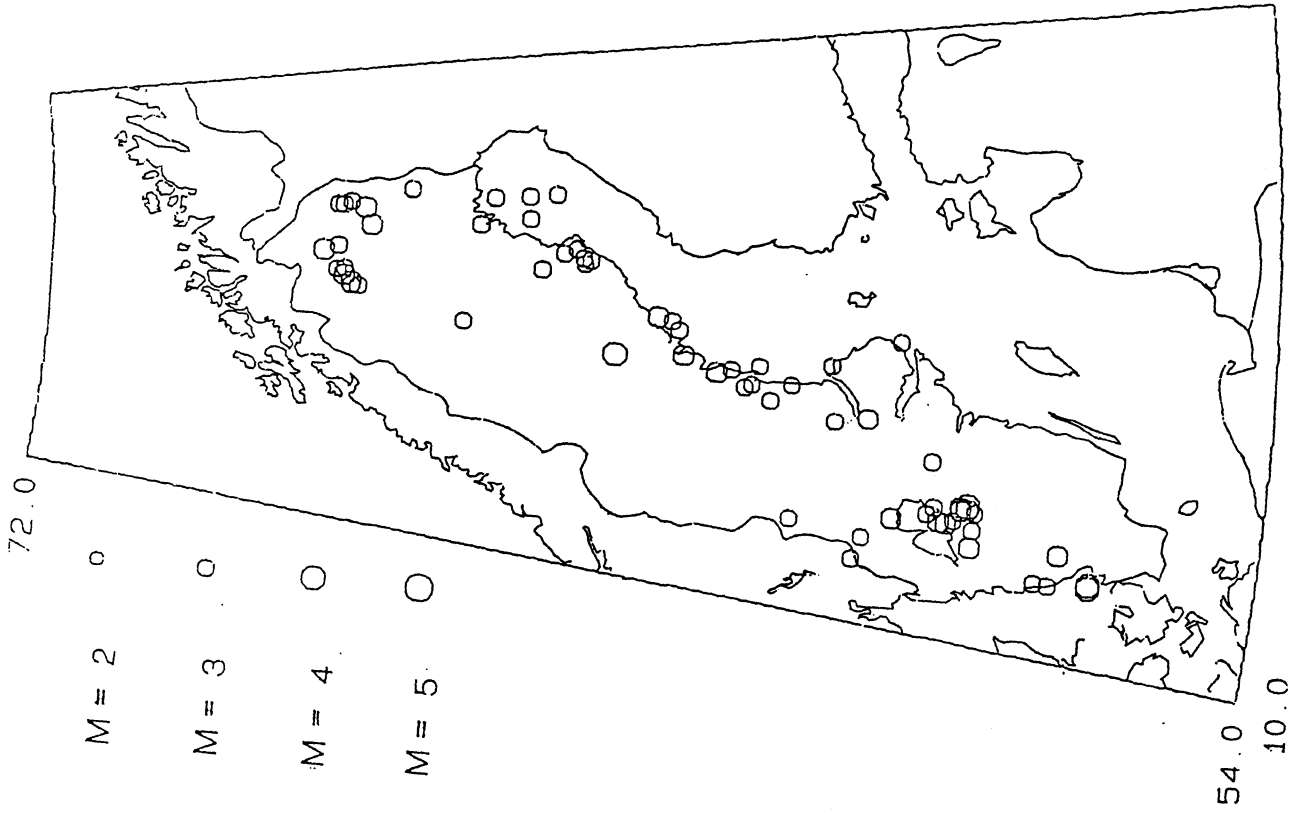


Figure 5-8 Seismicity of Sweden for earthquakes in 1963-1989 above the 99% threshold of 3.0. 28.0

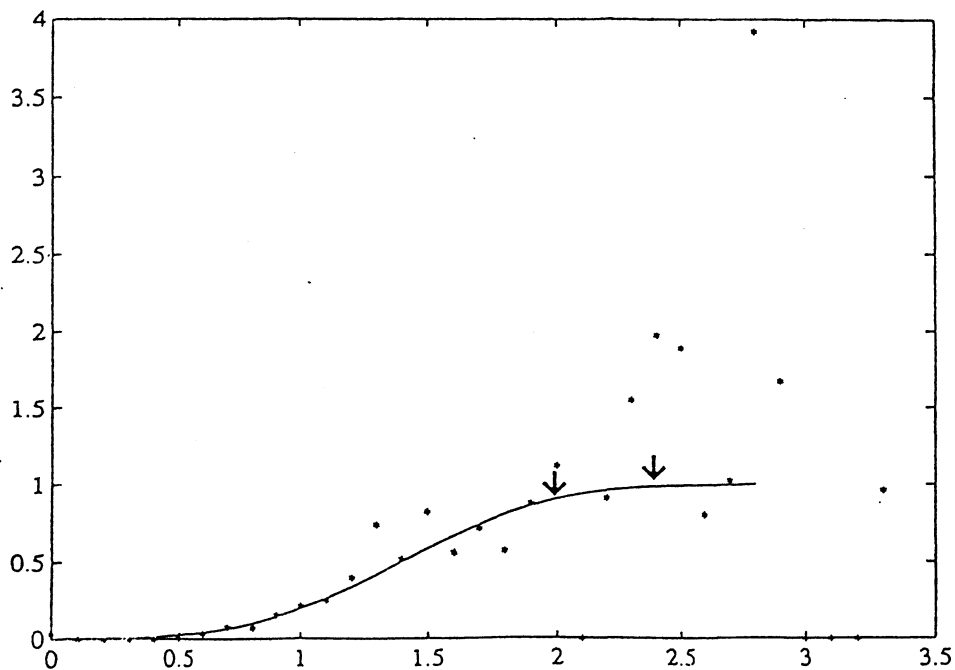
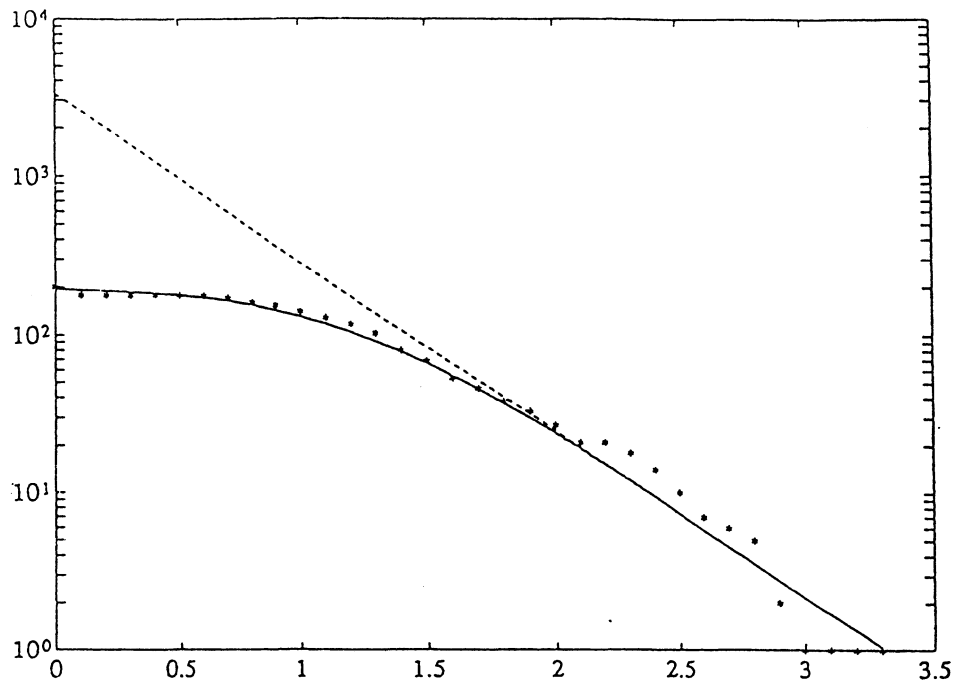


Figure 5-9 Observed cumulative number of earthquakes for Sweden south of  $61^{\circ}\text{N}$ , in 1980-1984 (during operation of the SKI network) and ratio between number observed and number predicted from the ideal Gutenberg-Richter relation.

number of sensors continued to increase in the late 1960s and later, and included the deployment of arrays. A small micro-earthquake network has operated near the Lovisa nuclear power plant since 1984 (Saari, 1990).

In Norway the deployment of TRO, BER and KON stations in the early 1960s marks the start of highly sensitive recording. Two more stations, KRK in the north and LHN, were operating during several years in the 1960s. However, a large part of Norway, from Bergen up to Tromsø, was without coverage by Norwegian seismograph stations before the 1980s and was, to a large extent, best covered by Swedish stations. The installation of the NORSAR array in 1969, although not primarily devoted to monitoring of local seismicity, increased the detectability of earthquakes in southern Norway.

Several permanent and temporal digital networks operated in Norway during the 1980s: SNS (1980-1983; Bungum et al, 1986), WNN (since 1984; Engell-Sørensen and Havskov, 1987), NORESS (since 1985), SEISNOR (since 1987; Kvamme and Hansen, 1989) and ARCESS (since 1987). There is thus a significant improvement in recent years of the types of recording instruments and number of stations. Norway is today the most densely instrumented country in Fennoscandia.

No threshold magnitudes have so far been presented for Finland but on the basis of the history of instrumentation the detectability should be at least as good as for Sweden. The obtained thresholds for Sweden can thus be used as a conservative approximation for Finland.

With the significant improvement in instrumental coverage around 1980 the estimated threshold for Southern Norway is between 2.0 and 2.5 from 1980 to 1984 according to Bungum et al (1986) and 2.2 from 1984 (Engell-Sørensen and Havskov, 1987). For northern Norway, the threshold after the introduction of SEISNOR and ARCESS in 1987 is 2.5 (Kvamme and Hansen, 1989).

For the whole of Fennoscandia, the North Sea and the Norwegian Sea, a recent study (Ahjos and Uski,

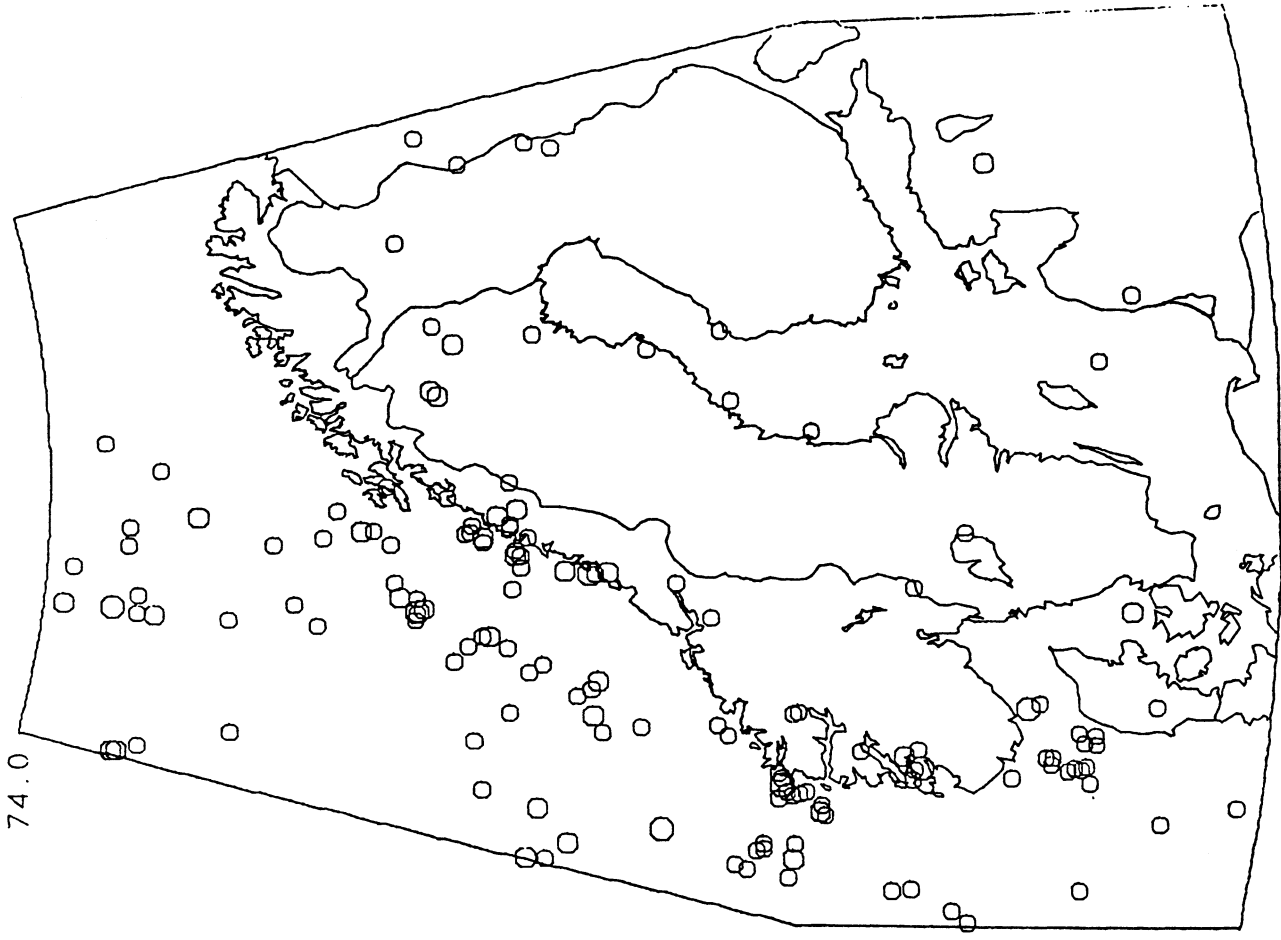


Figure 5-11 Seismicity of Fennoscandia above the general threshold of 2.7 for the years 1987-1989.

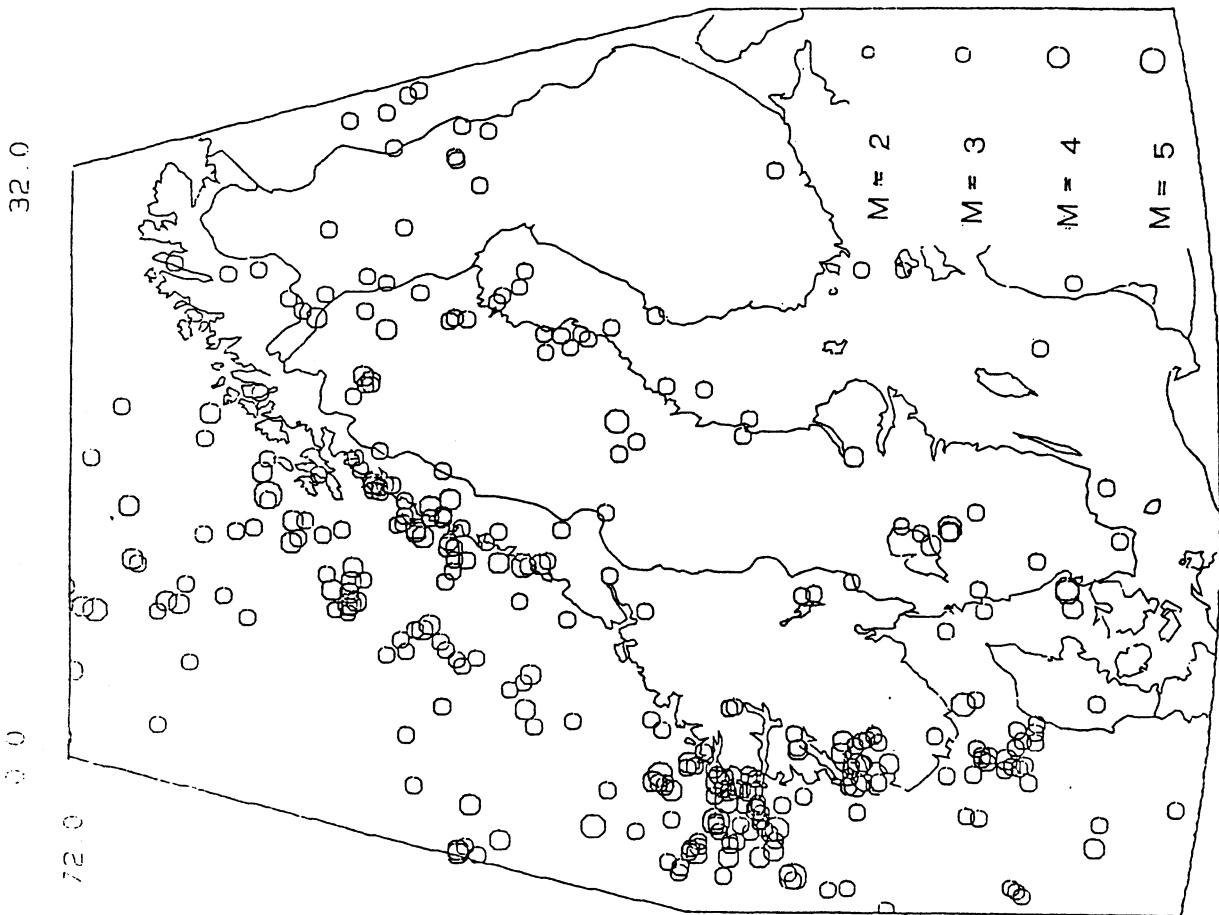


Figure 5-10 Seismicity of Fennoscandia above the general threshold of 2.7 for the years 1980-1989.

1991) indicates that the data are complete for magnitudes above 3.5 from 1973 and above 2.5 from 1985.

If thresholds are considered for Fennoscandia only, we estimate on the basis of the capability of the Swedish and Finnish networks that the threshold is probably better (ie smaller) than 3.0 in the period 1963-1979. However, the inhomogeneity for Norway before 1980 makes it unreliable to use this as a threshold for all Fennoscandia. Since 1980, when the new Norwegian stations were installed (Table 5-1), the threshold is approaching 2.7 (Figure 5-10), although probably does not reach this level for the whole of the offshore area until the inauguration of the northern Norwegian stations in 1987. Hence the best regionally consistent overview of the distribution of instrumental seismicity both onshore and offshore is provided by the complete set of events above 2.7 from 1987-1989 (see Fig 5-11).

### 5.3.3 Epicentre Location

The uncertainties in earthquake location are associated with the localisation method, the earth model, and the density and record quality of the stations. Today a number of different methods exist to locate earthquakes. Except for the old manual (graphical) techniques, most localisations use regression and iteration algorithms. Even if the computed (mathematical) error is small, the real error, ie, the deviation from the true location, may be large. Another source of error comes from the inaccuracy (simplification) of the applied earth model. In the case of Sweden the applied model is a flat-layered crust.

Due to the model inaccuracy and the sparsity of the SSSN network we estimate the location errors to be of the order of 10 - 15 km for Swedish earthquakes since 1963. For southern Sweden, during the life time of the FOA-operated network (1980-1984), the errors are most likely to be of the order of 5 - 10 km, although the mathematical errors are of the order of only a few kilometres (Slunga et al, 1984). Local earthquakes recorded with the SDU mobile station network probably have errors of only

June 15, 1985

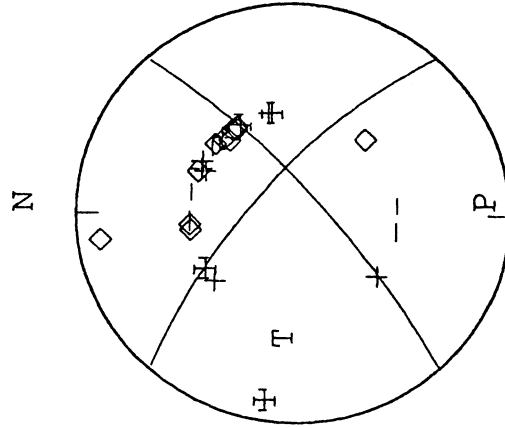


Figure 5-13 Example of a focal-mechanism solution determined from P-wave polarity data (hatched cross = full-weighted compression; + = half-weighted compression; diamond = full-weighted dilatation; - = half-weighted dilatation). Equal-area, lower hemisphere projection showing the two nodal planes, and maximum (P) and minimum (T) deviatoric stress axes for the Kattegat main shock.

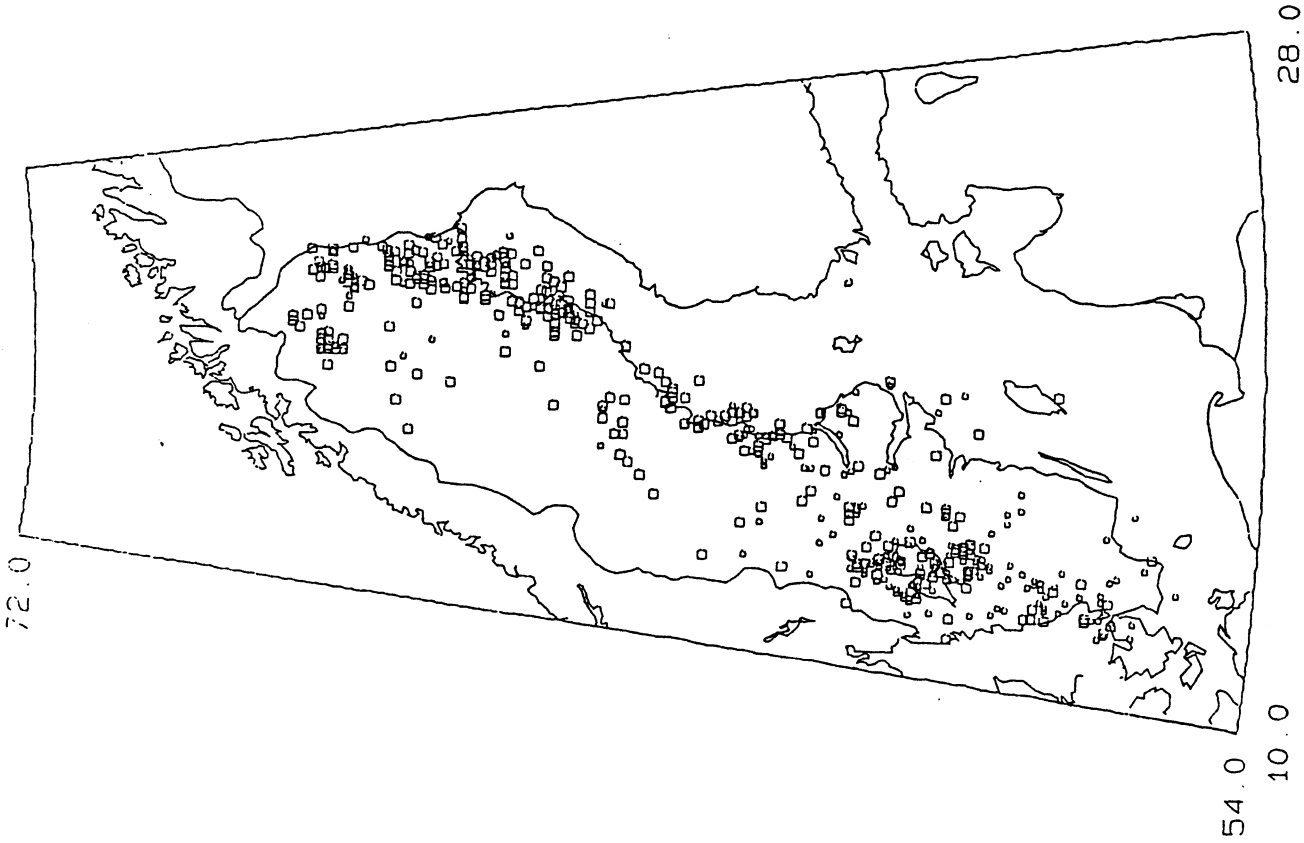


Figure 5-12 Seismicity of Sweden from 1963-1989 indicating locational uncertainty.

a few kilometres (see for example Wahlström et al, 1987, 1989). Figure 5-12 illustrates uncertainties of different sets of epicentres.

#### 5.3.4 Focal Depth

The focal depth is poorly known for most Swedish earthquakes. The depth determination is strongly dependent on all factors quoted above which are relevant for the epicentre location. Considering the sparsity of the SSSN network, the most robust depth determinations are made from near-field recorded aftershocks (assuming the focal depth of the main shock and the aftershocks to be similar), macroseismic data, observations of Rg waves (indicating depth less than about 3 km; Wahlström, 1980) and synthetic seismogram modelling. Examples where two or more of these criteria were used to determine the depth are the studies of the 1979 Bergshamra earthquake, depth less than 3 km (Kulhanek et al, 1981), 1983 Solberg earthquake, depth of about 40 km (Kim et al, 1985), and 1986 Skövde earthquake, depth of about 30 km (Arvidsson et al, 1992). A study by Arvidsson and Kulhanek (1990), based on synthetic waveform modelling, indicates another lower-crust event, depth approximately 35 km, in Swedish Lapland in 1988.

The macroseismic depths calculated in the catalogues by Kulhanek and Wahlström (1981, 1985 & 1992) are, although approximate, believed to be better estimates than those that can be obtained from instrumental travel-time data. Synthetic seismogram modelling of two events in Lapland give focal depths of about 12 km and 15 km respectively (Kim et al, 1988). Several earthquakes along the coast of the northern Baltic Sea and the Gulf of Bothnia yield recorded Rg waves, ie. indicating a depth less than 3 km (Wahlström, 1980). A list of Swedish earthquakes for which the focal depth has been derived with some certainty is given in Table 5-2.

Estimations of the focal depth from travel-time data from the denser FOA network in 1979-1984 indicate that a major part of the seismic energy is released in the upper crust, between 10 km and 15 km (Slunga, 1985).



Origin time	Location	Depth	Depth id.	Magnitude	Reference	
19670413	084619	68.1 N 20.8 E	15	S	3.7	6
19671129	092527	60.6 N 17.7 E	<3	R,M	3.0	1
19710728	232453	62.13N 17.31E	<3	R	3.1	1
19710804	120950	62.4 N 17.3 E	<3	R	2.3	1
19711006	074249	62.6 N 18.0 E	<3	R	2.6	1
19750811	182809	67.5 N 22.5 E	12	S	3.9	6
19760312	145620	61.3 N 16.9 E	<3	R	2.0	1
19770827	161454	59.0 N 12.3 E	10	M	2.2	3
19760702	115305	61.2 N 17.1 E	<3	R	2.3	1
19770905	234021	57.0 N 13.0 E	14	M	3.4	3
19790101	071729	63.5 N 16.0 E	11	M	2.5	3
19791111	235814	61.1 N 16.9 E	7	M	2.4	3
19791223	140912	59.63N 18.62E	<3	R,M	3.2	1,2
19791223	141240	59.66N 18.61E	<3	R	2.6	1,2
19791223	143329	59.6 N 18.7 E	<3	R	2.0	1,2
19800411	041912	57.92N 12.18E	11	M	2.7	4
19800725	214511	64.07N 20.25E	<5	M	2.3	4
19800913	075957	64.6 N 20.7 E	7	M	2.6	4
19801125	023951	58.44N 13.66E	8	M	2.6	4
19801217	181926	61.47N 16.96E	<5	M	2.2	4
19810213	063910	58.96N 13.81E	8	M	3.3	4
19811111	024851	57.09N 13.10E	9	M	2.9	4
19820926	134017	59.60N 16.17E	2	M	2.3	4
19830618	124343	64.28N 20.73E	8	M	3.0	4
19830712	190429	58.04N 14.54E	11	M	2.8	4
19830924	020820	58.20N 13.54E	4	M	2.0	4
19830929	050322	63.89N 17.53E	41	S,M	4.1	5
19831003	095040	59.74N 13.24E	6	M	2.2	4
19850615	004021	56.5 N 12.2 E	13	M	4.6	8
19860125	231325	61.83N 16.83E	25	S	3.2	7
19860401	095656	56.5 N 12.3 E	13	M	4.2	8
19860714	135037	58.47N 14.04E	30	S,A,M	4.5	9
19860714	144533	58.46N 13.99E	30	S,A	3.4	9
19860920	221504	58.89N 16.31E	19	S	3.6	7
19861102	074800	58.7 N 13.4 E	20	M	3.6	9
19870723	131619	61.86N 17.48E	25	S	3.0	7
19870725	953958	60.01N 12.36E	20	S	3.2	7
19880516	235020	67.43N 21.86E	35	L	3.4	7
19890725	104453	63.11N 18.86E	20	S	3.2	7

Depth identifiers: M: Macroseismic data; R: Rg waves;  
S: Synthetic seismogram; L: Arrival time location; A: Aftershocks.  
References:

- 1: Wahlström, 1980.
- 2: Kulhanek et al., 1981.
- 3: Kulhanek and Wahlström, 1981.
- 4: Kulhanek and Wahlström, 1983.
- 5: Kim et al., 1985.
- 6: Kim et al., 1988.
- 7: Arvidsson and Kulhanek, 1990.
- 8: Arvidsson et al., 1991a.
- 9: Arvidsson et al., 1991b.

Table 5-2 Swedish earthquakes for which the focal depth is well determined.

No	Date	Location		M	P	T	Plane 1			Plane 2			np	na	Me	Q	Reference		
					p	t	s	d	r	s	d	r							
1	19670413	084614.8	68.24N 20.37E	3.7	170	50	350	40	260	85	-90	80	5	-90	7	S	B	6	
2	19750811	182809.9	67.43N 22.37E	3.9	260	50	80	40	350	85	-90	170	5	90	10	S	B	6	
3	19791223	140912.9	59.63N 18.62E	3.2	153	2	246	59	36	54	50	271	51	131	12	P	B	1	
					28	-12	62	62	67	39	131	198	62	62	4	6	A	D	3
4	19800411	041912.1	57.92N 12.18E	2.7	166	5	89	-69	58	5	64	277	44	120	4	7	A	D	3
5	19800819	011316.5	61.41N 16.08E	2.6	124	-46	79	34	9	84	-66	114	25	-164	3	8	A	D	3
6	19801125	023951.5	58.44N 13.66E	2.6	119	-18	110	72	33	27	96	206	63	87	5	12	A	D	3
7	19810213	063910.4	58.96N 13.81E	3.3	129	-15	43	17	176	89	23	86	67	178	10	11	A	B	3
					110	12	224	61	0	62	61	230	39	132	10	P	D	2	
8	19810220	183122.3	60.23N 15.92E	2.5	145	51	55	-1	177	57	-42	293	56	-139	3	8	A	D	3
9	19811030	095256.3	55.70N 13.82E	2.8	7	-46	39	39	294	86	-107	192	17	-12	3	8	A	D	3
10	19811111	024851.6	57.09N 13.10E	2.9	136	-1	226	32	266	69	156	6	67	23	5	11	A	D	3
11	19820630	171511.9	55.93N 15.38E	2.8	156	-29	65	-2	114	71	-157	17	68	-20	4	8	A	D	3
12	19830712	190429.9	58.04N 14.54E	2.8	146	-35	55	0	106	66	-154	5	66	-26	7	8	A	D	3
13	19830929	050322.7	63.89N 17.53E	4.1	143	47	307	42	225	88	-82	329	8	-166		S	A	4	
					7	45	119	20	58	75	-50	165	42	-157	6	11	A	C	3
14	19850615	004021	56.5 N 12.2 E	4.6	179	4	271	25	312	70	165	47	76	21	33	P	A	9	
15	19860125	231325	61.8 N 16.9 E	3.2	357	33	243	33	120	90	-130	30	40	0	12	S,P	B	7	
16	19860401	095656	56.5 N 12.3 E	4.2	176	48	290	20	337	40	-154	227	74	-53	22	P	A	9	
17	19860714	135037	58.47N 14.04E	4.5	125	30	235	30	180	90	-45	270	45	-180	30	S,P	A	10	
					124	5	216	22	258	71	168	352	78	20	6	7	A	C	5
18	19860714	144533	58.46N 13.99E	3.4	133	14	227	14	180	90	-20	270	70	-180	8	S,P	B	10	
					107	-1	196	43	340	61	33	232	62	146	3	6	A	D	5
19	19860920	221504	60.0 N 16.2 E	3.6	304	52	40	5	340	60	-45	97	52	-141	16	S,P	B	7	
20	19861102	074800	58.7 N 13.4 E	3.6	350	72	227	11	122	59	-111	338	37	-60	20	P	B	10	
					112	-18	27	15	70	66	-178	339	88	-24	6	8	A	D	5
21	19870419	123952	67.78N 19.66E	3.4	269	48	155	20	189	40	-26	38	74	-127	10	P	B	7	
22	19870723	131619	61.7 N 17.5 E	3.0	24	24	126	24	75	90	-35	165	55	-180	14	P	D	7	
					166	-52	38	-25	107	75	-117	351	31	-30	3	5	A	D	8
23	19870725	053057.4	60.03N 12.37E	3.1	288	27	32	27	340	90	-40	70	50	-180	11	P	B	7	
					91	-12	16	49	39	47	148	152	67	48	4	6	A	D	8
24	19880516	235020.8	67.43N 21.86E	3.4	277	8	182	34	325	60	20	225	73	149	12	S,P	B	7	
25	1989 725	104453.5	63.03N 18.82E	3.2	50	62	152	7	215	45	-130	85	57	-57	13	S,P	B	7	
26	1990 524	095156.8	56.56N 12.06E	3.3	188	24	293	30	328	50	176	61	87	40	11	P	D	9	

M: Magnitude; P: Compressional axis; T: Tensional axis; t: Trend; p: Plunge; s: Strike; d: Dip; r: Rake;  
 np: Number of P-polarities; na: Number of amplitude data;  
 Me: Method used: A: amplitudes together with P-polarities, P: P-polarities, S: synthetic waveform modeling;  
 Q: Quality indicator A, B, C, D (see text).  
 References:

- 1: Kulhanek et al., 1981
- 2: Kulhanek et al., 1983
- 3: Slunga et al., 1984.
- 4: Kim et al., 1985.
- 5: Slunga and Nordgren, 1987.
- 6: Kim et al., 1988.
- 7: Arvidsson and Kulhanek, 1990.
- 8: Slunga and Nordgren, 1990.
- 9: Arvidsson et al., 1991a.
- 10: Arvidsson et al., 1991b.

Table 5-3 Earthquake focal mechanism parameters.

For the vast majority of recent Swedish earthquakes, lack of information of the aforementioned types prevents determination of the focal depth. From the calculations made and referred to above, it is obvious that earthquakes occur over the whole depth range of the crust. Thus, it is striking that two of the very largest Swedish earthquakes during the instrumental time, in Solberg 1983 and Skovde 1986, are located in the lower crust.

#### 5.3.5 Crustal Stresses and Earthquake Focal Mechanisms

Earthquake focal mechanism studies often represent the only way to extract information and understanding of the deformation in the crust, especially below a few kilometres depth. From the double-couple assumption of the earthquake source (eg. see Aki and Richards, 1980) a symmetrical pattern of the waveform with two possible focal planes are obtained. Independent information is needed to derive the actual fault plane from the two possible planes, eg. correlation with observed surface faulting or geological structures, or spatial distribution of aftershocks. Usually, however, none of these additional pieces of information exist with any certainty and the ambiguity in determining the actual fault plane persists. The best constrained case in Sweden so far is the Kattegat earthquakes (events 14, 16 and 26 in Table 5-3) and their probable connection to the neotectonic Skålderviken depression (Arvidsson et al, 1991). The focal mechanism for the Kattegat main shock is shown in Figure 5-13.

Focal-mechanism determinations for small earthquakes recorded only at short distances are problematic. Usually only data from a few stations with high-frequency recording are useful. The high frequencies are sensitive to local, small-scale structures which may introduce errors in the derived focal mechanisms. Small size events also give a small signal-to-noise ratio which makes the use of the signals more uncertain.

Methods applied to derive Swedish earthquake mechanisms are the classical first-motion direction (polarity) of P-waves (Kulhanek et al, 1981, 1983

Arvidsson et al, 1991, 1992), amplitudes of P- and S-waves (Slunga et al, 1984, Slunga and Nordgren, 1987, 1990, Slunga, 1989b) and synthetic waveform modelling (Kim et al, 1985, 1988, Arvidsson et al, 1992). Common problems for all methods are uncertainties in the location (not least focal depth) and earth model, but in wave form modelling these uncertainties can be minimised in an iterative procedure.

First motion studies can be robust when a large amount of data is at hand, say more than 20 polarities with good azimuthal spread. Care must be exercised when selecting the data, eg in the distance range 130 km to 170 km where Pg and Pn phases may be confused.

The method of using spectral amplitudes of P- and S-waves - together with P-polarities when available - as introduced by Slunga (1981) possibly fits data at short distances. A drawback is the heavy influence of the local structure where deflections of the applied model from the true earth may give large errors in the mechanism.

Waveform modelling is probably the most robust method, especially in combination with polarity observations. Possible deviations from the applied velocity model can be observed when the modelled seismogram is compared to the observed one. One advantage is that all the seismogram is used, not only the first part of the P- and/or S-coda as in the other methods.

Due to the different methods and the variation in the amount and quality of data, a quality and importance ranking of mechanism solutions has been done:

- A Well constrained focal mechanism with magnitude 4.0 or larger.
- B Well constrained focal mechanism with magnitude 2.5 - 3.9.
- C Poorly constrained focal mechanism with magnitude 4.0 or larger.
- D Poorly constrained focal mechanism with

magnitude 2.5 - 3.9.

A "well constrained focal mechanism" has been determined from waveform modelling, P-wave polarities, or amplitudes together with P-wave polarities, with good azimuthal coverage of data. The solution should be nonambiguous. That large earthquakes are ranked as more important than small reflects the greater seismotectonic significance of the former with larger stress release and deformation. Mechanisms of earthquakes below magnitude 2.5 are generally not considered reliable (cf above). However, a well constrained focal mechanism may be derived for an earthquake below magnitude 2.5 provided a sufficiently dense network is at hand.

Available mechanisms of categories A, B, C and D are listed in Table 5-3. Most of them belong to D but 16 events have quality A or B. These events have various faulting styles (Table 5-3; Figure 5-14). Some have a mechanism indicating extensional stresses (1, 2, 13, 15, 17, 19, 20, 21, 25). The four earthquakes with magnitudes above 4 (13, 14, 16, 17) are more or less anomalous relative to the ridge push hypothesis (Arvidsson et al, 1992). The mainly northwesterly oriented compressive stresses in south-central Sweden possibly relate to ridge push forces. However, the scatter of different types of mechanisms (Figures 5-14, 5-15), ranging from normal to thrust faulting, indicates that, as in Norway (Bungum et al, 1991), there may be several contributing factors beside ridge push.

#### 5.4 **PALAEOSEISMICITY**

##### 5.4.1 **Palaeoseismic Observations**

Similar problems of interpretation to those encountered in claims of neotectonic surface faulting beset palaeoseismic observations. Palaeoseismology depends on the discovery of permanent changes in superficial deposits consequent on earthquake vibration. The problem with palaeoseismic interpretations is that many of these effects are not so much the product of vibration as of gravitational instability triggered by vibration. The energy flow that is recorded,

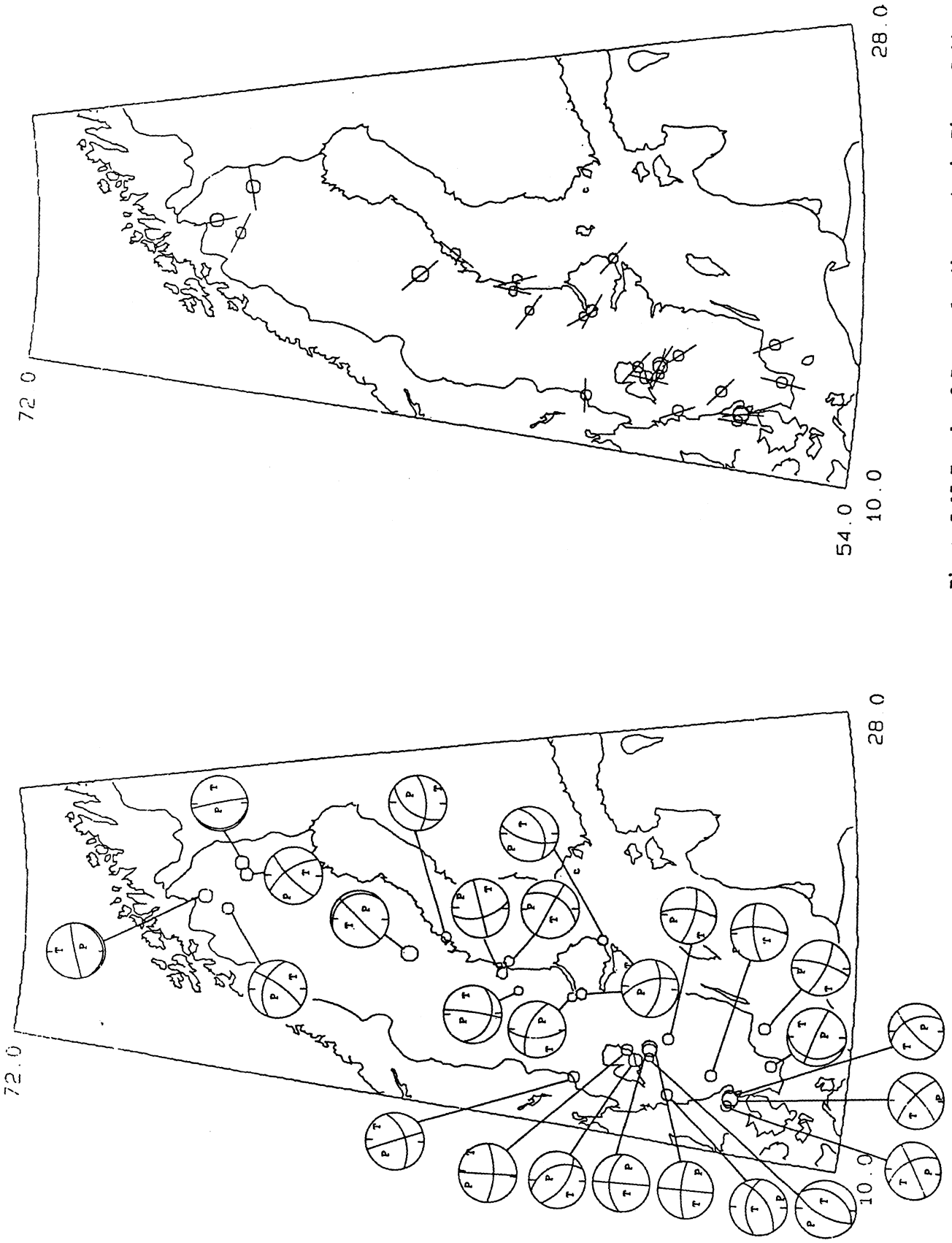


Figure 5-14 Lower hemisphere projections of focal-mechanism solutions for Swedish earthquakes. Symbols as in Figure 5-13.

Figure 5-15 Trends of P-axes for the events in Figure 5-14.

whether in a disturbed sediment, slump structure or landslide is that resulting from the force of gravity and hence almost all palaeoseismic phenomena are capable of being triggered by alternative non seismic processes, such as a simple slope failure or heavy rain. The chief diagnostic of palaeoseismicity is not the individual example but a whole series of examples that can be demonstrated to have formed synchronously, over a relatively large area.

The diagnostics of palaeoseismic processes have been established through studies of superficial effects of recent major earthquakes, their nature, appearance, location relative to the earthquake, significance with respect to the severity of ground motion etc. As with neotectonic surface faulting, palaeoseismicity may not provide the sole interpretation for the phenomenon. Important questions to be asked include:

- Is the phenomenon one that has been observed forming as a result of ground shaking in a recent earthquake?
- Is the deposit in question capable of explanation without an earthquake?
- How many other similar indicators have been found?
- Over what area have they been located?
- Can synchronicity be demonstrated?
- Is there any confidently demonstrated neotectonic fault movement in this region of the same age?
- Is there any other likely cause of the disturbance?

Even when simultaneity of a number of different examples can be demonstrated it is worth assessing whether there are any other potential regional scale disturbances likely to have affected all these deposits at the same time: viz. ice-dammed lake drawdown, major landslide, meteorite, torrential rain etc.

As with neotectonics it is possible to rank observations according to the degree to which they are consistent with an earthquake origin. This has not been attempted here.

#### 5.4.2 Fennoscandian Palaeoseismicity

By far the best studied potential palaeoseismic indicators in the region are the landslides and graded till deposits found in northern Sweden and Finnish Lapland. The widespread occurrence of landslides in this region was first noted by Kujansuu (1972) who identified about 40 large landslides (or earth-flow features) developed in till, on shallow slopes (typically 2-4 degrees) and with volumes of 0.5 - 1.5 million cubic metres. The slides had moved when the till had been highly liquefied. All but one of the slides showed a close correlation with fault-scarps identified by Kujansuu (1964). More of these landslides were discovered in Swedish Lapland by Lagerbäck (Lagerbäck and Witschard, 1983) again showing a striking correspondence with the late-glacial faults. Age dates for peat deposits formed adjacent to these landslides provided minimum ages of 8280 years BP in Finland (Kujansuu, 1972) and 8140 years BP in Sweden (Lagerbäck, 1990). These ages are consistent with formation immediately following deglaciation. One of the Finnish landslides discussed by Kujansuu appears to have developed adjacent to a wall of stagnant ice; another one described by Lagerbäck appears to have flowed over stagnant ice.

These landslides all appear to have formed around the same time, and this, allied with the low gradients on which they have formed and the remarkable extent of liquefaction required to create the flow-slides, lend support to an association with one or more earthquakes. The liquefaction of the till deposits may not, however, have solely been due to ground shaking and could reflect the expulsion of groundwater as a result of strain changes accompanying the fault movements. Earth flows as a result of the emergence of groundwater are known from a number of earthquakes (see Muir Wood and Steedman, 1992). For the



reverse faults of this region, the expulsion of water can be predicted to be concentrated around or beyond the ends of the faults.

In the region of the Lansjarv Fault, Lagerbäck has reported the widespread occurrence of liquefaction deposits filled with flame-shaped bulges and dewatering structures (Lagerbäck, 1990). The most spectacular of these are graded till sequences identified from the existence of shallow depressions in the till surface, without any visible boulders. Trenches through these deposits have revealed size sorting of till fragments down to a depth of 5-6 m, with a considerable reduction in porosity and increase in density. These graded tills have only been found on the hangingwall of the fault and beneath the highest contemporary shoreline. Lagerbäck (1990) has attributed these formations solely to the effects of prolonged ground shaking. Geotechnical considerations suggest that it is impossible to achieve the sorting of the sediments without prolonged shaking in the liquefied state, and while this could reflect a series of aftershocks following the initial seismic event, the pronounced compaction of these sediments requires some overlying load, such as a grounded iceberg. This in turn could explain why these graded tills are only found on the uplifted hangingwall of the fault where it was below the contemporary sea-level.

Outside northern Sweden and Finnish Lapland there are few well-documented studies of potential palaeoseismic exposures, although there do exist a number of poorly reported instances of deformed varves, slumps etc. (see for example Mörner, 1985). The attribution of these to earthquake shaking requires more detailed field investigations and dating studies, than appear to have been performed up to now. From what is already known however there is a marked difference in the degree to which clear evidence of palaeoseismic phenomena is encountered in northern Sweden relative to other parts of the country, suggesting that enhanced seismic activity during and following deglaciation was not uniformly distributed.

#### 5.4.3 Swedish 'Palaeoseismic Indicators'

One curious feature of Swedish literature on palaeoseismology, is that a whole range of phenomena with no obvious connection with earthquakes, have been assumed to be palaeoseismic indicators. The most widely cited of these is the disruption of bedrock as an indicator of strong ground motion. This notion was initiated by De Geer (see De Geer, 1938, 1940) and has subsequently been championed by a number of other authors most notably Mörner (see for example Mörner, 1978), as well as in a separate lineage of literature on 'boulder caves' (see below). None of the authors, including De Geer, have ever referenced empirical observations of recent earthquakes at which the disintegration of a crystalline bedrock surface, as a result of strong ground motion, has ever been observed. Instead the idea is kept in circulation by internal reference to other Swedish papers.

The ultimate source for all this work seems to have been a simple misunderstanding of earthquake-related phenomena by De Geer, that has been sustained by Mörner. In effect De Geer appears to have employed the term 'earthquake' in much the same way that it was used before about 1900 to encompass any sudden process taking place in the rocks close to the earth's surface (including what we would now categorise as volcanic eruptions, landslides, rock-slides, rockbursts and true earthquakes).

The disruption of a bedrock surface is not a process that can be directly correlated with earthquakes. Rockfalls have been found on steep slopes, following earthquakes (and commonly occur in the absence of earthquakes). Unlike landslides caused by the build-up of pore pressures as a result of liquefaction, the instability is inherent to the rockmass itself. The periods and amplitudes of earthquake ground motion, even close to the earthquake source, are incapable of causing the disintegration of relatively flat-lying crystalline bedrock. Hence bouldery tills, fragmented bedrock, boulder caves etc, should not be considered as palaeoseismic (ie. ground-motion) indicators. They may, as discussed below, directly reflect some other style of shallow stress-relief phenomenon.

Two other palaeoseismic indicators employed by Mörner that also do not appear to reflect any empirical association with earthquakes are: varve sedimentation rates, and the position of an esker, both in the vicinity of Stockholm. The movement of the line of an esker by about 5 km was attributed by Mörner to an 'earthquake' (Mörner et al, 1989), as was the existence of an overthickened varve (Mörner, 1978). Increased sedimentation has numerous potential causes, besides any potentially related to an earthquake, while there is no logical connection between a 5 km shift in the line of an esker and a seismic event. As with De Geer, it appears that (sustaining the 19th Century use of the term) any unusual phenomenon is termed an 'earthquake'.

#### 5.4.4 Shallow Stress-Release Phenomena?

There are a number of observations of the disruption of the bedrock surface in parts of Sweden, to form either bouldery moraines (De Geer, 1938) (if the disruption occurred close to the ice-front during deglaciation) or so-called boulder caves ( De Geer, 1940, Bergsten, 1943, Sjöberg R, 1987). Both boulder caves and bouldery moraines were attributed to earthquakes by De Geer, but it is clear that the disruption of the bedrock surface has a number of other possible explanations relating to ground-water pressure (beneath the front of the ice-sheet, see Talbot, 1990b), or frost-shattering and rockslides. Almost all the so-called boulder caves have formed within the large blocks of talus in massive rock-slides (Sjöberg R., 1987). However the attribution of rockslides to strong earthquake ground motion is in general too indirect unless a large number of slides can be dated to have formed simultaneously.

None of the most massive rockslides known from Norway in the past few centuries show any association with earthquakes (Ambraseys, 1985b). It is however possible that some of the disrupted Swedish rockmasses reflect shallow stress relief phenomena as the result of very high horizontal stresses at some period following deglaciation. As one example Agrell (1981) reported from a boulder

cave north of Stockholm at which "it seems as though the whole mountain has been blasted". Shallow stress-relief phenomena are relatively common around the southern Canadian border with New England and the Great Lakes (see Adams, 1989) and have been observed forming in the past few decades as a result of quarrying. Further research is required to date the rockslides and also identify those (if any) which genuinely cannot be explained as a result of frost shattering and gravitational collapse.

## 6 STRESS OBSERVATIONS

### 6.1 INTRODUCTION

The in situ stresses in the Earth's crust prior to excavation are an important parameter needed to design safe mines, underground excavations and vaults for nuclear waste in particular. Knowledge of the in situ stresses also provides an important insight into crustal dynamics.

Numerous measurements of in situ stress have been conducted throughout the world and published during the past 35 years, both for specific mining and civil engineering projects as well as for research programmes. One of the first compilations of stress magnitudes and stress directions over large areas was presented by Hast (1958). Based on a fairly large number of measurements in mines and rock engineering projects he demonstrated the existence of large, horizontal stresses in the Earth's crust. For more than twenty years Hast was collecting stress data, mainly from Fennoscandia, that supported his hypothesis that the horizontal stresses were in excess of the vertical stress.

In 1980, Zoback and Zoback (1980) presented a compilation and a map of horizontal stress orientations for the contiguous United States that inferred the principal stress directions from geological data, focal mechanisms of earthquakes and in situ measurements. They found the stress orientations to be quite uniform within a given geological domain of the continent and they were able to draw several conclusions about the tectonics of the area and how they could be related to plate tectonics.

Currently the World Stress Map Project of the International Lithosphere Program is compiling a global data base of in situ stress measurements in the crust (Zoback et al, 1989; Mueller et al, 1991). Results of the compilation demonstrate significant scatter in the stress field of Fennoscandia compared to many other intra plate regions. A similar scatter also seems to be the case for other Pre-Cambrian shield areas (Zoback et al, 1989; Brown and Windsor, 1990).

The content of this section covers a short history of stress measurements in Fennoscandia. (Descriptions of the methods of stress observation are to be found in a separate report to SKB.) The Fennoscandian Rock Stress Data Base is presented in Section 6.3. Results of compilation of data for the World Stress Map are presented in Section 6.4, together with the subset of data covering Europe. This section also highlights the Fennoscandian stress field in relation to the rest of Europe.

## 6.2 **SHORT HISTORY OF ROCK STRESS MEASUREMENT**

During the 1950s, in the design of safe underground mines and hydroelectric power stations, rock engineers became aware of the importance of a good understanding of rock stresses. This created the need for developing techniques to measure the virgin stresses.

### 6.2.1 **Sweden**

Measuring rock stress by the overcoring method with the magnetostrictive cell was first conducted in 1951 in the mines of Trafikaktieb-olaget Grangesberg-Oxelosund at the Grangesberg iron ore mine, Central Sweden, by Hast. A preliminary report on the subject was presented as a lecture to members of the Swedish Mining Association and later published in a Swedish journal for engineers.

After completing stress measurements in six mines in Sweden and Norway, Hast published the classical paper "The measurement of rock pressure in mines" (Hast, 1958). His results, in particular the measured excess of horizontal stresses over vertical stresses in the upper part of the Earth's crust, were controversial to the earth scientists of the late fifties. None of the mechanisms he suggested for generation of the excess horizontal stresses were relevant. Today we know that most intraplate regions of the world are characterised by uniformly oriented compression due to the plate tectonics.

Hast patented his stress measuring cell which prevented other groups getting access to stress measurements. Therefore, following the development

by Leeman, the Swedish State Power Board (SV) developed the two-dimensional door-stopper method, and later the three-dimensional overcoring method with strain gauges (Hiltscher, 1969). These methods were primarily used for measurements in underground hydropower caverns and tunnels. In 1979 the group at SV completed the development of a new overcoring technique that allowed measurements to be taken in 500m long diamond boreholes from the ground surface (Hiltscher et al, 1979). This was a major improvement in stress measuring techniques.

The original Leeman cell was later modified by Leijon. Improvements were made in the hole-cleaning technique, the installation tool, the readout equipment and the arrangement of the strain gauges (Leijon, 1986). The new equipment was developed at Lulea University of Technology and is named the LuT-cell. It is the most widely used overcoring stress measurement technique in Sweden today.

For almost two decades, the Stripa mine in Central Sweden, has been the site for field testing, to evaluate the feasibility of storing radioactive waste in hard rocks. In 1981/82 Doe et al (1983) carried out a programme of in situ stress measurements using hydro-fracturing in combination with a variety of overcoring techniques. This was the first comparison of hydraulic fracturing and overcoring techniques in the same deep borehole and the first hydraulic fracturing stress measurement in Sweden. In 1982 the Division of Rock Mechanics at the Lulea University of Technology built its first mobile hydro-fracturing system (Stephansson and Angman, 1986), which has now been used to measure stresses at twenty three sites in Fennoscandian bedrock (Bjarnason et al, 1989a).

Under states of stress where none of the principal stresses are parallel to the borehole the conventional hydro-fracturing is not applicable. To overcome this problem hydraulic tests on pre-existing fractures (HTPF) have been introduced (Ljunggren (1990).

### 6.2.2 Norway

The first stress measurements in Norway were carried out by Professor Hast in 1958. The Mining Department of the Norwegian Institute of Technology (NTH) started their first tests in 1964 with an early version of the USBM cell. This was followed by extensive development of the door-stopper method during the years 1965-67 (Li, 1967). Starting in the late 1960s scientists at NTH have been continuously refining the three-dimensional overcoring technique according to Leeman.

Today the majority of mining companies in Norway are using the rock stress measurement device of NTH in their mine planning and operation (Myrvang and Grimstad, 1981). During recent years a combination of triaxial stress measurements by SINTEF of NTH and simple hydraulic fracturing by the Norwegian Geotechnical Institute (NGI) has been carried out in unlined pressure shafts of hydroelectric power plants. Offshore Norway, numerous analyses of borehole breakouts have been conducted. The results are discussed in conjunction with the interpretation of the European Stress Map.

### 6.2.3 Finland

The first measurements of the state of stress in Finnish bedrock were conducted in the Tytyri limestone mine of the Lohja Co by professor Hast's measurement team in 1961. The company bought Hast's equipment and in the sixties, Lohja Co stress measurement group was the only one conducting stress measurements in Finland. It performed about 60 measurements at 9 different mines. The results were used mainly in mine planning. In 1970 a Leeman device modified by the Norwegian Institute of Technology (NTH), Trondheim, was purchased by the company for true triaxial measurements. In 1971 all equipment and contracts were transferred to a state-owned mining company, Suomen Malmi OY Finnprospecting.

In the 1980s measurement of stress became a standard design parameter for all major underground projects in Finland, both for mining and civil projects, mainly employing the Leeman-NTH device



(Matikainen, 1988). As of the summer of 1986, 170 measurements were completed at 45 different locations in Finland, mainly located in mining districts, major cities, and industrial areas being considered for underground storage facilities. Later in the 1980s, a number of hydraulic fracturing stress measurements and hydraulic testing of pre-existing fractures were conducted in deep boreholes at the potential sites for storage of radioactive waste (Klasson and Leijon, 1990). All the hydraulic fracturing stress measurements were conducted by personnel from RENCO AB of Sweden using the method and equipment of the Lulea University of Technology.

### 6.3 **FENNOSCANDIAN ROCK STRESS DATA BASE (FRSDB)**

The Nordic countries have a long tradition in rock stress measurements. The work by Zoback and Zoback (1980) stimulated a group of Nordic scientists to establish the Fennoscandian Rock Stress Data Base (FRSDB) in 1986. The main objectives of the FRSDB were to locate as much data as possible to determine any systematic variation with respect to rock types, geological structures, strength, elastic parameters etc. An additional goal was to establish regional trends in the stress regime within Fennoscandia (Stephansson et al, 1986, 1987). Specific measurements and the data trends are now widely used for rock engineering purposes in Fennoscandia. The data base also provides a foundation for further local and global stress research.

#### 6.3.1 **Current State of the FRSDB**

The rock stress data base was designed and implemented using KNOWLEDGEMAN 1.07 which is a general data handling software package for microcomputers. A listing of entries in the data base is shown in Figure 6-1. References to published data are always presented with: (i) site Latitude and Longitude coordinates; (ii) stratigraphy of the measuring site in accordance with the chronostratigraphic scheme of the geological map of the Baltic Shield (Stephansson and Ljunggren, 1988); (iii) along with the geology

Output of post # 100

FRDSB Version 2.0A

Country : Sweden Year : 1983  
 Site : FJÄLLBACKA  
 Measuring group : SWEDISH STATE POWER BOARD  
 Method : SSPB  
 Information given by : SSPB  
 INPUT INTO NRSDB BY L-O DAHLSTRÖM

References :  
 ROCK STRESS MEASUREMENTS IN LERVIK, FJÄLLBACKA. L. STRINDELL,  
 1983. REPORT L-645, SWEDISH STATE POWER BOARD.

Measuring Station : LERVIK, LEVEL 2

Coordinates : X= 0 Y= 0 Z= 0 (17.0, 15.2)  
 Long. : E11/17/00 Latt. : N58/36/05

Vertical overburden (m): 22  
 Topography : Slightly Hilly  
 Direction of measuring hole (Deg) = 0 Dip (Deg) = 0

Density (kg/m<sup>3</sup>) : 3000  
 Uniaxial Compressive Strength (MPa) : 125.5  
 Tensile Strength (MPa) : 5.3  
 Young's Modulus (GPa) : 50.0  
 Poisson's Ratio : 0.2

Magnitude and Direction of Principal Stress :  
 Sigma1 (MPa) = 28.2 Direction (Deg) = 56 Dip (Deg) = 55  
 Sigma2 (Mpa) = 17.4 Direction (Deg) = 203 Dip (Deg) = 30  
 Sigma3 (MPa) = 8.6 Direction (Deg) = 303 Dip (Deg) = 15

Vertical Stress (MPa) : 24.1  
 Maximum Horizontal Stress (MPa) : 20.5  
 Minimum Horizontal Stress (MPa) : 9.6  
 Direction of Maximum Horizontal Stress (Deg) : 38

Comments :  
 AVERAGE VALUE OF TWO MEASUREMENTS  
 LEVEL 2 MEASUREMENT HAS UNEXPECTED HIGH VALUES

Figure 6-1 Listing of entries in the Fennoscandian Rock  
 Stress Data Base for a stress measuring site in  
 Sweden.

of the test site employing a list of 90 rock types together with a list of different geological structures are used to describe the geology of the test site. For a number of the rock stress measurement sites, rock testing has been done and these data (uniaxial compressive strength, Young's modulus etc) are also stored in the data base. Magnitude and direction of principal and horizontal stresses are presented as the last entry for each measurement.

Stress data influenced by underground structures, such as mines, tunnels and excavations, are omitted, as are stresses interpreted from focal mechanism studies of earthquakes and mapping of geological structures.

The test methods used to measure the stress, the number of entries to the FRSDb for each method and its maximum depth of measurement are shown in Table 6-1. As of June 1990 the data base contained more than 500 entries.

Stress measuring method	Number of entries	Maximum depth (m)
Door-stopper	3	900
Overcoring NTH/LUT	142	1250
Overcoring Hast	136	880
Overcoring Hiltcher	87	665
Hydraulic fracturing	140	1000
Soft inclusion	1	570

Table 6-1 Current state of Fennoscandian Rock Stress Data Base

### 6.3.2 Stress Versus Depth

The variation of stress as function of depth can be simply extracted from the FRSDb. Principal stress versus depth for the Leeman triaxial overcoring

methods are well known to show an increase with depth, as demonstrated by many investigators (Klasson and Leijon, 1990). The stress gradients at about 500 m depth in the Baltic Shield are of special interest to nuclear waste repository design. The scatter in the data points when compiling all overcoring data is shown in Figure 6-2.

Linear regression analyses of maximum and minimum horizontal stresses versus depth for four different measuring methods are shown in Figure 6-3. The analysis of data using the overcoring method of Hast's measuring technique gives the largest stress gradient and the largest stress values at the bedrock surface, while hydraulic fracturing results give the smallest stress gradients and the smallest stresses at the bedrock surface. All hydrofracturing stress data in the FRSDB are calculated according to the second breakdown method (Doe et al, 1983). All of the reported vertical stresses were assumed to be equal to the stresses generated by the weight of the overburden.

The following conclusions can be made regarding the variation of stress with depth:

- There is a large horizontal stress component in the uppermost 100 m of the Fennoscandian bedrock.
- The variation of stress magnitude with depth depends on the rock stress measurement technique.
- Generally, the maximum and minimum horizontal stresses exceed the vertical stress (when the vertical stress is estimated from the weight of the overburden).
- Stress measurements from the Leeman, Leeman-NTH and Leeman-LuT overcoring methods have revealed minor differences in the magnitudes of the minimum horizontal stress,  $S_h$ , and the vertical stress  $S_v$ .

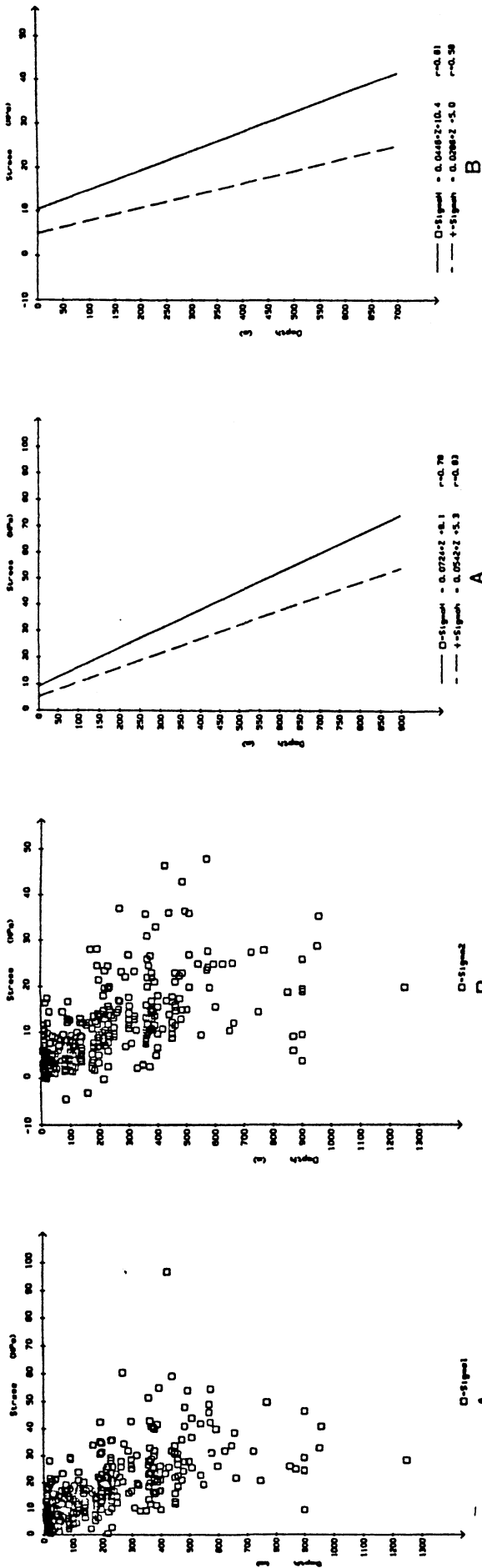


Figure 6-2 Variation of principal stress with depth in Fennoscandia from triaxial overcoring stress measurements: A) major principal stress; B) intermediate principal stress; C) minor principal stress; D) mean principal stress. After Stephansson et al (1986).

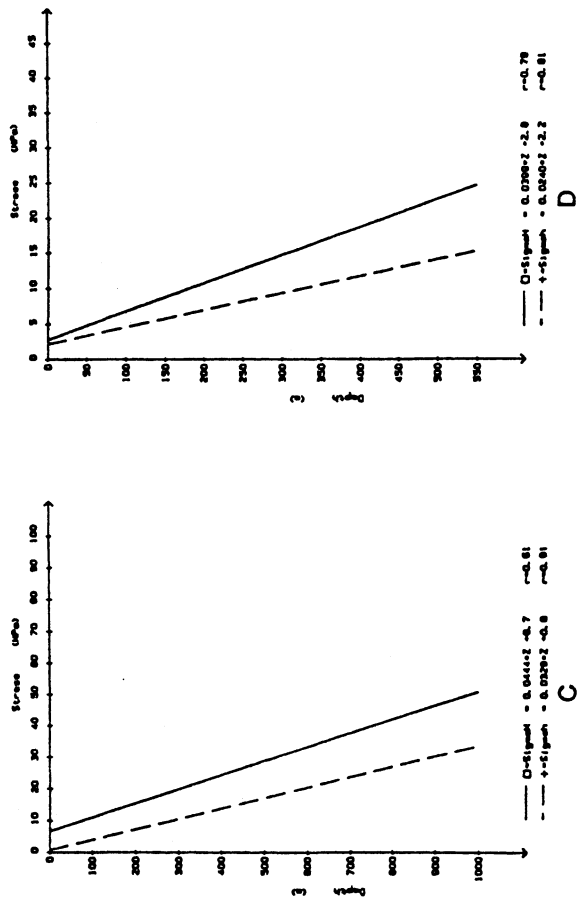


Figure 6-3 Linear regression analyses of maximum and minimum horizontal stress versus depth for four different rock stress measurement methods: A) Hast overcoring; B) Leeman-Hiltcher, Swedish State Power Board overcoring; C) Leeman-, Leeman-NTH-, and Leeman-LUT overcoring; D) hydraulic fracturing, Lawrence Berkeley Laboratory, Chalmers Technical University and Lulea University of Technology. Data from Stephansson et al (1986).

- Linear regression analyses of the principal horizontal stress versus depth using hydraulic fracturing techniques result in:

$$S_H = 2.8 + 0.04z \quad (\text{MPa}) \quad (6-1)$$

$$S_h = 2.2 + 0.024z \quad (\text{MPa}) \quad (6-2)$$

where  $z$  is the depth in meters ( $< 1000$  m).

- Linear regression analyses of the major, intermediate, and minor principal stresses versus depth for all Swedish overcoring measurements result in:

$$\sigma_1 = 10.8 + 0.037z \quad (\text{MPa}), \quad r = 0.68 \quad (6-3)$$

$$\sigma_2 = 5.1 + 0.029z \quad (\text{MPa}), \quad r = 0.72 \quad (6-4)$$

$$\sigma_3 = 0.8 + 0.020z \quad (\text{MPa}), \quad r = 0.75 \quad (6-5)$$

where  $z$  is depth in meters ( $< 1000$ ) and  $r$  is the goodness of fit.

- The regression analysis of the mean stress versus depth for overcoring rock stress measurements with the LuT cell yields:

$$\sigma_m = 0.1 + 0.04z \quad (\text{MPa}) \quad (6-6)$$

where  $\sigma_m = (\sigma_1 + \sigma_2 + \sigma_3)/3$  and  $z$  is in meters ( $< 1000$  m).

Leijon (1989) collected LuT-Gauge stress data from 18 mine sites in Sweden and presented them as shown in Figure 6-4 and Equation 6-6. The locationwise scatter expressed as standard deviations is shown in Figure 6-4 and, in relative form, also in Figure 6-5. This scatter reflects the combined effect of random measuring errors and true stress variations, mixed in unknown proportions. However, the data can provide estimates of the part attributable to measuring errors. Given such estimates, bound estimates for the in-situ stress variations can also be obtained as demonstrated by Leijon.

To estimate the upper bound of the in-situ stress variation with the LuT-Gauge, we assume the measuring error to be insignificant (ie. equal to zero). Stress variations will then account for all scatter. This corresponds to the solid line curves

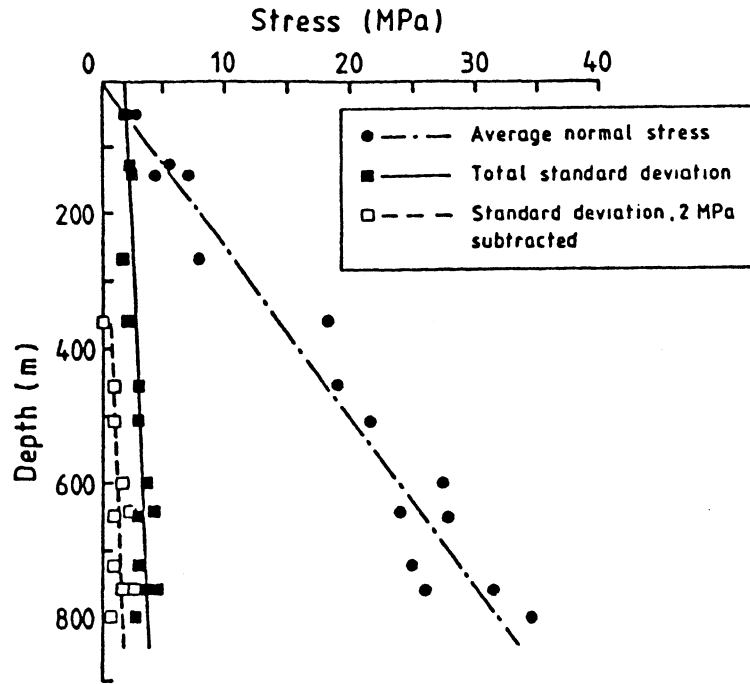


Figure 6-4 Values of mean stress plotted as a function of depth. Locationwise calculated averages and standard deviations. Curves fitted by linear regression. After Leijon (1989).

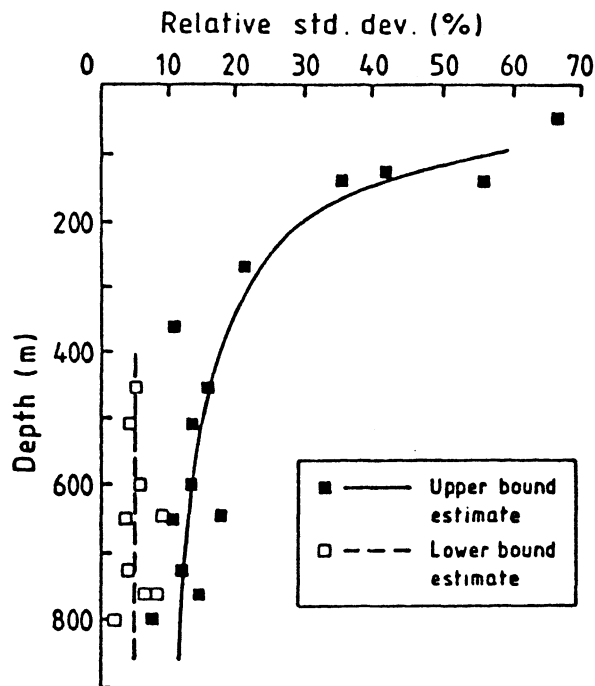


Figure 6-5 Relative standard deviations of the mean stress plotted as a function of depth. Locationwise calculated values. For depths larger than about 400 m, the curves indicate upper and lower bound estimates. After Leijon (1989).

in Figures 6-4 and 6-5. It appears that the standard deviation is about 2 MPa for the shallow measurements, and tends to increase slowly with depth.

The rate of growth with depth (ie. with stress magnitude) is of special interest. Following Leijon, this increase could arise from two sources. The first of these is best illustrated by considering the rock mass as a discontinuous array of infinitely stiff blocks. In such a rock mass, the variability encountered in random stress sampling will depend on the geomechanical contact conditions between the blocks and will increase proportionally with the applied boundary load. This implies that the relative standard deviation should be constant and independent of depth. The second source relates to the fact that neither the blocks nor the structures in a rock mass are infinitely stiff. Increased loading will therefore be accompanied by a consolidation of the rock mass. This will reduce the relative stress variations, and hence the relative standard deviation will decrease with depth.

The solid curve in Figure 6-5 should represent the superimposed effects discussed above. A sharp decrease in the relative standard deviation is noted for the uppermost 300 m. This would indicate that the consolidation effect is strong at low stress levels. At depth, the trend is uncertain, but a decrease in relative standard deviation is indicated. This would indicate a consolidation effect even at stress levels of the order of 20-30 MPa. Data are, however, not conclusive in this respect, as pointed out by Leijon (1989).

### 6.3.3 Stress Magnitude Discontinuities

In the discussion of stress gradients in the upper crust, it should be noted that a major discontinuity in the stress field with depth has been reported from several test sites. Five such stress discontinuities are reported in the Fennoscandian Shield (Matikainen, 1988; Stephansson, 1988). The maximum horizontal stress jumped about 20 MPa across a major sub-horizontal fracture zone at a depth of 320 m in a vertical



borehole at Forsmark, Central Sweden. A similar behaviour was measured at Lavia, Central Finland, where a stress jump of about 20 MPa was inferred from measurements below a major fracture zone at 420 m depth in Proterozoic granodiorite rocks. Pronounced changes in the stress fields have also been reported in the nappes around the headrace tunnels of the Vietas power plant in the Swedish Caledonides.

Hydraulic fracturing stress measurements were conducted adjacent to the remarkable post-glacial fault at Lansjarv, Northern Sweden (Bjarnason et al, 1989b). Evaluation of data according to the second breakdown method gave maximum horizontal stress  $S_H = 12$  MPa and minimum horizontal stress  $S_h = 6$  MPa at 500 m depth. A normal state of stress at this depth in the Pre-Cambrian rocks according to Equations A-1 and A-2 (Appendix A) would be  $S_H = 22.8$  MPa and  $S_h = 14.2$  MPa. The low stresses recorded at Lansjarv are interpreted to be a result of stress relief from the displacement of the adjacent post-glacial reverse fault ca. 9000 BP, during deglaciation (see Sections 3.3 and 9.2.4).

These examples demonstrate that stress discontinuities do exist in the hard rock of Fennoscandia. Therefore one has to be cautious in using generic stress versus depth relationships such as those presented in Equations A-1, A-2, A-3 and 6-1, 6-2, 6-3. Further, the state of stress can shift from a thrust faulting regime to a strike-slip regime or vice versa.

#### 6.3.4

#### Orientation of Stresses from FRSDB

From the very first compilation of stress orientation from the Fennoscandian Rock Stress Data Base it became obvious that there is a major scatter in the orientation of the maximum horizontal stress,  $S_H$  (Stephansson et al, 1986). This scatter holds for stress data in the areal extension as well as for stress orientations versus depth, Figure 6-6. At depths below 300 m,  $S_H$  is generally oriented in the NW-SE direction in Central Sweden and Central Finland.

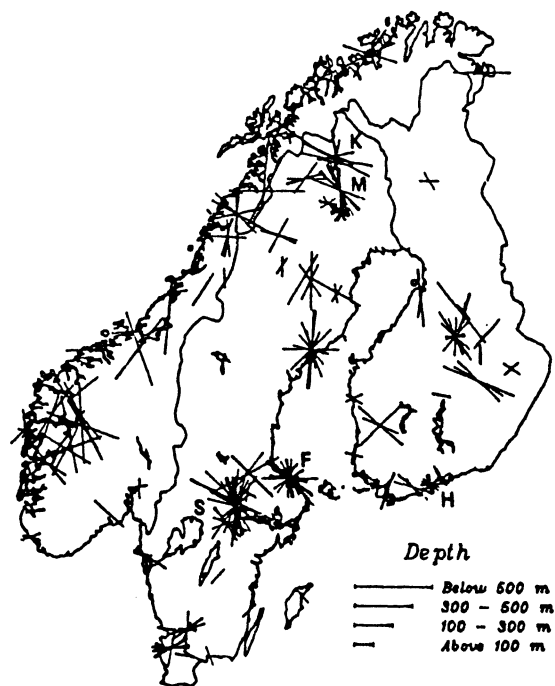


Figure 6-6 Trend of maximum horizontal stress at different depths in the Fennoscandian Shield. Data taken from the Fennoscandian Rock Stress Data Base. After Stephansson et al (1986).

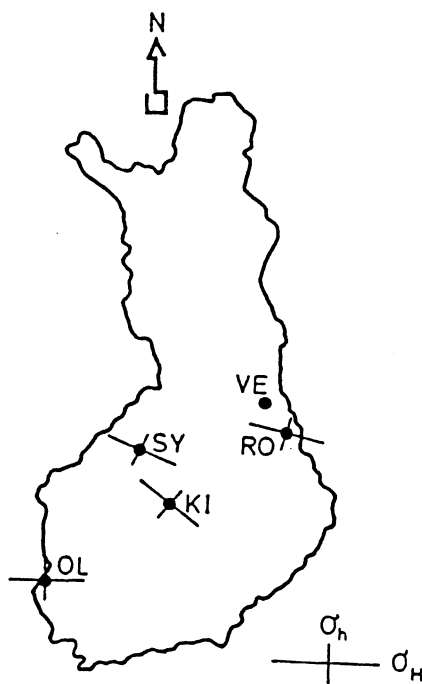


Figure 6-7 Measured directions of horizontal stresses in deep boreholes in Finland. Each cross indicates average value from hydraulic fracturing at a site. The plot shows directions only. VE = Veitsivaara, RO = Romuvaara, SY = Syyry, KI = Kivetty and OL = Olkiluoto. After Klasson and Leijon (1990).

Since the release of the map of  $S_H$  for Fennoscandia in 1986, there has been a series of deep hydrofracturing stress measurements conducted in Finland with application to their nuclear waste programme and site location for deep-seated gas storages (Klasson and Leijon, 1990). The measurements were conducted between 400 and 900 m depth in each of the boreholes. The average direction of  $S_H$  is shown in Figure 6-7 and the results range from NW-SE to E-W. Early data from the FRSDDB (Stephansson et al, 1986, 1987) also show a tendency for the maximum horizontal stress in Norway to align with the axis of the Caledonides. For the majority of test sites in Fennoscandia, one of the intermediate or minor principal stresses is vertical and its magnitude is approximately equal to the weight of the overburden.

An attempt was made to see if there was any correlation between the direction of  $S_H$  and the different orogenies in Fennoscandia. Six litho-chronostratigraphic units were selected according to their last major phase of tectonic deformation: Phanerozoic/Mezozoic, > 300 Ma; Caledonian, 400 Ma; Sveconorwegian, 1.2 - 0.9 Ga; Transscandinavian Belt, 1.8 - 1.65 Ga; Svecokar-elian, 2.0 - 1.75 Ga, and Archean, 2.9 - 2.6 Ga.

These orogenies coincide with the geological evolution and geological domains for the history of the Baltic Shield as presented by Gorbatshev and Gaal (1987) (see also Section 2.1). The stratigraphic units/domains and their extension are presented in Figure 6-8. The results of this correlation, are shown in Table 6-2, and as can be seen in Figure 6-9 there does not seem to be any simple orogenic control of the  $S_H$  direction.

### 6.3.5 Scatter in Stress Magnitudes and Orientations

The maximum horizontal stress in Fennoscandia almost everywhere exceeds the vertical stress, which is in agreement with a regional tectonic stressfield that develops from the Mid-Atlantic spreading zone. The large scatter in the magnitude and direction of the measurements obtained in the uppermost part of the crust must still be explained. One possible explanation for this

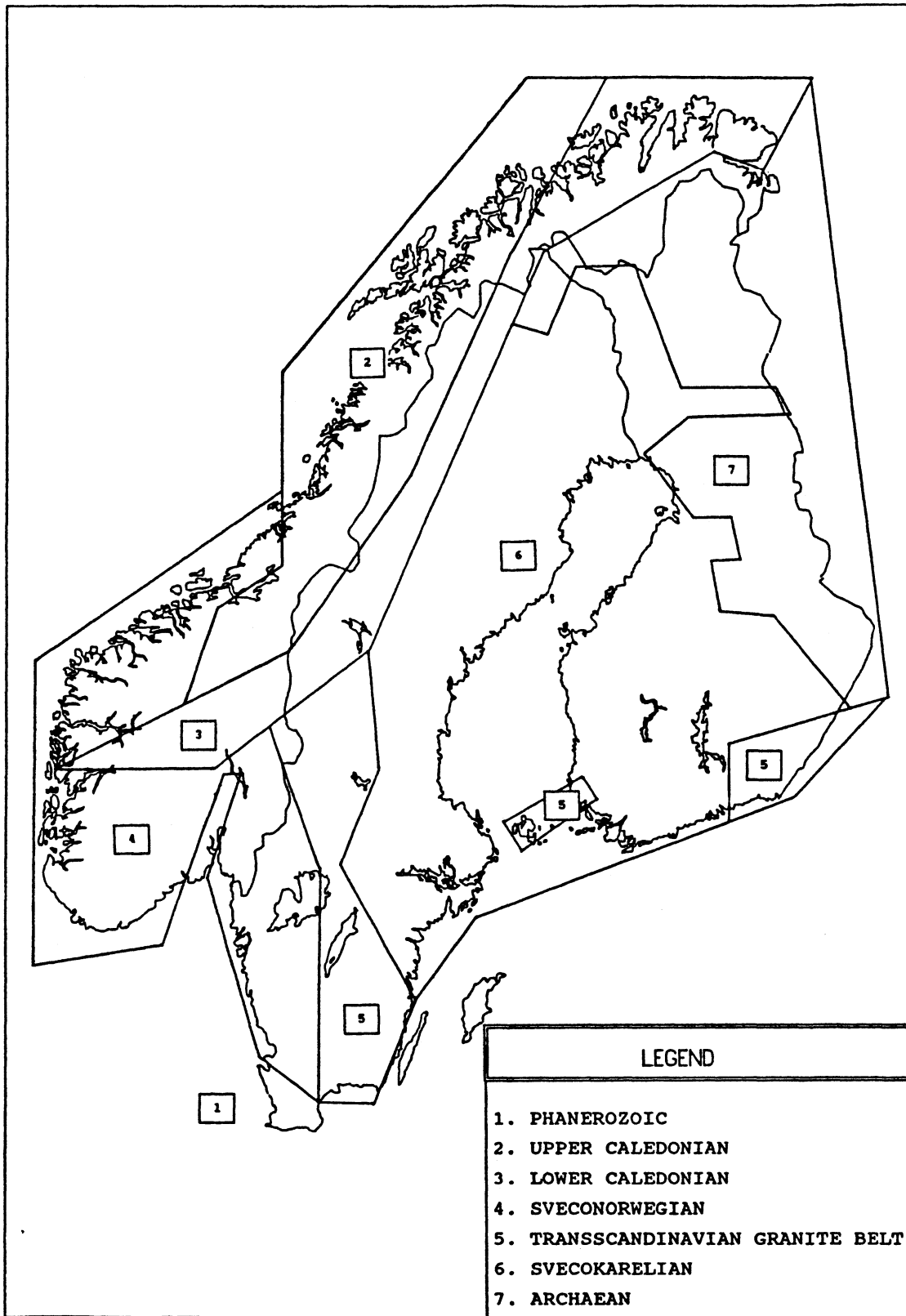


Figure 6-8 Stratigraphic units within the Baltic Shield.

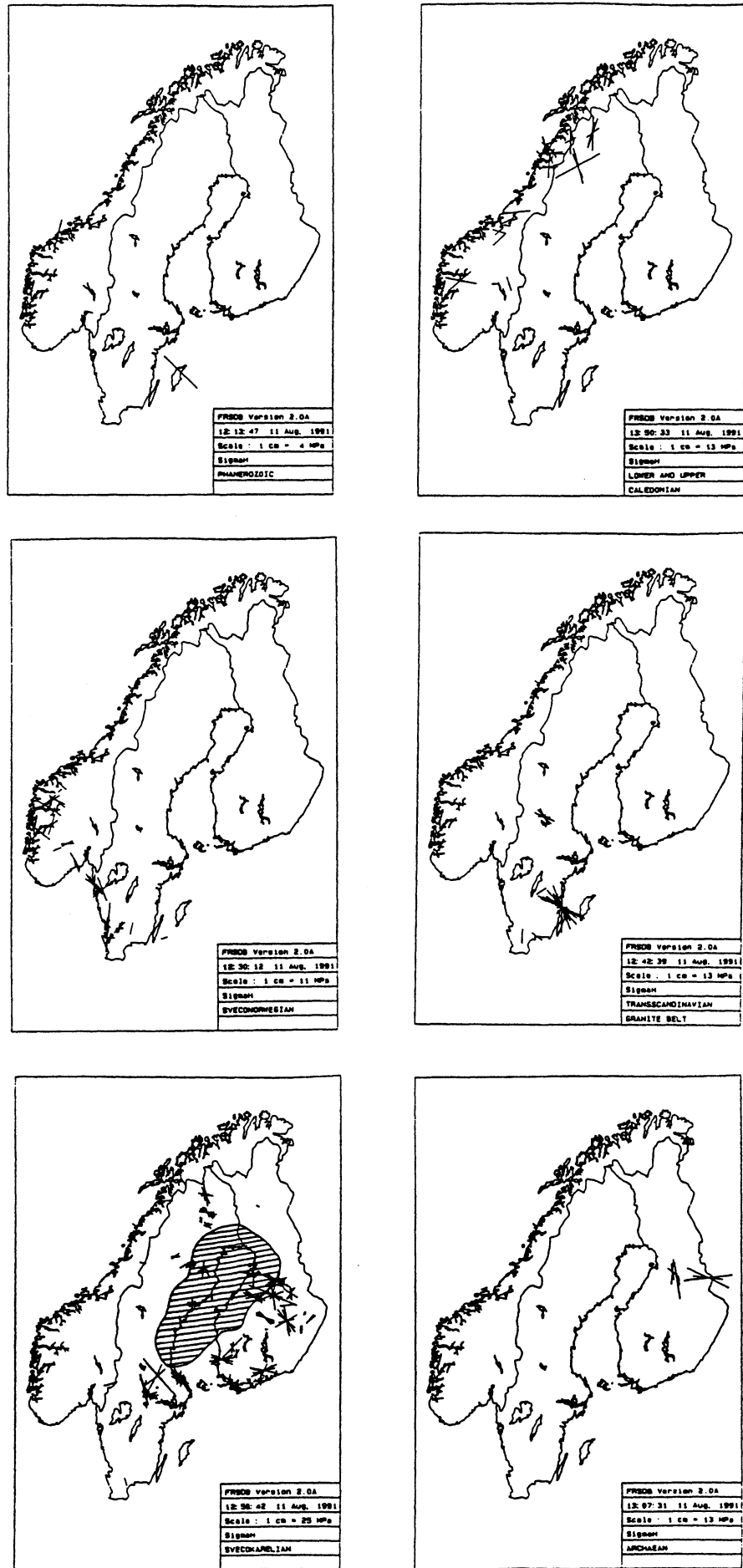


Figure 6-9 Orientation of maximum horizontal stress in different tectonic stratigraphic units.

	Orogenic Unit	Observation	Comment
A	Archaean	Only four locations, three in Finland and one at the iron ore district in Kirkenaes.	There is a considerable discrepancy between the orientation data from the different locations in Finland indicating a $S_H$ direction ranging from N-S to E-W.
B	Svecokarelian	-	There is a large scatter in orientation of $S_H$ . However, there is a weak tendency for a preferential orientation NNW-SSE.
C	Transcandinavian Granite Belt	This unit comprises five sites located in Sweden of which the two southernmost are rather shallow. Prominent NW-SE orientation of $S_H$ in the Siljan District of Central Sweden, agrees with the data from the Gravberg deep borehole (see Figure 6.9). The large number of data points on the Swedish east coast is a product of the Aspo Hard Rock Laboratory investigation.	There is good coincidence between the Aspo and Siljan data.
D	Sveconorwegian	Data came chiefly from two regions; southernmost Scania, and southwestern Norway.	The $S_H$ orientation in Scania is E-W to NE-SW. For southwest Norway there seem to be basically two $S_H$ orientations: NW-SE and NNE-SSW.
E	Caledonian	The Caledonian orogeny is generally divided into Upper and Lower levels (allochthonous and autochthonous), here lumped together. Almost 100% of observations are from overcoring.	There is a large scatter of data, but a weak tendency for stresses to line up parallel with the axis of the Caledonian mountains.
F	Phanerozoic	Data points are from the island of Gotland, Sweden, the northern Oslo Graben and one point from the west coast of Norway.	There is a clear NW-SE trend in the direction of $S_H$ . Perhaps, as in Central Europe, the youngest geological formations give the most distinct print of existing plate motions.

Table 6-2 : Correlation of Orientation of Maximum Horizontal Stress

scatter is that stress concentrations develop at the contacts between minor tectonic blocks delimited by the major fault system (see Stephansson, 1988). These stress concentrations could then cause scatter in the measurements. A consequence of the variation of discontinuity strengths is that stronger discontinuities can sustain higher stresses resulting in the scatter of stress magnitude and orientation.

These possible explanations have been studied using numerical models (Stephansson, 1989). A rock mass delimited by major faults and shear zones was subjected to a shear displacement along one edge of the model. Models consisting of large blocks resulted in relatively large stress concentrations at contact points, whereas the stresses in models comprised of small blocks did not vary significantly.

Down to 1000 m in the Earth's crust, where in situ stresses are measured, the interaction between rock mass blocks could cause a redistribution of stress. Higher stresses would develop at contact points of blocks and stress refraction would develop adjacent to shear zones and faults.

There are very few studies about scatter in stress magnitudes and direction due to variations in the geological structures. Leijon (1986) made a thorough study on the influence of geological structures and the number of tests in the determination of the principal stresses for hard rock masses. He studied two areas in the Maloberget mine, Northern Sweden where one site (locality 1) was located in a foliated and jointed biotite leptite, and the other site (locality 2) was situated in a homogeneous, sparsely jointed granite. He determined confidence limits for principal stresses by using Student's t-distribution and derived confidence limits for the stress orientation by means of Fisher-distributions. His results are summarised in Figure 6-10 and demonstrate that local rock conditions have a major influence on the confidence of results from individual overcoring stress measurements. This finding may have important implications for stress observations in other rocks in Sweden that possess a profound fabric.

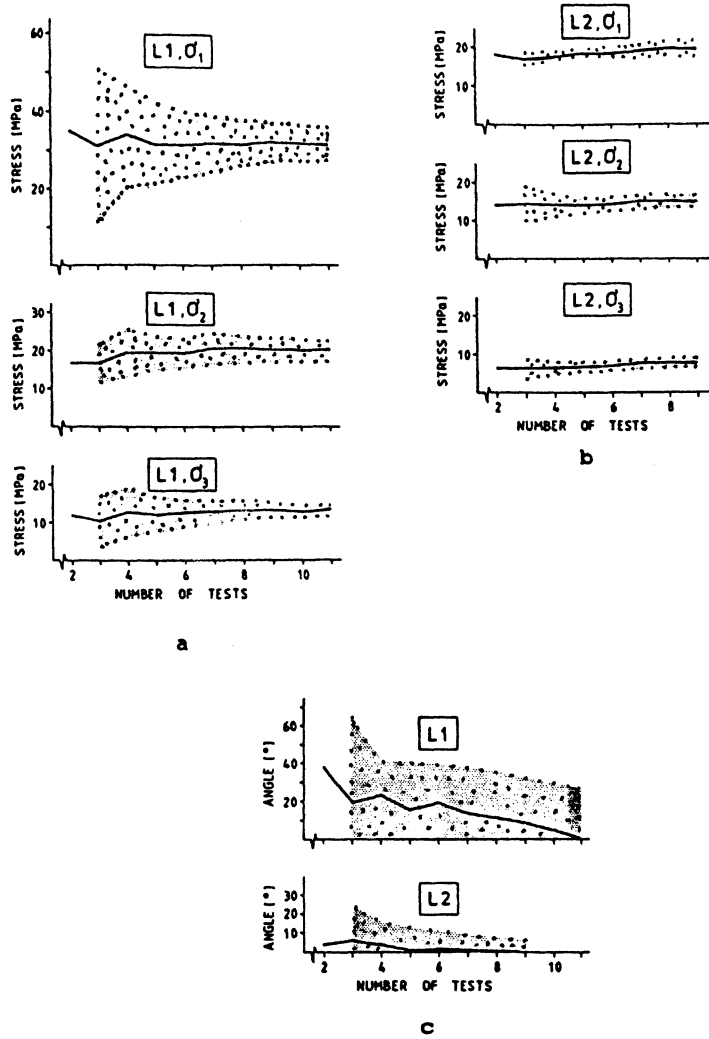


Figure 6-10 Scatter in stress magnitude and orientation for two different rock types in Malmerget Mine, northern Sweden. Location L1 is a foliated and jointed biotite leptite and L2 is a homogeneous granite. a) principal stress versus number of test for site L1; b) principal stress versus number of test for site L2; c) confidence of principal stress direction. Curve = sample mean, Shadow = 90% confidence interval.

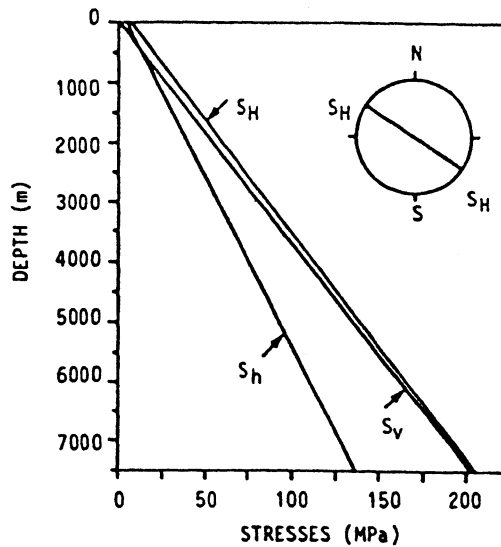


Figure 6-11 An estimate of stress profiles in the Siljan District. Orientation of  $S_H$  is shown in the upper right corner of the figure. After Stephansson et al (1990).



### 6.3.6 Stress State from Breakouts and Other Tests at Great Depth in the Siljan District

Estimates of the maximum horizontal stress,  $S_H$ , from breakouts are only available from Central Sweden. A deep well in the Siljan District was drilled at Gravberg to prospect for gas. The well was located just outside the meteorite crater and close to the outer rim syncline. The well was spud on the 1st of July 1986 and by 1987 had been drilled down to 6600 m. Many drilling problems were encountered including severe breakouts and borehole collapses. Borehole deviations of up to 45 degrees occurred and the drill string and logging tools were often jammed. Despite all these complications the pumping tests were completed in 1990.

Figure 6.11 shows the estimated stress profiles for the Siljan District (from Stephansson et al, 1990). At surface both horizontal stresses are larger than the vertical stress. Below approximately 500 m,  $S_H$  becomes smaller than the vertical stress, approaching a value of 0.65 times  $S_V$  for large depths. The maximum horizontal stress is larger than  $S_V$  at all depths but the difference is very small, see Figure 6-11. This estimate was later confirmed by the pump testing, geophysical logging analysis of borehole breakouts and fracturing test with heavy drilling mud.

The borehole at Gravberg has been measured by a four-armed dipmeter calliper logging tool, which makes it possible to estimate the breakout, the deviation and the azimuth for the boreholes as a continuous function of depth.

Breakouts started to appear at a depth of around 1500 m and remained more or less constant to a depth of 4800 m. Severe breakouts appeared around 5000 m depth. Cementing and reentering the borehole at 4500 m depth showed that breakouts appeared immediately when the drilling restarted. The magnitude of the breakout zones in ST-3 (sidetrack 3) is greater than in ST-2. Below 6325 m in ST-3 the hole has a more irregular shape and the overall volume of the hole is calculated to be double the theoretical volume of a 6 1/2 inch hole.

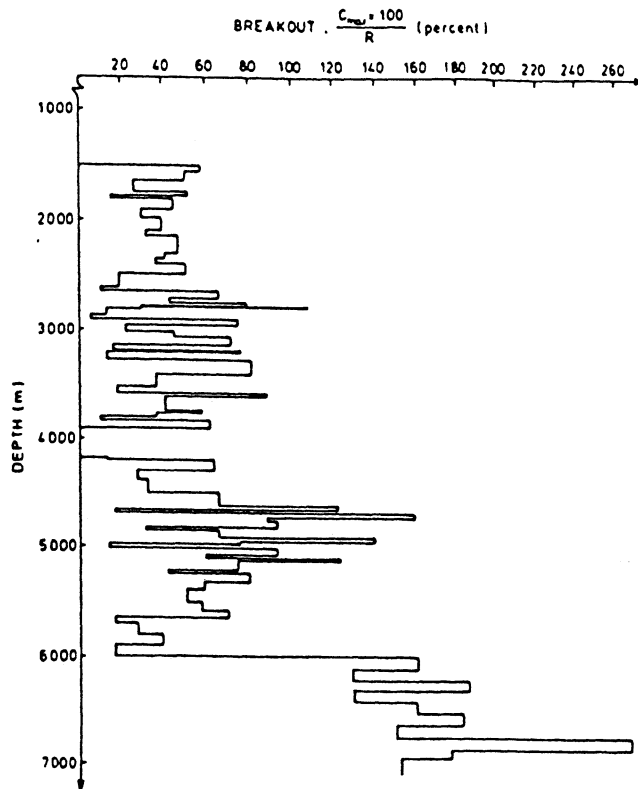


Figure 6-12 Breakouts versus depth at the Gravberg deep borehole.  $C_{max}$  is the maximum breakout and  $R$  is the diameter of the drillbit. After Stephansson et al (1990).

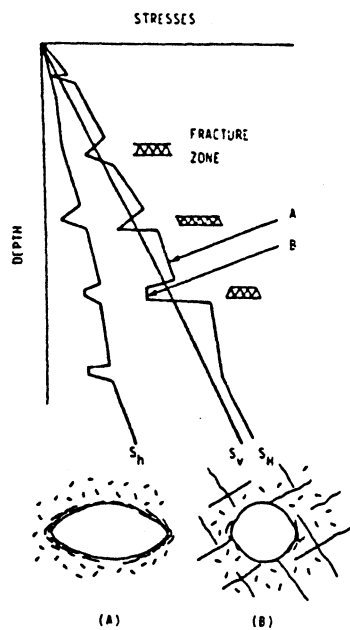


Figure 6-13 Suggested models for breakouts at the Gravberg well. Stresses are assumed to be low across the fracture zones. Spalling is the most common mechanism of failure for intact rocks (A) and numerical modelling has demonstrated lower stresses and less displacements in the surrounding of a deep borehole in jointed rock mass. After Stephansson et al (1989) and (1990).

The maximum breakout dimensions,  $C_{max}$ , presented as the percentage of the drill bit radius,  $R$ , as a function of depth, is shown in Figure 6-12. The diagram is constructed from the logs where sections of constant breakouts are defined and shown as an average value. The average direction of maximum horizontal stress ( $S_H$ ) is found to be N71°W with a standard deviation of  $S_n = 16$ .

The fracture zones that appeared in the borehole are characterised by no breakouts, an increase in drilling rate, an increase in sonic travel-times, a decrease in deep resistivity, an increasing amount of fracture associated minerals and finally fractures or effects of fracturing observed in the cuttings. The fact that these zones show no breakouts is a strong indication that the magnitude of stress is less in the zones than in the surrounding rock. The borehole is penetrating a rock mass composed of large blocks of the size of several hundred meters, bounded by major discontinuities or fracture zones in which the stress state is non-uniform, re-oriented and probably lower.

If this model of the rock stress changes versus depth is valid one would expect two different types of failure of the borehole wall, one for intact rock (A) and one for the fracture zones (B) as shown in Figure 6-13. The geophysical logs of the Gravberg well give clear evidence of the existence of fracture zones, where the calliper logs show only minor breakouts.

Numerical modelling using the distinct element code MUDEC has demonstrated a major reduction in the peak stresses and deformations around the periphery of the well for jointed rock mass (Stephansson et al, 1989, 1990). The maximum stress for a jointed rock is reduced by more than 30% and, for the depth of 7500 m, by almost 50% compared to the situation for homogeneous intact rocks. Although minor spalling can take place at the periphery of the borehole in a jointed rock mass, the borehole wall remains stable and the deformability of the joints prevent the build up of large stress concentrations. The few breakouts recorded in the fracture zones at Gravberg might also be a result of the lower stresses anticipated across the zones.

This suggested model for the breakouts at Gravberg can be checked only by conducting in-situ rock stress measurements by means of conventional hydraulic fracturing techniques in combination with hydraulic injection tests on pre-existing joints or fractures in the borehole.

#### 6.4 **FENNOSCANDIA IN THE CONTECT OF THE WORLD AND THE EUROPEAN STRESS MAP**

##### 6.4.1 **World Stress Map (WSM)**

The World Stress Map project of the International Lithosphere Program is compiling a global database of contemporary in situ stresses in the crust using a variety of geophysical and geological measurement techniques. The project is a collaborative effort which at present involves over 30 scientists from 10 different countries.

The results of the World Stress Map Project of the International Lithosphere Program are presented as a global data base incorporating contemporary in situ stress data in the crust using:

- (i) earthquake focal mechanisms;
- (ii) stress-induced wellbore breakouts;
- (iii) in situ stress measurements;
- (iv) young geological deformational features, including both fault slip and volcanic alignments.

A system to rank the quality of stress orientation data has been developed. Four qualities are used, ranked in order A ( $\pm 10-15^\circ$ ) > B ( $\pm 15-20^\circ$ ) > C ( $\pm 20-25^\circ$ ) > D ( $\pm >25^\circ$ ) where recorded data of the direction of the maximum horizontal stress has to be within specified limits. The most recent edition of the WSM is shown in Figure 6-14.

The main conclusions from the co-operative WSM Project are (Zoback et al, 1989):

- (a) most intraplate regions are characterised by a compressive stress regime, ie. thrust or strike-slip faulting dominate;
- (b) extensional stress regimes occur at high altitude and thermally elevated regions;

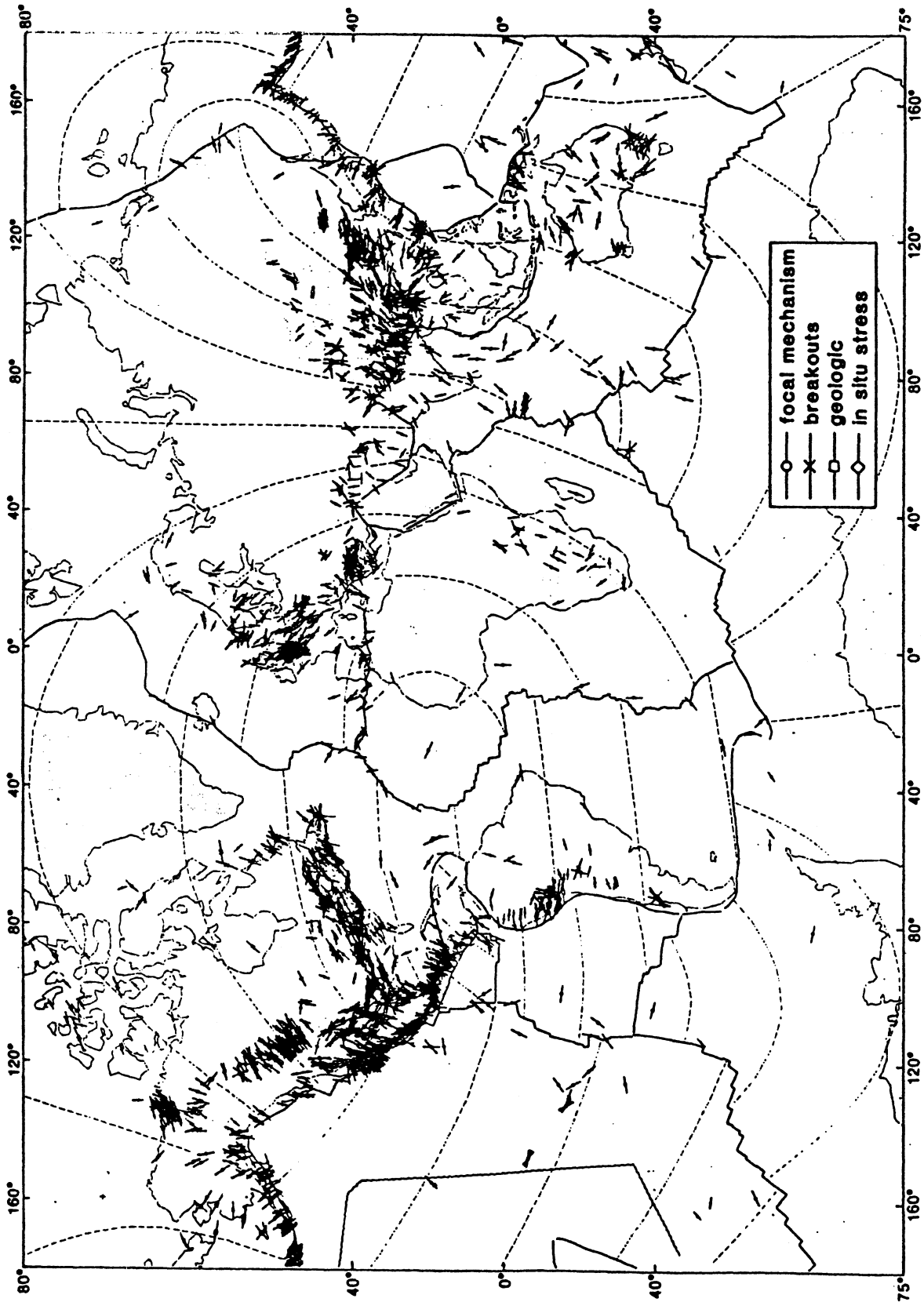


**Figure 6-14 World Stress Map.**  
 Transverse mercator projection,  $S_H$  orientations are plotted, length of lines are proportional to quality (A, B or C).

- (c) good positive correlation exists between relative plate movement and  $S_H$  -direction and the net boundary forces on the plate boundary are equilibrated by the intraplate stresses.

#### 6.4.2 The European Stress Data Base (ESDB)

Data on contemporary  $S_H$  orientation have been compiled for all Europe west of about  $30^\circ\text{E}$  including the continental shelf and oceanic regions. The in-situ stress measurements from FRSDB entered into the European Stress Data Base are shown in Figure 6-14. The European subset of the World Stress Map data base contained 1478 entries up to February 1991, Mueller et al, (1992).

The compilation of the stress data for the European part of the WSM followed the same procedure, format and quality ranking as defined and described for the WSM by Zoback et al (1989). The ranking system is based on the number of observations, the consistency of results and the reliability of the data as a tectonic (as opposed to local) stress indicator. The qualities range from A (high quality) to E. The qualities A to C are believed to record reliably the tectonic stress field, D quality data are of questionable quality, and E quality data provide no reliable information on stress orientation but are included for record keeping purposes only. All mean values and standard deviations presented in this section refer to the quality categories A to C as defined by the quality ranking, if not otherwise indicated. For the calculation of mean  $S_H$  -orientations versus azimuth in the circular statistics, a linear weighting for the different qualities of A:B:C:(D) = 4:3:2:(1) was used. Geographic north is chosen as reference direction for comparison with the orientation of faults, folds and other indicators of structural geology.

For Europe, as for the global WSM dataset, the stress data are obtained from the following sources: earthquake focal mechanisms; hydraulic fracturing stress measurements; borehole breakouts; overcoring stress measurements; and fault slip orientations. The majority of the data come from

depths greater than 5 km where information is almost exclusively derived from focal mechanisms, few of which are of A quality. Focal mechanisms were generally not included if they are judged to be sub-crustal. At medium depths (2 km - 5 km) data are very sparse; only hydrofracturing, breakouts and focal mechanism data are available. The breakout data from deep boreholes in Europe, which comprise many ranked as A and B quality, help to expand knowledge of the 2-5 km depth range and provide an important tie between the near surface and deep stress determinations.

#### 6.4.3 The European Stress Map (ESM)

All  $S_H$  -orientations for Europe are plotted on Figure 6-15a that contains a total of 767 data points of A to C quality. On Figure 6-15b,  $S_h$  -orientations are plotted for all extensional data points. A comparison of stress orientations with topography in general does not indicate a correlation between specific regimes and either high or low topography areas (Figure 6-15a). A generalised stress map of Europe (Figure 6-16) was determined by a visual average of orientations shown in Figures 6-15a and 6-15b, assisted by the focal mechanisms and style of faulting. Inward pointing arrows characterise regions of compressional tectonics, either strike-slip or thrust faulting (TF), with strike-slip component (TS) and true strike-slip (SS); outward pointing arrows indicate the orientations of extensional tectonism like normal faulting (NF) and normal faulting with strike-slip components (NS). This map is based on clusters of consistent stress observations, preferably from different stress indicators, as shown in Figures 6-15a and 6-15b.

Clearly the density of stress data varies considerably within Europe. The distribution of the type of stress indicators is also inhomogeneous: obviously focal mechanisms are concentrated in seismically active areas; borehole breakout data are mainly available in sedimentary basins; overcoring measurements come from mining regions; and geologic indicators come from volcanic areas or regions with recent tectonic activity and with especially good fault exposures. In regions where

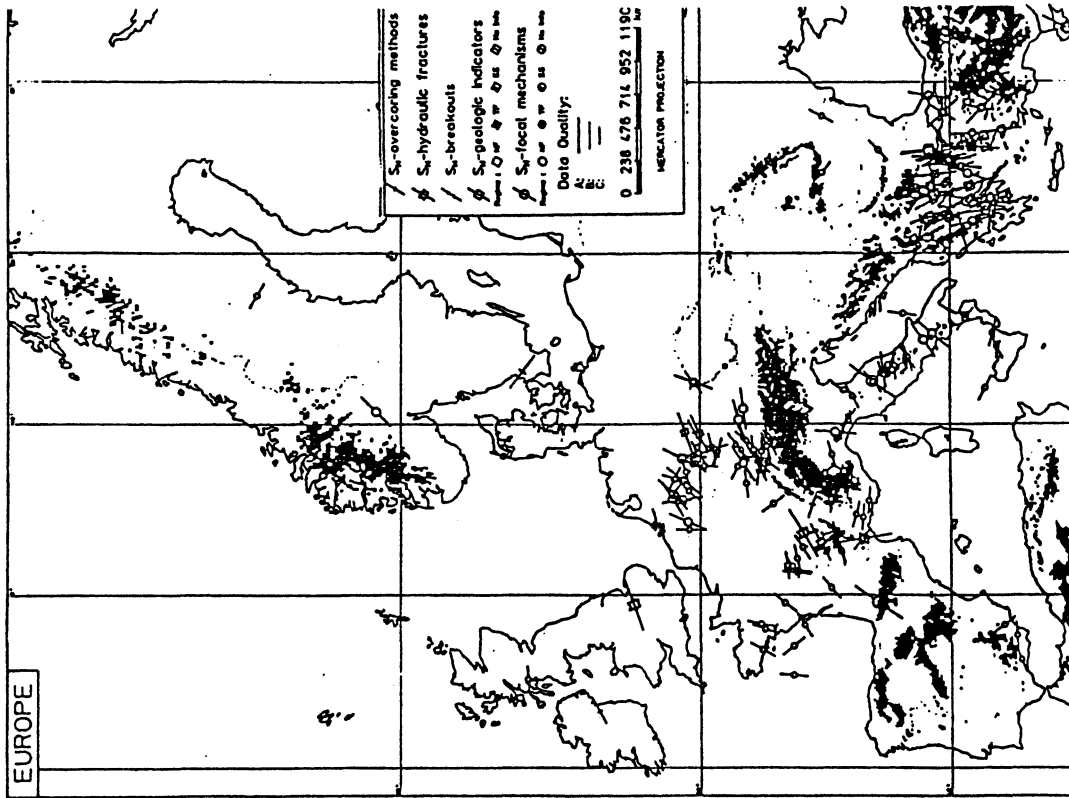


Figure 6-15b  $S_h$  orientations for the extensional subset of data of Figure 6-15a. After Mueller et al (1991).

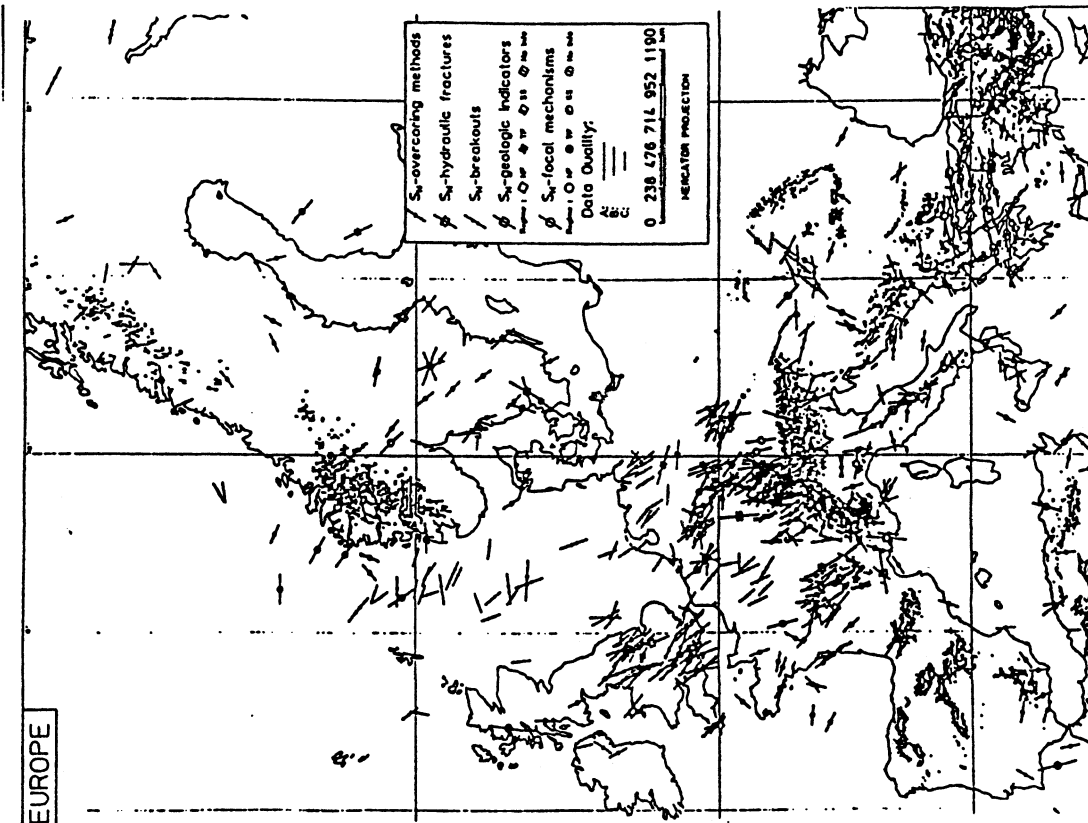


Figure 6-15a European Stress Map plotted on a regional topographic base. Maximum horizontal compressive stress orientations are plotted for all data in the quality categories A, B and C (length of line is proportional to quality). After Mueller et al (1991).



more than one type of stress indicator is available, the orientations generally did not show systematic differences.

The stress data indicate that: (1) much of western and northern Europe are subject to a strike-slip regime, which is characterized by NW to NNW compression and NE to ENE extension; (2) areas of extension include the Aegean Sea and western Anatolia, the lower Rhine Embayment, the western Appenines and parts of France; (3) there is no distinct correlation between stress regime and geological units such as sedimentary basins or orogenic belts; (4) there is no systematic variation of  $S_H$  -orientation with depth; and most importantly (5) the  $S_H$  -orientations and stress regimes are regionally uniform. The data on the maps in Figures 6-15a and 6-15b have been used to define three regions of characteristic stress orientation and relative magnitude:

- (a) western Europe, with a well-constrained mean  $S_H$ -orientation trending NW to NNW;
- (b) northern Europe, with more scattered  $S_H$ -orientations around a WNW-ESE mean;
- (c) the Aegean Sea and western Anatolia, with a nearly E-W oriented  $S_H$  -direction and thus, with a N-S extension.

This division in regions, or stress provinces, is based on the distribution of the observed data. Thus these regions do not necessarily geographically coincide with physiographic provinces.

#### 6.4.4 Relationship of the Fennoscandian Stress Province to Central Europe

Europe can be broadly subdivided into two major geologic provinces: the Fennosarmatian craton and a zone of Phanerozoic orogenic belts. The Pre-Cambrian Fennosarmatian craton extends from the Tornquist-Teisseyre line, a suture zone of at least Late Pre-Cambrian age in the west, to the Ural mountains in the east. In the north, Fennosarmatia borders on the Scandinavian Caledonides. This

Pre-Cambrian craton represents an old consolidated platform and includes the Baltic Shield, the Ukrainian Shield and the Russian Platform. The craton has a thick lithosphere (commonly >110 km), relatively low heat flow (<50 mW/m<sup>2</sup>) and relatively little internal Phanerozoic deformation. Lithospheric thickness, derived from the dispersion of surface waves, increases from approximately 90 km in the south and east to more than 170 km in Fennoscandia, the maximum thickness in Europe (see Section 2.1).

West and southwest of Fennosarmatia, lie three Phanerozoic orogenic belts: (1) the Early Paleozoic Caledonides in Scandinavia and the British Isles; (2) the Late Paleozoic Variscan belt, and (3) the late Mesozoic/Cenozoic Alpine belt. In comparison to Fennosarmatia, lithospheric thickness, heat flow, degree of recent tectonic deformation, and stress regimes in these Phanerozoic orogenic belts vary considerably as discussed below.

(a) Western European stress province

Within the western Europe stress province (roughly covering the region between 45° N and 55° N latitude and 10° W to 17° E longitude), the stress data show a uniform NW to NNW S -orientation with a mean value of N 145° E ± 26°. Figure 6-17 displays the azimuthal histogram of the S<sub>H</sub> -orientations for Western Europe. The predominance of strike slip faulting (number of normal fault, strike slip fault and thrust fault events of A to C quality = 62/106/58 respectively) suggests that the intermediate principal stress is dominantly vertical, however there is a significant fraction of both normal faulting and thrust faulting events which are generally regionally segregated as described in the subsequent section.

(b) Fennoscandian stress province

Fennoscandia is presently undergoing crustal uplift (maximum uplift 0.9 m/100yr at the centre of the area in the northern Baltic Sea) as a result of post-glacial rebound. A smoothed contour plot of the post-glacial land uplift is displayed in Figure 6-18 with the S<sub>H</sub> -orientations superimposed. The data shown in Figures 6-15a and 6.15b indicate that

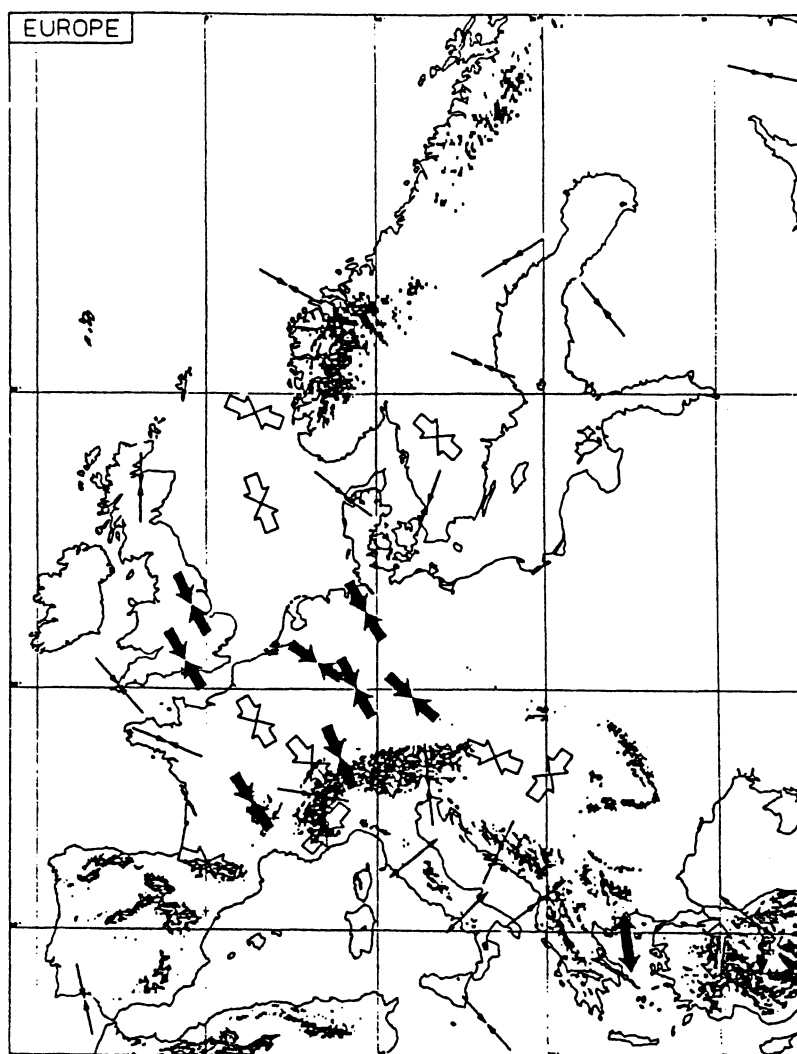


Figure 6-16 Generalized European stress map. After Mueller et al (1991).

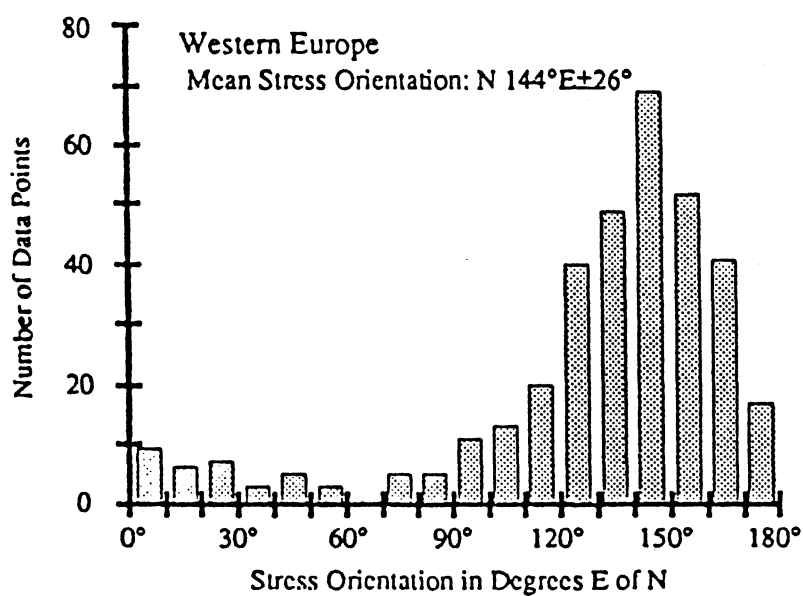


Figure 6-17 Azimuthal histograms of the stress orientations (A, B and C qualities) for Western Europe. After Mueller et al (1991).

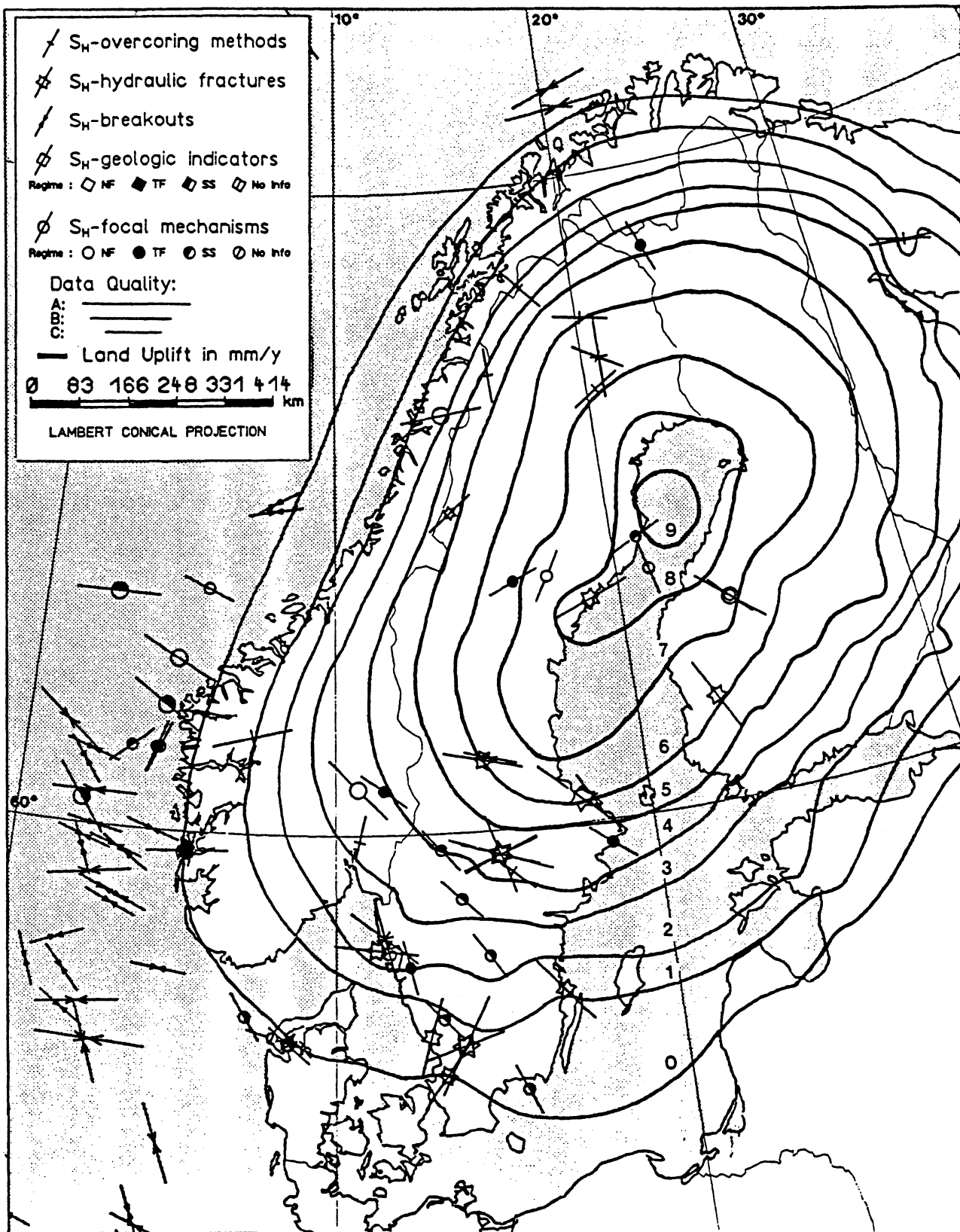


Figure 6-18  $S_H$ -orientations for Scandinavia plotted on a map of surface uplift rates (mm/yr) for glacial rebound (after Bakkelid, 1986; Ekmann, 1977). This map is from Mueller et al (1991).

the  $S_H$  -orientation in Fennoscandia is not as consistent as in western Europe.

Stephansson (1988) presented three possible sources of stress in the Fennoscandian region: (1) locked in creep stresses due to the ice loading and remaining flexural stresses from the subsidence from glaciation; (2) topography; and (3) stresses created from ridge push from the Mid-Atlantic Ridge, which he considered to be the most important, Figure 6-19. Bungum et al (1991) related a dominance of normal faulting earthquakes in Norway on the landward side of the continental margin and thrust faulting earthquakes on the oceanic side to post-glacial uplift of Fennoscandia. They further relate the stress orientations from locations at a distance from the continental margin to ridge push forces.

A combination of plate boundary forces with local sources (eg. flexural stresses from glacial rebound) are most likely responsible for the stress field in Northern Europe. Possible causes for some scatter in tectonic stresses could reflect: (a) the shift of the Mid-Atlantic ridge spreading axis at about 70° north latitude by a major fracture zone (Jan Mayen Fracture Zone), which is located quite close to the area of varying stress orientations in Northern Scandinavia and thus may indicate an influence of lateral variation of plate boundary forces; (b) a locally radial ridge push component due to the Iceland hot spot, which is superimposed on the lateral plate boundary forces, Harper (1990); and (c) the physical properties of Fennoscandian lithosphere (low heat flow, thick lithosphere), which act to reduce the mean stress level of the lithosphere, and permit local effects due to lateral inhomogeneities in the crust such as density or strength to have an important influence on the stress field.

With respect to the last of these, simple finite element modelling of the European intraplate stress field indicates that the general NW-SE direction of  $S_H$  stress can be well modelled by using only the plate boundary forces ridge push to the northwest and continental collision along the southern boundary (Brudy, 1990). Introduction of lateral variations of lithospheric thickness by Brudy and

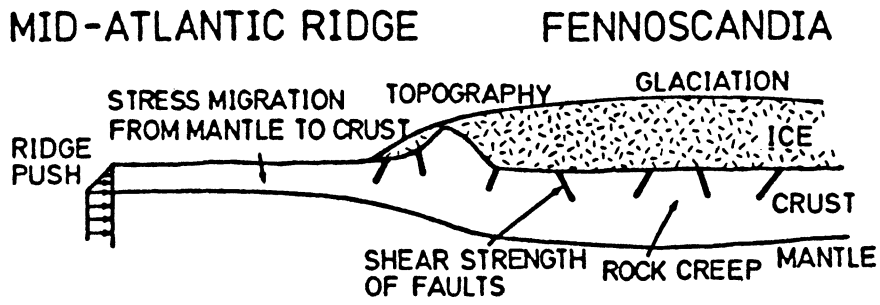


Figure 6-19 Schematic stress generating mechanisms in Fennoscandia.

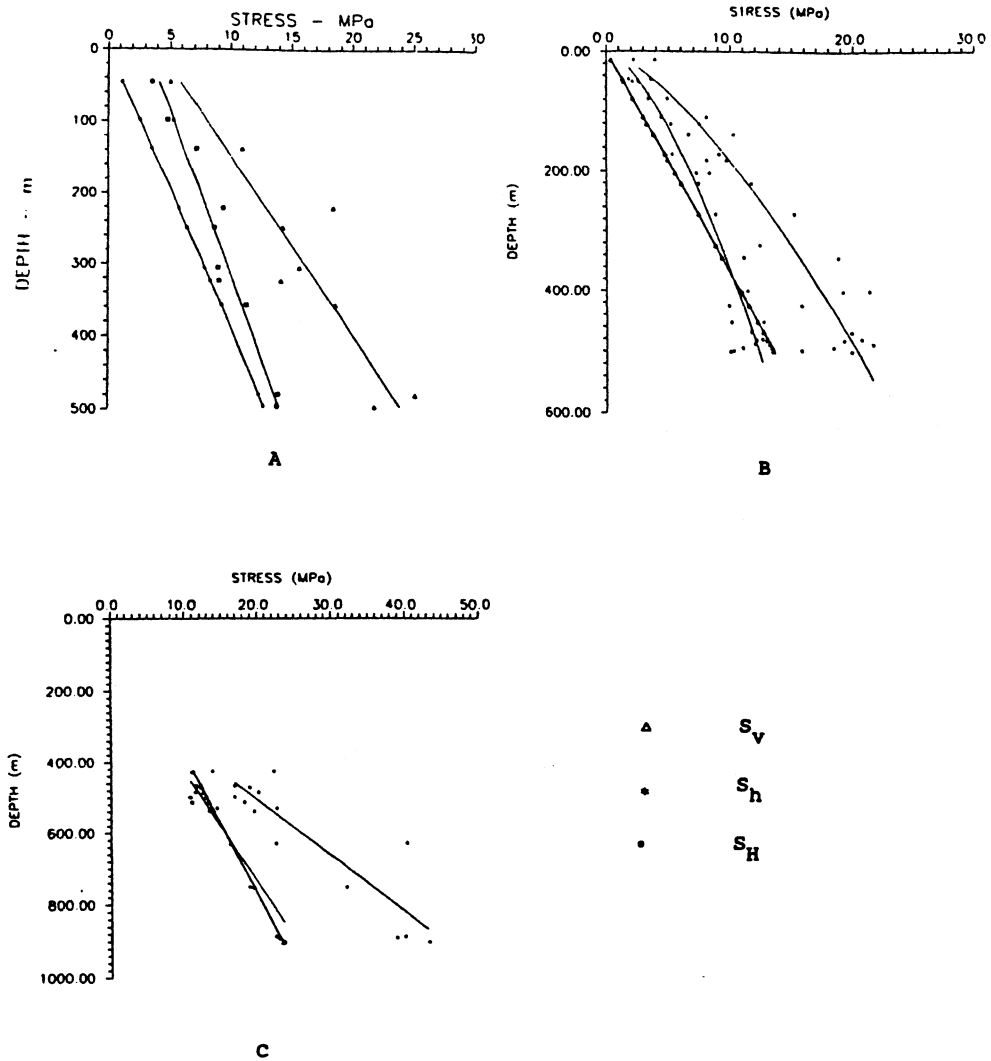


Figure 6-20 Hydraulic fracturing stress measurement profiles for three sites in the gulf of Bothnia: A) Lulea; B) Gidea; C) Syyry. After Ljunggren and Bjarnason (1990) and Klasson and Leijon (1990).

lithospheric strength by Grunthal and Stromeyer (1992) produced a stress field with a better fit locally to the observed data.

Another cause of variation may reflect the influence of rock discontinuities (joints and faults) which exhibit a wide range of shear strengths and friction angles under low effective normal stresses. Conversely, under high effective normal stress the shear strength and friction angles do not vary appreciably. This characteristic supports the general trend, that close to the bedrock surface where the average stress is low, there is a large scatter in stress data whereas deeper in the crust the state of stress becomes more uniform (Mueller et al, 1992). Currently there is no method to distinguish between the different local stress generating mechanisms.

#### 6.4.5 In-situ Stress Measurements Around the Centre of the Rebound Dome

One hypothesis tested in this project is the relation of the seismicity and in-situ stress state in Fennoscandia to glacial rebound. Unfortunately the crest of the rebound dome chiefly underlies the northern Gulf of Bothnia (see Figure 4-6). We have, however, analysed in more detail the in-situ stress data within the onland area of greatest rebound, and taken the 6 sites with stress data that are within the area of a rate of uplift exceeding 7mm/year, see Figure 6-18.

The stress data consist of hydraulic fracturing at Lulea (L), Gidea (G) in Sweden and Syyry (S) in Finland and overcoring for the remaining ones. Stress versus depth for the Lulea, Gidea and Syyry boreholes are presented in Figure 6-20. At Gidea and Lulea the stress data indicate thrust fault conditions close to the surface. However, below 400 m (Gidea) and 700 m (Lulea) depth, respectively, the results indicate that the strike-slip condition is prevailing. At Syyry, Finland, the situation seems to be the opposite: between 400-600 m depth there are indications of strike-slip conditions whereas deeper measuring points give thrust fault conditions.

The horizontal stresses versus depth at Gidea could

be interpreted as having a bi-linear relation with the inflexion point at around 300 m or a gradually decreasing stress gradient with depth, as is presented in Figure 6-20.

For the overcoring stress data within this region (Figure 6-18), only the measurements at the mines Nasliden (Sweden) and Vihanti (Finland) in FRSDB have stress information as a function of depth, Table 6-3. The results at both these sites show clear thrust fault conditions for the complete measuring interval (200 m to 450 m, 200 m to 600 m) and there are no clear indications for the stress conditions to change above or below these measuring intervals.

Stress	Nasliden mine				Vihanti mine			
	210m	260m	360m	460m	215m	365m	485m	570m
	(MPa)				(MPa)			
$S_v$	3.5	6.0	9.0	7.5	14.0, 8.1	20.7	24.0	24.0
$S_h$	9.5	14.0	7.0	10.0	14.0, 18.0	31.0	43.0	48.0
$S_H$	14.0	21.0	16.0	30.0	23.0, 25.0	43.0	48.0	48.0

Table 6-3 Measured stresses with overcoring technique versus depth for Nasliden mine and Vihanti mine

Interpretation of hydro-fracturing stress measurements in vertical boreholes at Gidea and Lulea in Sweden, where the vertical stress is assumed to be the weight of the overburden, indicate a transition from thrust faulting stress condition to strike-slip stress condition at a depth of 400 - 600 m. This is an interesting observation with importance for the location and design of a final repository for spent nuclear fuel. However, one would prefer stress measurements at greater depths (> 800 m) to be able to confirm this change in the stress regime on the margins of the area of maximum uplift. Further, there is a need for a comparison of the stress data from this area with the rest of Fennoscandia to find out if this is a local effect.